Claudia G. Flores González

Risk Management of Natural Disasters

The Example of Mexico

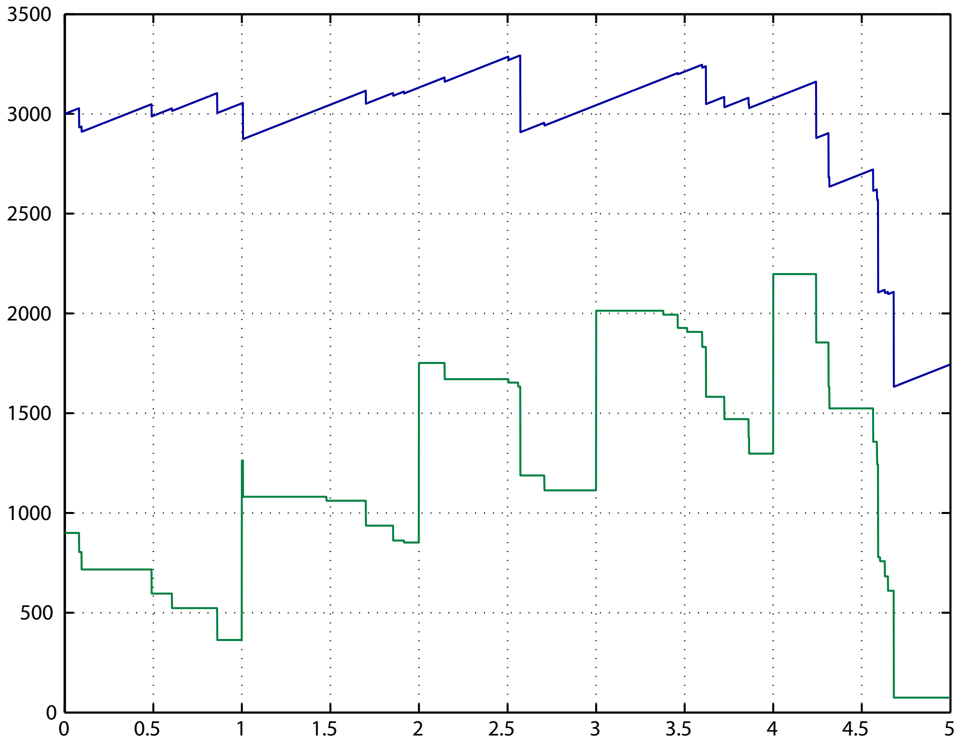

universitätsverlag karlsruhe

Claudia G. Flores González

Risk Management of Natural Disasters

The Example of Mexico

Risk Management of Natural Disasters

The Example of Mexico

von
Claudia G. Flores González

universitätsverlag karlsruhe

Dissertation, genehmigt von der Fakultät für Wirtschaftswissenschaften
der Universität Fridericiana zu Karlsruhe, 2005
Referenten: Prof. Dr. rer. nat. Christian Hipp,
Prof. Dr. rer. nat. Karl-Heinz Waldmann

Impressum

Universitätsverlag Karlsruhe
c/o Universitätsbibliothek
Straße am Forum 2
D-76131 Karlsruhe
www.uvka.de

Universitätsverlag Karlsruhe 2006
Print on Demand

ISBN 3-86644-005-7

PREFACE

Theoretical models of risk theory used in risk management were developed at the beginning of the XX century. At that time, the occurrence of natural disasters and other types of events was considered as being completely unpredictable. Nowadays, we have early warning systems and funds for disasters, and thus risk reduction is feasible. Moreover, we know more about the stochastic nature of some geophysical processes. The core of this book is to update risk management according to these new advances and challenges.

In the present research, two new tools in the risk management were developed: the theory of an arrival process taking into account an early warning system and consequently the theory of risk management for risk-averse governments. New models and procedures presented open up several new lines of research.

Although Poisson-based models and their generalizations are widely used in the practice and in many occasions produce acceptable results, sometimes are not rich enough to be applied directly in risk management issues. The global climate change and the lack of reliable historical data bases release the importance of exploring new mathematical tools to perform statistical studies of extremes. One possibility explored in the book and being the major contribution is the use of multifractal models. In the future, if the process shows multiscaling properties, we could take advantage of the abundant information at small scales to make statistical inference at the relevant scales for extremal events.

Wojciech Szatzschneider[1]
February 2006

[1] Chairman of the graduate program in Financial Mathematics of the Anáhuac University, Mexico City

CONTENTS

LIST OF TABLES

LIST OF FIGURES

TO MY GRANDMOTHER
Benjamina,

TO MY MOTHER
Gloria

AND
IN MEMORY OF MY FATHER
Víctor Manuel

INTRODUCTION

The purpose of this research are the economic aspects of disasters. We focus on the study of risk management of natural disasters from the perspective of complex systems, using the example of Mexico. The term *risk management* is used in several disciplines, with different meanings. We define *risk management* as the discipline that provides quantitative tools for the manager or decision maker to compare —or better help to compare— different alternatives to make decisions that deal with the availability of money under uncertainty.

We found a number of unexplored problems in actuarial sciences. In particular, the lack of models for governmental funds and its management. Whereas the management of private funds is well studied in the literature, we did not find an actuarial model conceived from the governmental perspective.

Although we based this research on the example of Mexico, our results can be useful for other countries in which the government plays a fundamental role absorbing losses and risk can not easily be absorbed with taxes. We develop the theory of an arrival process taking into account an early warning system and we use it to create appropriate actuarial models. Then, we formulate a stochastic optimization problem to find an investment strategy for the management of a fund from the perspective of a risk-averse government. The solution is given with the use of the Föllmer-Schweizer strategy.

Our risk-reserve model (considering the existence of an early warning system) can be useful for (re)insurance companies.

Nowadays, we are aware that natural disasters research should be done from a complex systems perspective. Natural disasters are the result of the interaction of innumerable sociological, economical and geophysical factors. This research was done under supervision of Prof. Dr. Christian Hipp within the framework of the Interdisciplinary Postgraduate Program "Natural Disasters" of the German Research Foundation (DFG) and the University of Karlsruhe (TH). This program focuses in endowing the participants with the ability to understand and evaluate the relevant relationships of natural disasters and with the ability to propose and implement adequate solutions needed for an optimal disaster management.

In Mexico, hydro-meteorological disasters are of frequent recurrence and high severity, causing enormous losses. Since recent years, there is overwhelming evidence that some hydro-meteorological processes of relevance in hydro-meteorological disasters, like rainfall intensity or river flows, exhibit multiscaling behavior. Therefore, our perception of the phenomena drastically changes depending on the sampling scale. In addition, available databases for natural disasters research are incomplete and imprecise, thus the need of multidisciplinary skills to make the best possible use of information. For this reason, the last part of our research is focused on random multiplicative cascade models for rainfall, their relationship with some hydrological models and future relevance in risk management of natural disasters. We consider that it is very important to incorporate these advances in risk management. This part of our research was supervised conjointly by Prof. Dr. rer. nat. Christian Hipp and Dr. Alin Andrei Cârsteanu[2]. The last chapter is the result of a conjoint work with Dr. Jorge Castro[3] and Dr. Alin Andrei Cârsteanu.

This book is organized as follows:

Part I: Risk management of natural disasters in Mexico

Mexico is a developing country that has experienced almost all types of natural disasters. Furthermore, it is one of the few countries that has a natural disasters fund.

We analyze the case of Mexico from a multidisciplinary perspective; we distinguish relevant relationships for our goals; and we elaborate the synthesis used as basis for the conceptual formulation.

Part II: Quantifying the economic impact of early warning systems

It is of crucial importance to incorporate the notion of early warning systems in insurance mathematics. Starting from the study presented in Part I, we developed the concept of an arrival process considering an early warning system, in order to create actuarial models. We also considered the impact of sociological factors for the actuarial modelling.

[2] Department of Mathematics at the Center for Research and Advanced Studies (CINVESTAV), Mexico City

[3] Department of Physics at CINVESTAV, Mexico City

Part III: Management strategy from a governmental perspective

We formulated a stochastic optimization problem using the results of Part II to find an investment strategy for the management of a fund from a governmental perspective, and we solved it using the Föllmer-Schweizer strategy.

Part IV: The scale-problem in rain-rate time series

Some processes of relevance in hydro-meteorological disasters, like rainfall intensity and river run-offs, require special mathematical treatment for their analysis, since their behavior changes among scales. We discussed the potential and relevance of multifractal models for rain in hydro-meteorological disaster risk management and obtained an asymptotic expression that enlarges the interpretation of an empirical parameter. Furthermore, in cooperation with Dr. Jorge Castro and Dr. Alin A. Cârsteanu, we derived an intensity-duration-area-frequency (IDAF) function for the small-scale, large-intensity limit of multifractal fields and parameterized it from tropical rainfall.

Acknowledgements

I am grateful to the German Research Foundation (DFG), the Mexican National Council of Science and Technology (CONACyT), and the Mexico's Ministry of the Environment (SEMARNAT) for sponsoring this project. I thank all the members of the Interdisciplinary DFG Postgraduate College "Natural Disasters" and of the Chair of Insurance for their help, the very pleasant work environment, and the productive discussions.

I thank Prof. Dr. Christian Hipp for supervising this research, and Prof. Dr. Karl-Heinz Waldmann for being co-referent. For his continued encouragement and co-supervising, I am thankful to Dr. Alin Andrei Cârsteanu. I would particularly like to thank Dr. Wojciech Szatzschneider for giving me the enthusiasm for research and independent thought and being my mentor over a number of years.

My thanks to Yasmin A. Flores González for improving Figures 1.1 and 3.1. I thank Marie-Claire Barba-Flores for helping make style corrections.

I have been very fortunate in having the support of my family to study abroad. I am also thankful to my friends for making my stay in Europe an incredible nice experience. Finally, I have to thank Andreas Keller for supporting my career with great patience, love and devotion.

Claudia G. Flores González
February 2006

As far as the laws of mathematics refer to reality, they are not certain; and as far as they are certain, they do not refer to reality.

Albert Einstein (1879 - 1955)

Part I

RISK MANAGEMENT OF NATURAL DISASTERS IN MEXICO

1. GENERAL INFORMATION ABOUT MEXICO

We begin this part of our research introducing the reader into the context of our study case.

1.1 Geographical location and territorial division

The official name of Mexico is *United Mexican States*. Its extremal latitudes and longitudes are 32° 43'06"N, 14° 32'27"N, 118°27'24"W and 86°42'36"W. The total surface is $1,964,375\,\mathrm{km}^2$: $1,959,248\,\mathrm{km}^2$ of continental territory and $5,127\,\mathrm{km}^2$ of islands.

Mexico is a federal republic. The country is divided in 31 federal states and a Federal District (Distrito Federal). A map of Mexico with its geographical location is shown in Fig. 1.1. Every federal state is divided in municipalities. The Federal District is divided in 16 delegations. The national territory is divided in 2443 municipalities and delegations.

In this thesis, we group the states and the Federal District in the following regions:

North: Baja California, Baja California Sur, Coahuila, Chihuahua, Durango, Nayarit, Nuevo León, San Luis Potosí, Sinaloa, Sonora, Tamaulipas and Zacatecas.

Center: Aguascalientes, Colima, Federal District, Guanajuato, Hidalgo, Jalisco, Michoacán, Estado de México, Morelos, Querétaro, Puebla, Tlaxcala and Veracruz.

South: Campeche, Chiapas, Guerrero, Oaxaca, Quintana Roo, Tabasco and Yucatán.

Fig. 1.1: Political map of Mexico, see Tab. 1.1

1 Aguascalientes	17 Nayarit
2 Baja California	18 Nuevo León
3 Baja California Sur	19 Oaxaca
4 Campeche	20 Puebla
5 Coahuila	21 Querétaro
6 Colima	22 Quintana Roo
7 Chiapas	23 San Luis Potosí
8 Chihuahua	24 Sinaloa
9 Durango	25 Sonora
10 Guanajuato	26 Tabasco
11 Guerrero	27 Tamaulipas
12 Hidalgo	28 Tlaxcala
13 Jalisco	29 Veracruz
14 México	30 Yucatán
15 Michoacán	31 Zacatecas
16 Morelos	32 Distrito Federal (D.F.)

Tab. 1.1: States of the Mexican Republic and the Federal District (D.F.), see Fig. 1.1

	1990	1995	2000
Total population	81,249,645	91,158,290	97,483,412
Population growth rate (average) [a]	2.6	2.0	1.9
Global fertility rate [b]	3.2	2.9	2.4
Crude mortality rate	5.1	4.6	4.3
Life expectation	70.8	73.6	75.3
Median age	19.0	21.0	22.0

Tab. 1.2: Demographic statistics of Mexico. Source: [Ins03]
[a] The growth rates correspond to the period 1970-1990, 1990-1995 and 1990-2000 for the years 1990, 1995 and 2000, respectively.
[b] The rate for 1990 corresponds to 1992.

Age group	Total	Men	Women
0-4	10,635,157	5,401,306	5,233,851
5-9	11,215,323	5,677,711	5,537,612
10-14	10,736,493	5,435,737	5,300,756
15-19	9,992,135	4,909,648	5,082,487
20-24	9,071,134	4,303,600	4,767,534
25-29	8,157,743	3,861,482	4,296,261
30-34	7,136,523	3,383,356	3,753,167
35-39	6,352,538	3,023,328	3,329,210
40-44	5,194,833	2,494,771	2,700,062
45-49	4,072,091	1,957,177	2,114,914
50-54	3,357,953	1,624,033	1,733,920
55-59	2,559,231	1,234,072	1,325,159
60-64	2,198,146	1,045,404	1,152,742
65-69	1,660,785	779,666	881,119
70-74	1,245,674	589,106	656,568
75-79	865,270	411,197	454,073
80-84	483,876	217,330	266,546
>85	494,706	209,654	285,052
Not specified	2,053,801	1,033,675	1,020,126
Total	97,483,412	47,592,253	49,891,159

Tab. 1.3: Demographic structure according to the national census of 2000. Source: [Ins03]

1.2 Demographic structure

The demographic structure of Mexican population is pyramidal (see Tab. 1.3). The fertility rate has a diminishing trend (see Tab. 1.2). It diminished from 5.7 in 1976 to 2.2 in 2003[1] ([Ins03]). The estimated crude mortality rate for the period 2000-2003 is 4.5 ([Ins03]).

1.3 Population distribution and Mexico City

Mexico has a problem of population distribution. Population is concentrated in few urban areas. In 2000, 18.25% of all inhabitants resided in Mexico City, the country's capital, and 30.76% in other cities with more than 5000 inhabitants. Cities like Guadalajara, Jalisco, and Monterrey, Nuevo León, have more than 3 million inhabitants each. Whereas, the population density in Baja California Sur was 5.94 inhabitants per km^2 in the year 2000, and in the Federal District (D.F.) 5562.53 inh. per km^2.

In 2000, 26% of the population resided in the northern region, 58% in the center region, and 16% in the southern region ([Ins03]).

Mexico City is the second largest city in the world. The metropolitan area covers almost all of the Federal District (D.F.) and a part of the State of Mexico.

The annual growing rate of the metropolitan area is 0.3% in D.F. and 2.4% in the State of Mexico ([AC03]).

According to the last census, the city had 17,786,983 inhabitants in 2000 ([AC03]); 48.38% of them resided in D.F. and 51.62% in the State of Mexico. The D.F., where the city center is located, represents 0.1% of the national territory and 8.83% of the population resides there.

1.4 Marginalization and income poverty

In Mexico, some regions have been historically excluded from the benefits of economical development. That is, not all population has equal access to the basic services (water, electricity, sewer system, paved roads, education). There are several degrees of marginalization in this country has led to the development of *indexes* to quantify marginalization intensity.

[1] This rate is the estimation of Conapo for the period of 2000-2003

According to the National Council of Population (CONAPO) (see [Con03]), the classification of the states and the Federal District with respect to its marginalization index for the year 2000 is the following:

Very high marginalization index: 1^{st} Chiapas (3,920,892 inhabitants), 2^{nd} Guerrero (3,079,649 inhabitants), 3^{rd} Oaxaca (3,438,765 inhabitants), 4^{th} Veracruz (6,908,975 inhabitants) and 5^{th} Hidalgo (2,235,591 inhabitants). 20% of the population reside in these states.

High marginalization index: 6^{th} San Luis Potosí (2,299,360 inhabitants), 7^{th} Puebla (5,076,686 inhabitants), 8^{th} Campeche (690,689 inhabitants), 9^{th} Tabasco (1,891,829 inhabitants), 10^{th} Michoacán (3,985,667 inhabitants), 11^{th} Yucatán (1,658,210 inhabitants), 12^{th} Zacatecas (1,353,610), 13^{th} Guanajuato (4,663,032 inhabitants) and 14^{th} Nayarit (920,185 inhabitants). 23% of the population reside in these states.

Medium marginalization index: 15^{th} Sinaloa (2,536,844 inhabitants), 16^{th} Querétaro (1,404,306 inhabitants), 17^{th} Durango (1,448,661 inhabitants), 18^{th} Tlaxcala (962,646 inhabitants), 19^{th} Morelos (1,555,296 inhabitants) and 20^{th} Quintana Roo (874,963 inhabitants). 9% of the population reside in these states.

Low marginalization index: 21^{st} State of Mexico (13,096,686 inhabitants), 22^{th} Colima (542,627 inhabitants), 23^{th} Tamaulipas (2,753,222 inhabitants), 24^{th} Sonora (2,216,969 inhabitants), 25^{th} Jalisco (6,322,002 inhabitants), 26^{th} Chihuahua (3,052,907 inhabitants), 27^{th} Baja California Sur (424,041 inhabitants), 28^{th} Aguascalientes (944,285 inhabitants). 30% of the population reside in these states.

Very low marginalization index: 31^{th} Nuevo León (3,834,141 inhabitants), 29^{th} Coahuila (2,298,070 inhabitants), 30^{th} Baja California (2,487,367 inhabitants) and 32^{th} Distrito Federal (8,605,239 inhabitants). 18% of the population reside in these states and the Federal District.

The number of inhabitants in every state corresponds to the census of 2000, and the percentages were calculated considering that the total population in 2000 was 97,483,412. More information about the marginalization index of CONAPO and its calculation is in [Con03].

We wish to stress that marginalization is not distributed equally in each state (incl. the Federal District) and municipalities (or delegations), so we can not say

	1990	1995	2000
Population that speaks a native language	6.50%	6.02%	6.20%
Rural population [a]	28.7%	26.5%	25.4%

Tab. 1.4: Population that speaks a native language and rural population. Source: [Ins03]
[a] Population living in communities with less than 2500 inhabitants.

that all the population living in a given state or municipality suffers the same degree of marginalization or is marginalized.

Chiapas has the highest marginalization index in the country and the Distrito Federal (D.F.) has the lowest. In Chiapas, 22.94% of the people older than 15 are illiterate (D.F.: 2.91%), 50.31% of the people older than 15 have not finished elementary school (D.F.: 12.16%), 19.33% reside in houses without sewer system or bathroom (D.F.: 0.44%), 12.01% have no electricity (D.F.: 0.17%), 24.99% have no drinking water at home (D.F.: 1.47%) and 40.90% reside in houses with earth-floor (D.F.: 1.34%).

Marginalization in Mexico is associated with the distribution of the population in the national territory ([Con03]). A number of small and isolated communities are dispersed in the country, making it difficult to bring them drinking water, electricity, telephone, schools and paved roads. For cost-benefit reasons, most of social politics have been focused on urban communities ([Con03]).

In 2000, 50.99% of the population resided in communities of less than 5000 inhabitants and 25.4% in communities of less than 2500 inhabitants. 61% of Chiapas population resides in communities with less than 5000 inhabitants. In Oaxaca 64%, and in Guerrero, 53.44%.

Income poverty (poverty line: 2 US dollar daily per capita) and marginalization are highly correlated. Actually, rural poverty is often characterized by a combination of low-income, unsatisfied of basic needs and lack of public services.

In Tab. 1.5, we present the indicators of the interrelation between severity of income poverty and marginalization degree in Mexico for the year 2000. The municipalities of the country where ranked according to the marginalization degree calculated by the National Council of Population (CONAPO) and the FGT index of poverty severity degree (see [Con03]).

In Mexico, as in other Latin American countries, the geographical distribution of income poverty and marginalization has been historically correlated with the distribution of native people. A study of the Economic Commission for Latin

Marginalization degree	Total	Degree of poverty severity				
		Very high	High	Medium	Low	Very low
Total	100.0%	2.7%	7.7%	8.7%	25.6%	55.3%
Very high	4.6%	1.9%	1.9%	0.6%	0.1%	- - -
High	14.0%	0.7%	5.0%	5.0%	3.2%	0.1%
Medium	12.0%	0.0%	0.8%	2.5%	8.3%	0.4%
Low	15.7%	- - -	0.0%	0.5%	10.4%	4.8%
Very low	53.7%	- - -	- - -	- - -	3.6%	50.0%

Tab. 1.5: Population of Mexico grouped by the degree of marginalization and poverty severity of the municipality of residence. Total population: 97,483,412. Source: [Con03]

America and the Caribbean (ECLAC) found that, with exception of Querétaro, the nine federal states with highest poverty levels are those with the most Native Mexicans ([ECL95]). The National Council of Population (CONAPO) also observes a high correlation between marginalization, poverty and number of natives. During centuries, this population suffered a process of displacement from their original territories to regions that have been historically excluded from the benefits of national development ([Coo83], [Con03]).

The number of Native Mexicans is not easy to estimate. The National Institute of Geography, Informatics and Statistics (INEGI) uses the language as estimation criteria (see Tab. 1.4).

According to the census of 2000, 6,044,547 inhabitants older than 5 speak a native language and about 61% resides in the following federal states:

1. Oaxaca (1,120,312), 18.53% of the total,
2. Chiapas (809,592), 13.39% of the total,
3. Veracruz (633,372), 10.48% of the total,
4. Puebla (565,509), 9.35% of the total, and
5. Yucatán (549,532), 9.09% of the total.

(see [Ins03]).

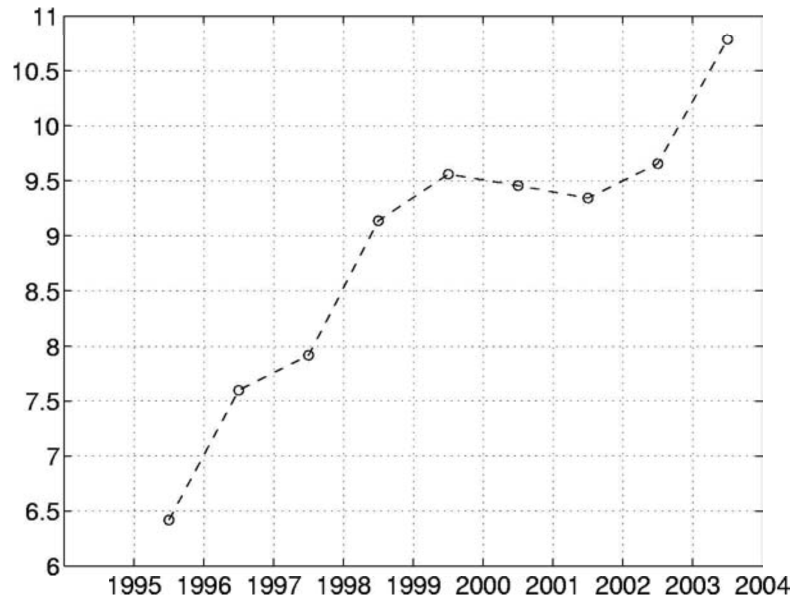

Fig. 1.2: Average market exchange rates (Mexican pesos per US dollar). Source: [Ins03]

Although this indicator is very useful as an approximation, it should be noticed that natives preserve their culture but not necessarily their language. The National Council of Population estimates no less than 12 million people ([Con03]).

1.5 Financial statistics

1.5.1 Exchange rates

The average market exchange rates for the period (1995-2003) are plotted in Fig. 1.2. The monthly average exchange rate of August 2004 is 11.3957. The daily exchange rates (FIX) used to calculate these averages are determined by the Central Bank of Mexico (Banco de México).

1.5.2 Interest rates

The data displayed in Fig. 1.3 is provided by the International Monetary Fund ([IMF03]). Annual and quarterly interest rates are arithmetic averages of monthly interest rates reported by Mexico.

Money market rate: the rate on short-term lending between finacial institutions.

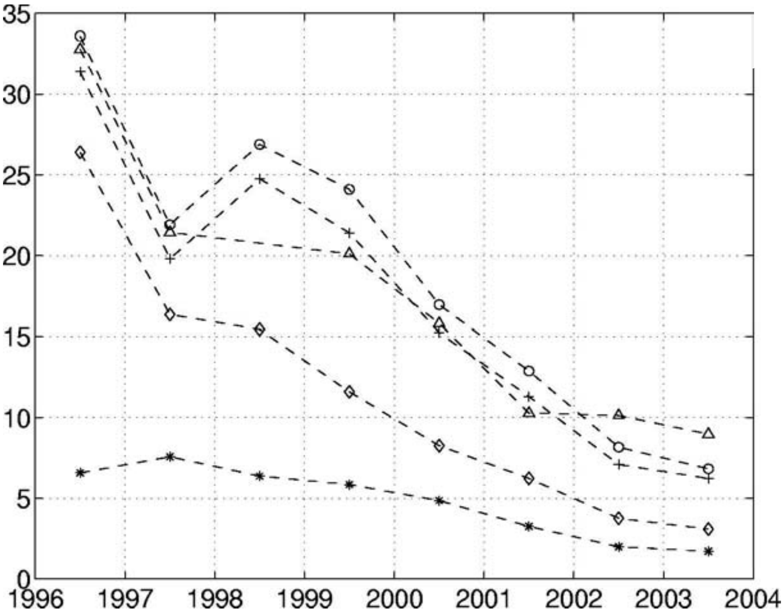

Fig. 1.3: Annual interest rates (1996-2003): money market rate (o), treasury bill rate (+), savings rate (∗), deposit rate (◇) and government bond yield (△) Source: [IMF03],[IMF04]

Treasury bill rate: the rate at which short-term securities are issued or traded in the market.

Deposit rate: usually refers to rates offered to resident customers for demand, time, or *saving deposits*.

Government bond yield: this rate represents yields to maturity of government bonds or other bonds that would indicate longer term rates.

1.5.3 Gross Domestic Product (GDP)

The GDP at purchaser prices is defined by the World Bank as "the sum of gross value added by all resident producers in the economy plus any product taxes and minus any subsidies not included in the value of the products. It is calculated without making deductions for depreciation of fabricated assets or for depletion and degradation of natural resources." ([Wor04]). The Gross Domestic Products of the years 1999, 2002 and 2003 are displayed in Tab. 1.6.

The rural economy[2] generated only 4% of the GDP in the years 2000 and

[2] It includes forestry, hunting, fishing, cultivation of crops and livestock production.

	1999	2000	2003
GDP	481.1	648.5	626.1
Annual GDP growth	3.7%	0.7%	1.3%
GDP implicit price deflator (annual growth)	15.2%	6.9%	6.5%

Tab. 1.6: Gross Domestic Product (GDP) in billions of US dollars. The exchange rate corresponds to August 2004. The GDP implicit price deflator is the ratio of GDP in current local currency to GDP in constant local currency. Source: [Wor04]

	1990	1991	1992	1993	1994
Revenue	117,710	177,372	210,446	194,813	220,382
Expenditure	137,146	149,448	164,364	190,657	225,229
Unforeseeable exp.	83,383	77,236	73,600	75,747	77,737
Deficit	19,436	-27,924	-46,082	-4,156	4,846

Tab. 1.7: Government finance (1990-1994), million of Mexican pesos. Source: [Ins03]

2003 (see [Wor04]). The value added in services represented 69.6% of the GDP in 2003 and the remaining 26.4% corresponds to the industrial economy (see [Wor04]).

The economy of the *Center* region generates 60% of the GDP, whereas 10% comes from the south of the country (see [AC03]). The remaining 30% is generated by the north region.

1.5.4 Government finance

A summary of annual balances of the government for the period (1990-2003) is given in Tabs. 1.7, 1.8 and 1.9. Within this period, only in 1991 and 1992 was a surplus observed. Nevertheless, the total balances of 1991, 1992 and 1994 include the extraordinary revenues from the privatization of banks and telephone services. The years of the so-called "Tequila" crisis were 1994 and 1995.

1.6 Insurance sector in Mexico

This section is based on information provided by the Swiss Re ([Sig02], [Sig04]).

In 2003, the premium volume of the insurance sector in Mexico was 10,920 USD million; 6,690 USD million correspond to non-life insurance premium vol-

	1995	1996	1997	1998	1999
Revenue	280,144	392,566	503,554	545,176	674,348
Expenditure	294,926	404,045	546,726	612,475	754,389
Unforeseeable exp.	124,950	171,673	219,246	219,781	285,149
Deficit	14,781	11,479	43,172	67,300	80,041

Tab. 1.8: Government finance (1995-1999), million of Mexican pesos. Source: [Ins03]

	2000	2001	2002	2003
Revenue	868,268	939,115	989,353	1,133,184
Expenditure	952,083	996,951	1,124,451	1,233,141
Unforeseeable exp.	362,681	365,177	379,348	400,926
Deficit	83,815	57,836	135,098	99,957

Tab. 1.9: Government finance (2000-2003), million of Mexican pesos. Source: [Ins03]

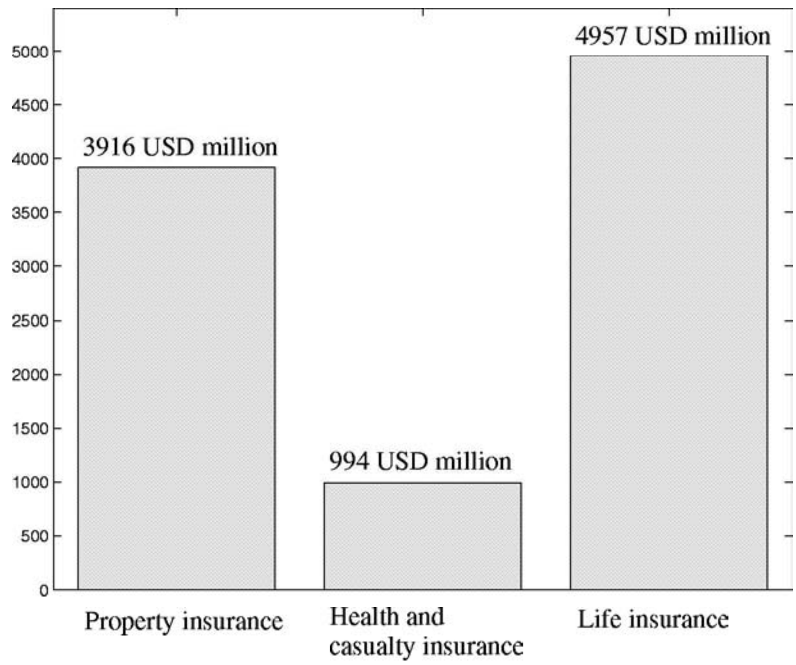

Fig. 1.4: Premium volume in Mexico, year 2000. Source: [Sig02]

umes. In the same year, the share of world market was 0.37% and the country was ranked in place 27. The premium volume of Mexico represented 26% of total premium volume of Latin America.

Three years before, in 2000, the premium volume of the insurance sector in Mexico was 9,866 USD million. This represented 25.3% of the total premium volume of Latin America (39,000 USD million). Nevertheless, the insurance market in Latin America is very small. Its premium volume represents 1.6% of the total premium volume worldwide. Although the technical results were improved year by year, the investment results got worse as a consequence of the "tequila" crisis, the high interest rates and inflation. In 2000, for the first time, the total result was negative.

Mexico has a high exposure to natural disaster risks. Therefore, indemnity insurance depends on the international reinsurance capacity. The penetration of non-life insurance[3] in Mexico was 0.9% in 2000 and 1.10% in 2003. The non-life insurance density[4] was 50 in 2000 and 65.3 in 2003.

[3] premiums in % of GDP in the respective year

[4] premiums per capita in USD in the respective year

2. NATURAL DISASTERS RISKS IN MEXICO

Mexico is a country which has to deal with several natural disaster risks: floods, hurricanes, heavy rain, drought, frost, forest fires, landslides, earthquakes, tsunamis and vulcanism. A list of the largest natural disasters in Mexico (1900-1999) is displayed in Tabs. 2.2, 2.3, 2.4 and 2.5 (at the end of this section).

An overview of the incidence of natural disasters in Mexico that caused more than 100 deaths or extraordinary economic losses in the period (1900-1999) is shown in Fig. 2.1. We considered the drought periods as a single disaster, as well as the two volcanic eruptions of 1982. We estimated that the mean number of major natural disasters per year is 0.86 in this period. It is important to notice that this value is only a reference because of the imprecision of the data. However, nearly one major natural disaster per year reflects already the size of the problem, and we should also consider that the incidence of natural disasters causing less damage is higher, as we can see in the information published in [CEN01]. This underlines the importance of developing strategies for the management of natural disasters risks in Mexico.

The lack of reliable statistical information about the number of victims and economic losses from natural disasters in Mexico in the past, made it difficult to develop risk management strategies. The estimation of the number of fatalities of Mexico City's earthquake in 1985, for example, disagrees considerably from source to source. The publication *Prontuario de contingencias del siglo XX mexicano* (Mexican Contingencies Compendium of the 20^{th} Century) says that 4,287 people died, and 37,000 lost their homes or were injured ([CEN01]). The German IDNDR[1] Committee ([CEN01]) and Munich Re ([Mun00]) use the estimation of 10,000 victims. The Swiss Re ([Sig99]) estimates that the earthquake of 1985 in Mexico City caused 15,000 fatalities (dead and missing).

In the case of historical economical losses, the error margin is also considerable. In Tab. 2.1, we present the data compendium by D. Bitrán. Although this

[1] International Decade for Natural Disaster Reduction

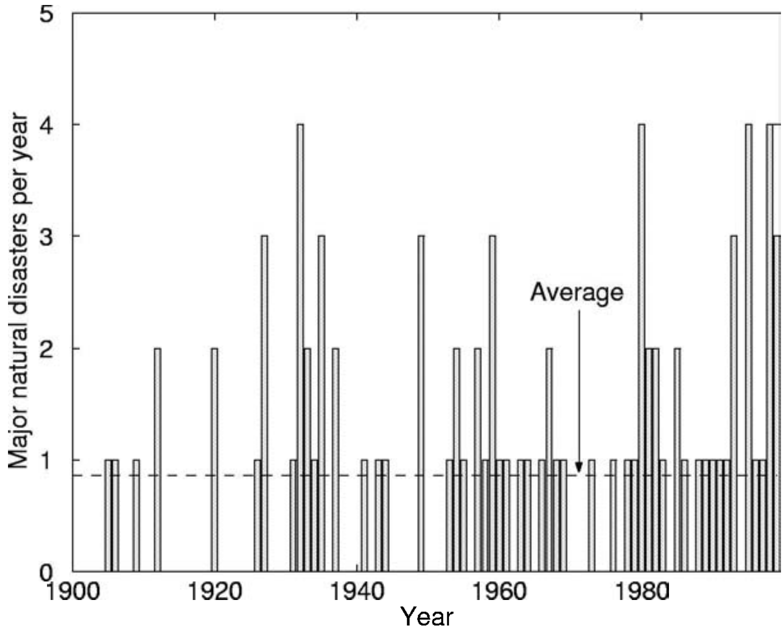

Fig. 2.1: Incidence of major natural disasters in Mexico (1900-1999).

data comes from disperse information, and estimations were obtained using different methodologies, Bitrán's compendium is one of the most complete works available ([CEN01]).

After Mexico City's earthquake of 1985, the need to create an institution devoted to the study of technical aspects of disaster prevention was recognized. As a response, the Mexican government established the National Civil Protection System (SINAPROC). The National Center for Disaster Prevention (CENAPRED) was created in September 1988, with the economic and technical support of the Japanese government. The CENAPRED was inaugurated in May 1990. This institution is subordinated to the Ministry of the Interior (SEGOB). Its main responsabilities are research, education and information about disaster prevention. The National University (UNAM) collaborates with SINAPROC and CENAPRED through academic research, and it participates in the technical consultant committee of CENAPRED.

Year	Event	Fatalities	Losses
1980	droughts in the north and others	3	310.4
1981	n.a*	n.a	n.a
1982	hurricane “Paul”, eruption of “Chichonal” volcano and others	50	314.0
1983	n.a	n.a	n.a
1984	explosion (storage tank) “San Juanico” and others	1000	26.3
1985	earthquake in Mexico City; heavy rainfalls in Nayarit and other	about 5000	4159.8
1986	fires	0	1.5
1987	snowfalls	6	0.3
1988	hurricane “Gilbert”, fire in oleoduct and others	692	2092.9
1989	fires	0	648.0
1990	hurricane “Diana” and others	391	94.5
1991	explosion (petroleum plant) and others	11	167.5
1992	sewer-line explosions in Guadalajara and others	276	192.5
1993	hurricane “Gert” and others	28	125.6
1994	droughts and others	0	3.8
1995	hurricanes “Opal” and “Ismael” earthquake in Guerrero-Oaxaca, explosion (gas pipeline) and others	364	689.6
1996	frosts and others	224	5.3
1997	hurricane “Pauline” and others	228	447.8
1998	heavy rains in Chiapas and others	199	2478.8
1999	earthquakes and floods	313	1100

Tab. 2.1: Economic losses of disasters in Mexico in USD million (1980-1999). The exchange rates used to convert the losses in Mexican pesos to USD correspond to the year of occurrence. Source: [CEN01]
* n.a.=not available

Year	Event	State
1905	flood	Guanajuato
1906	flood	Jalisco
1909	flood caused by hurricane	Nuevo León
1912	flood earthquake	Querétaro México
1920	earthquake and landslides [a]	Veracruz
1926	hurricane	Veracruz, Yucatán and Campeche
1927	two earthquakes flood	Baja California Michoacán
1931	earthquake	Oaxaca and D.F.
1932	earthquake earthquake and tsunami[a] flood	Colima and Jalisco Colima Coahuila
1933	hurricane hurricane	Tamaulipas Tamaulipas, Tabasco and Veracruz
1934	flood	Coahuila
1935	heavy rains and landslides [a] hurricane	D.F. Veracruz
1937	heavy rains and landslides [a]	Michoacán
1941	earthquake	Colima, Guerrero, Jalisco and Michoacán
1943	birth of “Paricutín” volcano and lava flow	Michoacán
1944	heavy rains	Chihuahua and Durango
1949	flood heavy rains hurricane	Sinaloa and Sonora Hidalgo Sinaloa

Tab. 2.2: Natural disasters in Mexico that caused more than 100 deaths or extraordinary economic losses (1900-1950). Source: [CEN01]
[a] concatenated events.

Year	Event	State
1953	hurricane	Guerrero
1948-1954	drought	north and center regions
1954	landslide	Jalisco
1955	hurricanes "Gladys", "Hilda" and "Janet" [a]	Veracruz, San Luis Potosí, Yucatán, Quintana Roo and Tamaulipas
1957	earthquake hurricane	D.F., Guerrero and Oaxaca Sinaloa
1958	flood	Michoacán
1959	landslide flood hurricane	Veracruz Tabasco Colima and Jalisco
1960	flood	Sinaloa and Sonora
1961	hurricane "Tara"	Guerrero
1963	flood	Tabasco
1960-1964	drought	north and center regions
1966	hurricane "Inés"	Tamaulipas
1967	hurricane "Beulah" hurricane "Katrina"	Tamaulipas and Nuevo León Guerrero, Nayarit and Sonora
1968	hurricane "Naomi"	Colima, Jalisco, Sinaloa, Sonora, Durango, Coahuila and Chihuahua
1969	flood	Veracruz and Oaxaca

Tab. 2.3: Natural disasters in Mexico that caused more than 100 deaths or extraordinary economic losses (1951-1970). Source: [CEN01]
[a] the hurricanes occurred consecutively.

Year	Event	State
1973	earthquake	Puebla, Oaxaca and Veracruz
1976	hurricane “Liza”	Baja California Sur and Sonora
1970-1978	drought	north and center regions
1979	earthquake	D.F. and Guerrero
1980	flood heavy rains hurricane “Allen” earthquake	Baja California Baja California Tamaulipas Oaxaca and Puebla
1981	flood flood	Veracruz and Guerrero Sinaloa
1982	hurricane “Paul” two volcanic eruptions[a]	Sinaloa Chiapas
1983	flood	México
1985	earthquake heavy rains	D.F. and Michoacán Nayarit
1986	flood	Veracruz
1988	hurricane “Gilbert”	Yucatán, Quintana Roo, Campeche, Nuevo León, Tamaulipas and Coahuila
1989	forest fire	Quintana Roo
dec. 1990- jan. 1991	hurricane “Diana” flood	Veracruz and Hidalgo Sonora, Baja California Sur, Sonora, Sinaloa and Chihuahua
1991	flood	Zacatecas
1992	flood	Nayarit
1993	flood hurricane “Gert” flood	Baja California Veracruz, Hidalgo, Tamaulipas and San Luis Potosí Baja California Sur

Tab. 2.4: Natural disasters in Mexico that caused more than 100 deaths or extraordinary economic losses (1971-1994). Source: [CEN01]
[a] the eruptions of “Chichonal” volcano occurred on March 28th and April 4th.

Year	Event	State
1995	hurricane “Ismael” hurricane “Opal” earthquake earthquake	Sonora and Sinaloa Veracruz, Tabasco, Yucatán, Quintana Roo and Campeche Guerrero and Oaxaca Colima and Jalisco
1993-1996	drought	north and center regions
1997	hurricane “Pauline”	Oaxaca and Guerrero
1998	hurricane“Isis” heavy rains hurricane “Mitch” forest fire	Sonora and Sinaloa Chiapas Tabasco, Yucatán, Campeche and Quintana Roo Oaxaca, Chiapas and Durango
1999	earthquake earthquake heavy rains	Puebla and Oaxaca Oaxaca Puebla, Hidalgo, Veracruz, Tabasco and Oaxaca

Tab. 2.5: Natural disasters in Mexico that caused more than 100 deaths or extraordinary economic losses (1995-1999). Source: [CEN01]

3. MEXICO'S FUND FOR NATURAL DISASTERS (FONDEN)

Mexico's Fund for Natural Disasters (FONDEN[1]) is the name of the financial mechanism that Mexico's federal government uses to assign and transfer budget resources to the dependencies and entities of the federal public administration in case of a natural disaster. We define natural disaster as the natural phenomena or phenomenon, whether concatenated or not, which occur within time and space limits, are the cause of severe damage and whose recurrence is difficult or impossible to foresee[2].

3.1 History

In order to reduce the country's vulnerability to the economic impact of natural disasters and to support rapid recovery when they occur, the Mexican government established in 1996 the Mexico's Fund for Natural Disasters (FONDEN).

The first version of FONDEN's Mandate ([Min00b]) was published on February 29^{th}, 2000. Months later, this mandate was modified in order to allow the use of FONDEN's resources to avoid the irreparable loss of the cultural patrimony of the country [Min00a].

On March 31^{st}, 2001, a second version of FONDEN's mandate ([Min01]) was published in the Official Journal of the Federation. One year later, on March 15^{th} 2002, a new version of the Mandate was issued ([Min02]) and it nullified the previous one. The current version of FONDEN's Mandate was published on May 23^{rd}, 2003 [Min03].

[1] Fondo de Desastres Naturales

[2] This definition is a translation of "desastre natural: el fenómeno o fenómenos naturales concatenados o no que cuando acaecen en un tiempo y espacios limitados, causan daños severos no previsibles y cuya periodicidad es difícil o imposible de proyectar" ([Min03], Chapter I, §1, par. XII)

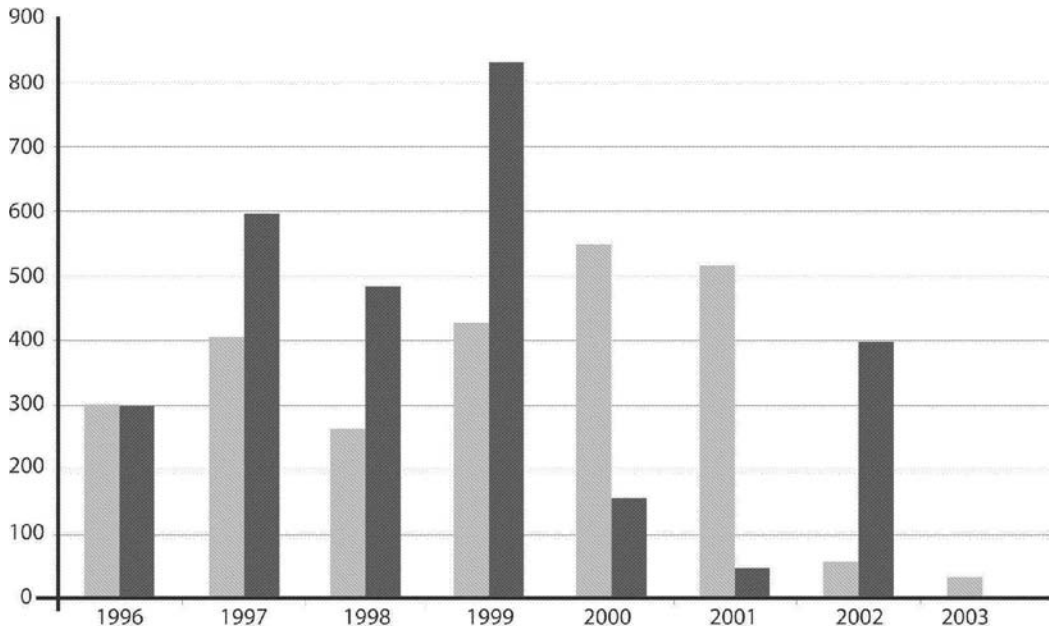

Fig. 3.1: FONDEN budgets (light-colored columns) versus utilization (dark-colored columns) in USD Million equivalent (1996-2003). Source: [Mex03].

3.2 FONDEN's goals

Through FONDEN, the Mexican government provides resources to mitigate the effects of natural disasters whose magnitude surpass the capacity of local governments and public federal entities to help the victims, and to repair damage. It is a last-resort fund that complements the efforts of local governments along with the National System for Civil Protection (SINAPROC) and other public institutions with programs or obligations directly related with the reaction after a natural disaster.

According to FONDEN's Mandate [Min03], the federal government assigns economic resources to

1. support the potential victims in case of imminent danger;

2. support, in complementary form and under the restrictions specified in

[Min03], the reparation of damage in public goods;

3. support, complementary to the existent programs, the fight of forest fires and the rehabilitation of the affected zones;

4. mitigate damage to the houses of those with low-income victims who are unable to purchase property insurance;

5. partially compensate the income-losses of victims providing resources for the implementation of temporary employment programs;

6. consolidate, restructure or, if it is the case, rebuild the archeological, artistic and historical monuments that satisfy the specifications established in [Min03];

7. provide temporary aid to the dependencies and semigovernmental entities for the reparation of insured infrastructure before they receive the insured sum; and

8. provide resources for the acquisition of specialized equipment and other goods in order to react optimally in case of emergency or natural disaster, and for its installation.

3.3 FONDEN's management

Within the federal financial statement, FONDEN is accounted as unforeseeable expenditure (Ramo 23). The Ministry of Finance and Public Credit (SHCP) is responsible of managing post-disaster resources, whereas the Ministry of the Interior (SEGOB) manages the resources to attend emergencies.

The resources administrated by SHCP are divided into two parts: budget and trusteeship. FONDEN's trusteeship acts as a reserve and it is constituted with the annual surpluses of FONDEN's budget.

In case of imminent danger or high probability of disaster, SEGOB can declare a situation of emergency and provide resources to attenuate the effects of the possible disaster. From FONDEN's budget for the fiscal year 2004, 42.86% are resources for prevention.

FONDEN's assistance should be provided within a budget established at the beginning of every fiscal year. Almost every year since its creation, FONDEN's resources have been insufficient to meet all the government obligations established in FONDEN's Mandate, see Fig. 3.1. For the fiscal year 2004, the authorized budget was 350 million of Mexican pesos (about 34.43 USD million).

The process of budgetary planning of a fund like FONDEN is complex and often politically difficult [Fre02]. In 1998, for example, six changes to the budget were required to provide additional funds for natural disasters. The same year, about 270 USD million[3] were authorized and nearly 500 USD million[4] were required [Sub99]. When FONDEN's resources are exceeded, the government reallocates funds within the overall federal budget ([Guy00]). However, as pointed out in Levis & Murdock (1999), "Shifting resources in response to disaster needs disrupts fragile compromises formed to create initial budgets" (see [Fre02]).

From the period 1996-1999, 70% of FONDEN's budget funded losses for heavy rains and hurricanes, 19% for drought and rimes losses, and 10% for earthquakes. Fire accounted for 1% of FONDEN's payments (see [Guy00], [FM01]). In Table 3.1, we find more details of the FONDEN's funded losses (1996-1998) by type of disaster and state.

We wish to stress that the three states that received more help from FONDEN in the period 1996-1998 were Chiapas, Guerrero and Oaxaca. As we mentioned before, these states have very high marginalization rates. Most of the funded losses were for heavy rains and hurricanes. These states are also high-exposed to earthquakes ([CEN01]).

[3] 2558.6 million of Mexican pesos of the year 2000

[4] 4175 million of Mexican pesos of the year 2000

Federal state	Total	Droughts and rimes	Heavy rains and hurricanes	Earth-quakes	Fires
Total	9210,9	2844,3	6230,1	19,4	117,2
1 Aguascalientes	11,1	11,1	- - -	- - -	- - -
2 Baja California	159,2	13,6	145,7	- - -	- - -
3 Baja Cal. Sur	162,6	4,3	158,3	- - -	- - -
4 Campeche	2,7	2,7	- - -	- - -	- - -
5 Coahuila	370,6	348,0	22,5	- - -	- - -
6 Colima	11,9	0,4	11,5	- - -	- - -
7 Chiapas	2787,2	77,5	2684,1	- - -	25,6
8 Chihuahua	352,6	342,3	- - -	- - -	10,2
9 Durango	382,3	367,3	14,9	- - -	- - -
10 Guanajuato	137,8	78,5	59,2	- - -	- - -
11 Guerrero	1942,7	84,4	1858,3	- - -	- - -
12 Hidalgo	53,8	53,8	- - -	- - -	- - -
13 Jalisco	67,4	64,5	2,9	- - -	- - -
14 México	89,7	31,0	47,7	- - -	11,0
15 Michoacán	92,4	47,5	- - -	19,4	25,6
16 Morelos	13,7	0,9	- - -	- - -	12,8
17 Nayarit	7,5	7,5	- - -	- - -	- - -
18 Nuevo León	131,6	99,6	- - -	- - -	32,0
19 Oaxaca	1210,1	103,3	1106,8	- - -	- - -
20 Puebla	77,5	77,5	- - -	- - -	- - -
21 Querétaro	31,9	31,9	- - -	- - -	- - -
22 Quintana Roo	7,5	7,5	- - -	- - -	- - -
23 San Luis Potosí	125,4	125,4	- - -	- - -	- - -
24 Sinaloa	270,7	159,4	111,3	- - -	- - -
25 Sonora	201,4	201,4	- - -	- - -	- - -
26 Tabasco	14,2	14,2	- - -	- - -	- - -
27 Tamaulipas	296,1	289,2	6,9	- - -	- - -
28 Tlaxcala	42,7	42,7	- - -	- - -	- - -
29 Veracruz	53,9	53,9	- - -	- - -	- - -
30 Yucatán	0,6	0,6	- - -	- - -	- - -
31 Zacatecas	102,3	102,3	- - -	- - -	- - -

Tab. 3.1: FONDEN's funded losses (1996-1998) in millions of Mexican pesos for the year 2000. Source: [Sub99]

4. RISK MANAGEMENT OF NATURAL DISASTERS IN MEXICO

In developing countries like Mexico, the government plays a fundamental role absorbing the losses of natural disasters. The low insurance density, the poverty and the macroeconomic problems are some causes of the low participation of private capitals in the risk management of natural disasters.

The Mexican government does not satisfy the risk-neutral assumption usually applied for governments, because losses can not be easily internally absorbed with tax revenue (see [Guy00], [FM01]). The loss of Mexico City's earthquake of 1985, for example, was equivalent to 14% of tax revenue ([FM01]). In addition, the government deficit has been usually positive in the period 1990-2003 (see Subsection 1.5.4).

After analyzing the information presented in Secs. 1.4 and 1.5, we can only corroborate the risk-averse hypothesis in the case of the Mexican government.

A number of recommendations have been made to the Mexican government for the management of FONDEN from an economical point of view (see e.g. [Guy00], [FM01] and [PV99]), but besides estimating occurrence probabilities and mean losses, we did not find an actuarial study about FONDEN.

We can classify strategies for financing reconstruction in ex-ante and ex-post disaster (see [WP02]). Traditional examples of governmental ex-post strategies are: taxes, borrowing and aid (see [WP02]). Among ex-ante financing tools we have:

1. reserve funds,
2. insurance, and
3. contingent credit.

A summarized cost-benefit analysis of these strategies is shown in Tab. 4.1. Certainly, FONDEN has more obligations than financing reconstruction, but the

	Reserve fund	Insurance	Contingent credit
Cost before event	Contribution during years before event	Premium during years before event	Holding fee during years before event
Benefit after event	Only reserved funds and interest available	All needed funds available	All needed funds available
Cost after event	None	None	Additional debt service, reduction in ability to take out future debt
Incentive for mitigation?	Only if risk is known	Yes	No

Tab. 4.1: Costs and benefits of ex-ante financing tools. Source: [WP02]

above mentioned ex-ante strategies can also be explored in our case.

As pointed out in [WP02], ex-ante risk management demands the understanding of probability and this is a complication for some policy makers. If the future event does not occur, they sometimes perceive the money spent for the emergency as lost. Intuitively, we guess that money for emergencies should have some sense. How could we quantify the effect of emergencies? Which technical justification could we present to policy makers for the allocation of emergency resources? We did not find an actuarial model that could help us solve this question.

It can also happen that policy makers perceive a surplus as a signal that they can save money for the next year, because the budget was "too high". As experts in quantifying risks, actuaries understand that this is not so. Nevertheless, whereas the justification of building reserves in the insurance industry is well studied and understood, we did not find a mathematical model useful for justifying the existence of reserves from the governmental perspective.

After a discussion in an internal meeting at the Mexican Ministry of Finance (SHCP) on January 10th, 2003, the information given to us was that, at present, the Mexican government would not like to base the management strategy for FONDEN in acquiring debt. So, we decided to leave out the possibility of borrowing for this research. This option can be explored in further research.

If we assume that the government is risk-averse, spreading risk among taxpayers is not a possibility. In the case of aid, we hope to use this resource only if everything else fails!

If we do not want to manage the fund by borrowing money, then we can consider

- investment in the capital markets;
- alternative risk transfer instruments;
- Excess-of-Loss (XL) reinsurance; and
- Stop-Loss reinsurance.

After analyzing all these possibilities, we decided to focus our research in developing a basis model considering investment in the capital markets and Excess-of-Loss (XL) reinsurance. We leave the other possibilities for further research.

Although we know that one premise for FONDEN's management in reality is not to invest in the stock market, we found that for risk-averse governments this could be a good alternative in combination with risk-transfer instruments. So, we decided to explore it.

We did not consider alternative risk transfer instruments in this research, because we think that before recurring to them we should first identify our basic risk processes.

In the private industry, it is theoretically allowed to allocate funds to the reserve at every moment. In the case of Mexico's governmental fund this is not so. The moment and the amount of the contributions are restricted. The fund is linked to a trusteeship which has the function of reserve. If not all the money was disbursed at the end of the fiscal year, this residual will be transferred to the reserve. The transfer of budget's surpluses is the only valid way to build it.

Given the difficult economic situation in developing countries, it is not possible to ask for a large amount of money without a very well founded explanation about the estimation of the initial budget. We conclude that what is needed is the development of actuarial techniques for the estimation of the minimum budget in a governmental framework.

We realized that the above restrictions for the budget and the reserve make a fundamental difference between governments and companies. This should be included in the basis for the development of actuarial mathematics applied to governmental questions in the future. Also, the difference is so relevant, that applying usual insurance mathematics to give advice to governments can be misleading.

For example, we found that estimating the budget that minimizes ruin is inadequate in a governmental context subject to the above mentioned restrictions.

In the case of Mexico, as it may be for many other governments, improving the budget planning in order to hedge a predetermined contribution to the natural disasters fund's reserve is more important than avoiding ruin along the year.

As we mentioned before, FONDEN's rules of operation establish that in case of high probability of a natural disaster or imminent danger, the local governments can ask for a declaration of state of emergency to obtain resources faster. Hence taking measures to attenuate the effects of a possible disaster. For this reason, it becomes necessary the development of a mathematical model considering this type of outcome.

In our model we distinguish two types of natural disasters: those with warning, and those without warning. We assign costs for the false warnings and we consider the positive effect of an effective warning.

Finally, we wish to emphasize that, according to our study, the temporary unavailability of emergency resources, as well as the positive effect of an effective warning, have a relevant influence to the budgetary planning, the transfer of risks and the determination of a management strategy [Flo03].

Part II

QUANTIFYING THE ECONOMIC IMPACT OF EARLY WARNING SYSTEMS

5. EARLY WARNING SYSTEMS

We define *early warning* as a warning arriving in time before an imminent natural hazard (see [PM01]). The basic structure of an early warning system has three consecutive phases:

i) forecasting,

ii) warning and

iii) reaction.

(see [PM01]). In Fig. 5.1, we show the main components of an early warning system in a schematic representation.

The *forecasting phase* is based on a scientific and technical analysis of data from measurement stations. Its goal is to give a trustworthy forecast of natural phenomena in magnitude, time behavior and location. If a natural phenomenon, which could have catastrophic consequences is forecasted, a warning is issued.

The top priority of forecasting models is the prediction of the time between the warning and the occurrence of the natural phenomenon (t_{crit}). The precise prediction of the event magnitude and its future progression is in many cases not so important as estimating t_{crit}.

From the predictions of t_{crit}, we can have an idea of how much time we have for the warning and the reaction phases by type of disaster. For example, droughts and volcanic eruptions can be foreseen with months of anticipation; flood warnings usually happen within 24 hours of anticipation; and earthquake predictions within seconds of anticipation (see [PM01]).

There are a variety of forecasting methodologies. Some of them are essentially deterministic (e.g. forecasting volcanic eruptions) and others are based on the extrapolation of a continuous time-dependent process (e.g. flood forecasting).

During the *warning phase*, information is circulated. The success of this phase depends on technical, social and political factors. Political problems can arise when deciding if endangered populations should be warned. Miscommunication between forecasting experts and authorities should not be underestimated, as there can be serious consequences, like in the case of the volcanic eruption of the Nevado del Ruiz, Colombia, in 1985. The warning of geologists was not taken seriously and approximately 25000 people died (see [PM01]).

Important decision criteria to spread a warning or not is the margin of error of the forecast, the possible consequences of the natural event and the economic cost of the reaction phase. Actually, it is difficult for decision makers to evaluate the benefits of spreading a warning. Too many false alarms can diminish the reliability of official announcements.

If authorities decide to spread the warning, endangered populations should be informed as quickly as possible. Information and communication technology can facilitate this task; but however, in some countries like Mexico (see Sec. 1.4), there are regions without access to these developments.

The *reaction phase* is dominated by sociological factors. This is the time to carry out emergency plans. In many countries, organizational and administrative problems often impede a working emergency management. Other problems, often underestimated, are distortions in the risk perception of natural disasters, ignorance about how to react in case of an emergency, difficulties to understand what experts are trying to communicate, and mistrust in the authorities (civil, military or governmental). In addition, poverty, marginalization, war, delinquency, bands of guerrillas, terrorism and epidemics can also complicate the emergency management.

As an example, we explain the basic ideas of earthquake early warning systems.

5.1 Earthquake early warning systems

In spite of the short time period for the warning and the reaction phases, in some cases it is possible to take actions for loss prevention. For example: the shutdown of computers, disk drives, high precision facilities, airport operations, electronic facilities, high energy facilities, gas distribution, refineries, nuclear power plants and water pipelines; the rerouting of electrical power; stopping or slowing trains and subways; alerting hospital operating rooms; the opening of fire station doors; starting emergency detonators; leaving elevators in a safe position; shutting off oil pipelines; issuing audio alarms, and moving to a safe state in nuclear facilities (see [WB04]). Some of these measures have been implemented or are under

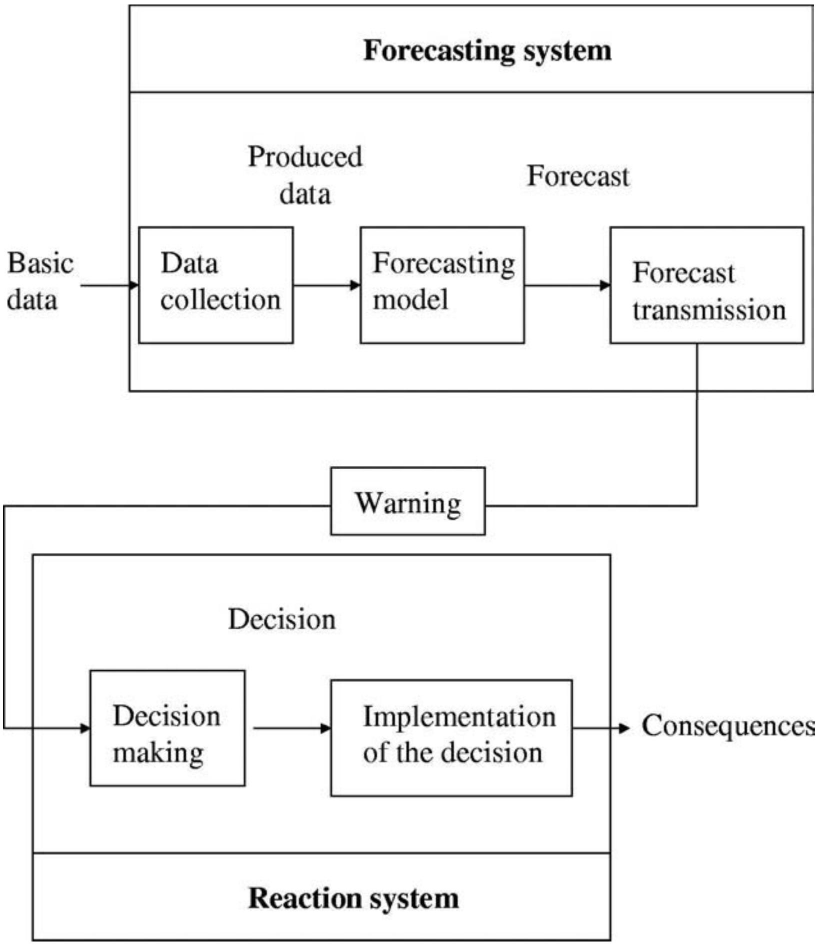

Fig. 5.1: Diagram of a warning system. Source: [PM01]

consideration in Japan, Mexico, Taiwan, California, Romania, Turkey and other countries ([WB04]).

Mexico has a public earthquake early warning system ([MW04]). It was implemented because was foreseen that an earthquake of magnitude greater than M7, with epicenter in the coasts of Guerrero, between Acapulco and Zihuatanejo, could occur. This event would have catastrophic consequences for Mexico City.

The Mexican Seismic Alert System (SAS) transmits a warning to Mexico City if an earthquake is forecasted at the above mentioned coast segment. An alert is technically possible, because the warning issued in Guerrero is transmitted to different points in Mexico City using electromagnetic waves and they travel faster than seismic waves. The distance between the Guerrero subduction zone and Mexico City is about 320 km (see the map of Mexico of Fig. 1.1). Therefore, the warning time lasts about 60-70 seconds ([Cen04], [MW04]).

The warning is spread out automatically depending on the magnitude of the forecasted earthquake:

Public alert: seismic energy, measured at the beginning of an undergoing earthquake, produces a forecast for an earthquake of magnitude greater than M6.

Preventive or restricted alert: seismic energy, measured at the beginning of an undergoing earthquake, produces a forecast for an earthquake of magnitude below M6.

Public alarms are mainly transmitted by radio and television. The alarm is also transmitted to schools, the subway and some buildings. Take into consideration that the number of alerted people varies depending on the time of the day in which the alert is issued.

To conclude this chapter, we wish to stress that the success of every early warning system not only depends on a good forecasting, but also on the capacity to reach authorities and endangered population as soon as possible, and on the decisions following the alert.

6. QUANTIFYING THE ECONOMIC IMPACT OF EARLY WARNING SYSTEMS

Within the last years, substantial progress in early warning systems for some types of natural hazards has been reached. These models are subject to constant improvement and are already fundamental for damage reduction. It is of crucial importance to incorporate these advances into insurance mathematics. This research presents a first step towards this direction.

In some countries, private and public sectors share natural disaster risks. However, to model this partnership mathematically, we need models for both parts. With this motivation, we developed a model for the reserve of an insurance company and for a governmental fund for natural disasters considering an early warning system. We conceived simplified arrival processes for expenditures (governmental fund) and claims (reinsurance company) using the information that we identified as fundamental.

In Part III, we use our model to find an optimal management strategy for the above mentioned governmental fund using financial mathematics.

6.1 Information problem

The first step was finding out what information regarding warning systems is essential for our goals. Observing that the natural hazard's forecasting and anticipating economic needs under uncertainty are two problems of different nature.

As we explained above, the natural hazard's forecasting intends to predict the occurrence of it in the near future. For economic planning under uncertainty, we need mathematical models to describe *economic damage* due to natural disasters stochastically. We also wish to stress that not all natural hazards become natural disasters.

We identify two main arrival processes involved in our problem: the early warnings (ex-ante) and the claims (ex-post). The main challenge for the development of a parsimonious mathematical model was that both processes are dependent and not simultaneous.

We explored different possibilities for the modelling, some of them focused on t_{crit} and the dependence between the arrivals of warnings and natural disasters. We modelled the warning system as a continuous stochastic model that should generate different cases: false warning, non-warned disaster, not enough time to react, the error $t_{\text{crit}} - t_{\text{obs}}$, where t_{obs} is the observed time between the warning and the disaster. Additionally, we explored the convenience of modelling the economic benefit of a hitting warning as a separate random variable.

As a main result, we conceived a simplified model that captures the essence of our problem with a minimum of information. We realized that, if t_{crit} is small enough, we can exploit performance statistics of early warning systems for the actuarial modelling.

The main idea is to take advantage of the only fact we have for sure: every warning system is fallible. From this axiom, we deduce that we have essentially three different types of errors:

Type I a warning was issued and nothing happened ($\mathbb{P}$[Error type I] $= \alpha_1$),

Type II a disaster occurred and no warning was issued ($\mathbb{P}$[Error type II] $= \alpha_2$),

Type III a warning was issued and a disaster occurred, but the system failed in the warning or the reaction phase ($\mathbb{P}$[Error type III] $= \alpha_3$).

In order to estimate the probability of an error type III (α_3) from data, we require the development of standard criteria for the classification of events in order to generate suitable data bases. This is a topic for further research in sociology. Up to now, data bases for natural disasters are very imprecise and there are no standards to structure them.

We can estimate α_1 and α_2 from statistical information. If we don't have enough information available or if the information is too imprecise, we recommend generating synthetic data bases.

6.2 Arrival process of natural disasters

Assume that the arrival process of claims corresponding to the type of natural disaster covered by the fund $\{N(t),\ t \geq 0\}$ is compound Poisson with rate $\lambda > 0$. Then the inter-arrival times are given by the sequence of independent identically distributed random variables (i.i.d.r.v.) (T_i), $i = 1, 2, \ldots$. The probability of n claims within the time interval $(0, t]$ is $P(N(t) = n) = \frac{(\lambda t)^n e^{-\lambda t}}{n!}$ and $\mathbb{E}[N(t)] = \lambda t$.

The sequence of i.i.d.r.v. $(T_i)_{i \geq 1}, T_i \sim \exp(\lambda)$ is the sequence of inter-arrival times of $N(t)$. Let $(W_i)_{\{i \geq 0\}}$ be the sequence of arrival times $W_n = \sum_{i=1}^{n} T_i$. In other terms, $W_n = \inf\{t \geq 0,\ N(t) = n\}$.

The probability density of W_n is given by

$$f_{W_n}(t) = \lambda e^{-\lambda t} \frac{(\lambda t)^{n-1}}{(n-1)!},\ t \geq 0. \tag{6.1}$$

Then, $W_n \sim \Gamma(n, \lambda)$ and $\mathbb{E}[W_n] = \frac{n}{\lambda}$.

The number of claims from warned disasters in $(0, t]$ is $N^*(t) = \sum_{i=1}^{N(t)} U_i$, where $U_i \sim$ Bern$(1 - \alpha_2)$ is defined by

$$U_i = \begin{cases} 1 & \text{if a warning was issued for the disaster} \\ & \text{that originated the claim,} \\ 0 & \text{otherwise.} \end{cases} \tag{6.2}$$

It is easy to verify that the arrival process of claims from warned disasters $(N^*(t))$ is compound Poisson with rate $\lambda^* = (1 - \alpha_2)\lambda$, inter-arrival times $T_i^* \sim \exp(\lambda^*)$ and arrival times $W_n^* \sim \Gamma(n, \lambda^*)$. The arrival process of non-warned disasters $(\check{N}(t))$ is compound Poisson with rate $\check{\lambda} = \alpha_2 \lambda$, inter-arrival times $\check{T}_i \sim \exp(\check{\lambda})$ and arrival times $\check{W}_n \sim \Gamma(n, \check{\lambda})$. Furthermore, $N^*(t)$ and $\check{N}(t)$ are independent processes and $N(t) = N^*(t) + \check{N}(t)$. This is the so-called disaggregation property of Poisson processes.

Finally, we consider the error type III. Using again the disaggregation property of Poisson processes, we decompose the arrival process of warned disasters into two independent Poisson processes. So, we represent the process of warned disasters $N^*(t) = \widetilde{N}(t) + \widehat{N}(t)$ as the sum of the counting process of disasters with non-working warning $(\widetilde{N}(t))$ and disasters with working warnings $(\widehat{N}(t))$. $\widetilde{N}(t)$ and $\widehat{N}(t)$ are Poisson processes with parameters $\widetilde{\lambda} = \alpha_3 \lambda^* = \alpha_3(1 - \alpha_2)\lambda$ and $\widehat{\lambda} = (1 - \alpha_3)\lambda^* = (1 - \alpha_3)(1 - \alpha_2)\lambda$, respectively. We define the arrival process $\overline{N}(t)$ as the sum of the arrivals of non-warned disasters $(\check{N}(t))$ and disasters preceded by a non-working warning $(\widetilde{N}(t))$. That is, $\overline{N}(t) = \check{N}(t) + \widetilde{N}(t)$. It is easy to verify that the arrival process of natural disasters is the sum of $N(t) = \overline{N}(t) + \widehat{N}(t)$.

6.3 Arrival process of warnings

Let the arrival process of warnings, $\{\kappa(t),\, t \geq 0\}$, be a Poisson process with fixed parameter σ. From now on, we will denominate emergency to the phases following the warning. Let $\mathcal{T}_i$ be the duration of the ith-emergency. We can consider the duration of the emergencies $\mathcal{T}_i$ as i.i.d.r.v., $\mathcal{T}_i \sim$ Erlang(k, μ), $i = 1, 2, \ldots$. It means,

$$f_{\mathcal{T}_i}(t) = \frac{(\mu k)^k}{(k-1)!} t^{k-1} e^{-k\mu t} \tag{6.3}$$

for $t \geq 0$, where $\mu > 0$ and $k \in \mathbb{N}$. We have $\mathbb{E}[\mathcal{T}_i] = \mu^{-1}$ and $\sqrt{\text{Var}[\mathcal{T}_i]} = (\sqrt{k}\mu)^{-1}$. k specifies the degree of variability and is known as the shape parameter.

Note that μ is related with the mean duration of the emergency. That is, $h = \mu^{-1}$. Then, for a 72-hours warning $h = 72(24)^{-1}(365)^{-1} \approx 0.00822$ and $\mu = 121.67$. For flooding in Germany, e.g., forecasts succeed between 12 and 48 hours before the event and we usually have 12-hours warnings ([dkv03]).

The parameter σ in our model is associated with the number of warnings expected per year. If, e.g., 4 warnings are expected, then $\sigma = 4$.

We suggest an Erlang distribution for the random variables $\mathcal{T}_i$, because it allows a variance equal to or smaller than the mean μ^{-1}. If desired, it is possible to model the arrivals of warnings and disasters considering a queueing model of the type $M/E_k/s$ with $\mathcal{T}_i$ as the "service times". Note that if we set $k = 1$, then we have the usual queueing model with exponential "service times". An emphasis on the queueing model is, however, beyond the scope of this thesis.

By the disaggregation property of Poisson processes, we separate the arrival process of warnings $\kappa(t)$ into two independent Poisson processes: $\kappa^*(t)$ and $\breve{\kappa}(t)$. The arrival process of effective warnings, $\kappa^*(t)$, has parameter $\sigma^* := (1-\alpha_1)\sigma$ and the arrival process of false warnings, $\breve{\kappa}(t)$, has parameter $\breve{\sigma} := \alpha_1\, \sigma$.

Note that the number of warned disasters and the number of technically-successful warnings should be the same. Hence, $\kappa^*(t)$ and $N^*(t)$ are Poisson processes with the same intensity. Using the equality $\sigma^* = \lambda^*$, we obtain an expression for σ in terms of λ:

$$\sigma = \frac{1-\alpha_2}{1-\alpha_1}\lambda. \tag{6.4}$$

Parameter	Equivalence
$\lambda^* = \sigma^*$	$(1-\alpha_2)\lambda$
$\check{\lambda}$	$\alpha_2\lambda$
$\widetilde{\lambda}$	$\alpha_3(1-\alpha_2)\lambda$
$\widehat{\lambda}$	$(1-\alpha_3)(1-\alpha_2)\lambda$
$\overline{\lambda}$	$(\alpha_2+\alpha_3-\alpha_2\alpha_3)\lambda$
σ	$(1-\alpha_2)(1-\alpha_1)^{-1}\lambda$
$\check{\sigma}$	$\alpha_1(1-\alpha_2)(1-\alpha_1)^{-1}\lambda$
η	$\left(1+\alpha_1(1-\alpha_2)(1-\alpha_1)^{-1}\right)\lambda$

Tab. 6.1: Poisson parameters in terms of the mean number of disasters per year (λ) and the probabilities of error ($\alpha_1, \alpha_2, \alpha_3$).

6.4 Arrival process of expenditures (claims)

In the previous sections, we decomposed the arrival processes $N(t)$ and $\kappa(t)$ into independent processes. A summary of all parameters in terms of $\alpha_1, \alpha_2, \alpha_3$ and λ is given in Tab. 6.1.

For the stochastic modelling, we consider a simplified arrival process of expenditures (claims). We model the arrival process of expenditures using a Poisson process $\{J(t),\ t \geq 0\}$ with parameter η, where

$$\eta = \widehat{\lambda} + \overline{\lambda} + \check{\sigma}. \tag{6.5}$$

That is,

$$\eta = \widehat{\lambda} + \widetilde{\lambda} + \check{\lambda} + \check{\sigma}. \tag{6.6}$$

The process of technically-successful warnings, $\kappa^*(t)$, is implicit in Eqs. (6.5) and (6.6).

6.5 Final comments

The model's conception is the result of an interdisciplinary analysis. It was developed to serve as basis for further research in risk management of natural disasters from an actuarial perspective.

Although the assumption of independent claims and expenditures is too simple, this kind of models (e.g. the Lundberg model) have proven its usefulness to develop techniques for more general risk processes.

We distinguish between ex-post aggregate claims of disasters which occurred after an optimal ex-ante disaster management, and ex-post aggregate claims which have a different background by using different stochastic models, respectively. We do not model any relationship between the size of the losses and the frequency of the extreme natural event.

7. RISK RESERVE MODEL

The classical Lundberg model for the risk reserve (capital) of an insurance company is given by

$$R_t = x + ct - S(t), \quad t \geq 0, \tag{7.1}$$

where

$$S(t) = \sum_{i=1}^{N(t)} S_i \tag{7.2}$$

denotes the aggregate claims process up to time t, x is the initial capital, c is the instantaneous premium rate and $N(t)$ is the arrival process of the claims. The individual claims S_i, $i = 1, \ldots, N(t)$, are i.i.d.r.v.. The Lundberg model is widely used in practice and is the basis for several fundamental results in actuarial mathematics. Nevertheless, this model was conceived before the existence of early warning systems, so that it does not consider the possibility of loss mitigation.

We denote $\widehat{S}(t)$ to the aggregate claims up to time t from disasters that were preceded by a working emergency management and $\overline{S}(t) := S(t) - \widehat{S}(t)$ are the rest of the claims. If early warning systems have an effect in the claim sizes, this should be reflected in the probability distribution. For this reason, we classify claims according to the alert phase.

Define the aggregated claim process

$$\widehat{S}(t) \quad = \quad \sum_{i=1}^{\widehat{N}(t)} \widehat{S}_i, \quad \widehat{S}_i,\ i = 1, \ldots, \widehat{N}(t), \text{ i.i.d.r.v.} \tag{7.3}$$

$\overline{S}(t)$ is defined in analogy to Eq. (7.3).

As a result, we obtain a variant of the classical Lundberg model considering the effect of a warning system:

$$R_t = x + ct - \widehat{S}(t) - \overline{S}(t), \quad t \geq 0. \tag{7.4}$$

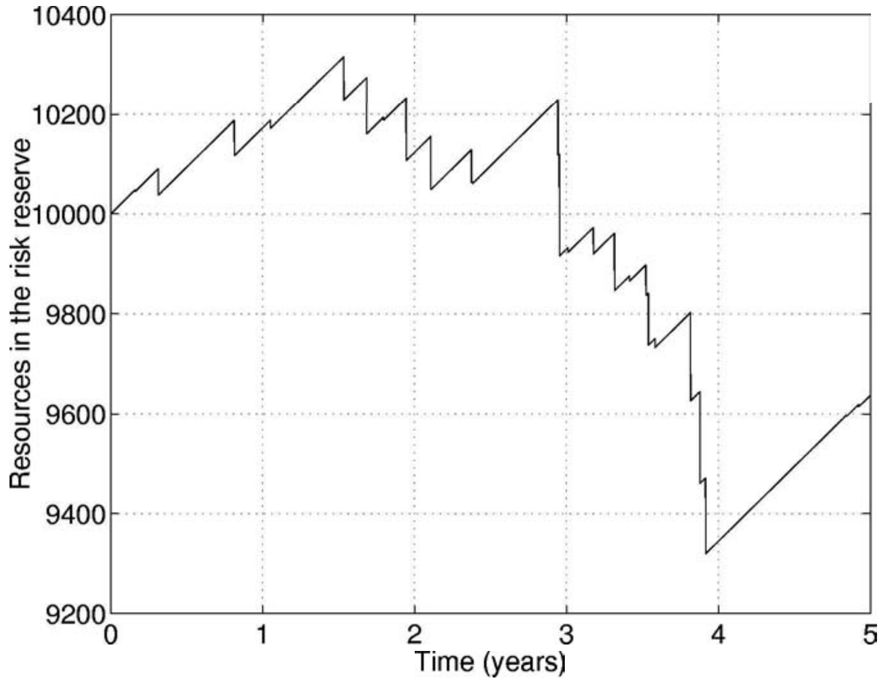

Fig. 7.1: Simulation of the risk reserve

The expectation of the total aggregate claims up to time $t \geq 0$ is

$$\mathbb{E}[\widehat{S}(t) + \overline{S}(t)] \quad = \quad (\widehat{\lambda}\mathbb{E}[\widehat{S}_i] + \overline{\lambda}\mathbb{E}[\overline{S}_i])t. \tag{7.5}$$

The variance is given by

$$\text{Var}[\widehat{S}(t) + \overline{S}(t)] \quad = \quad (\widehat{\lambda}\mathbb{E}[\widehat{S}_i^2] + \overline{\lambda}\mathbb{E}[\overline{S}_i^2])t. \tag{7.6}$$

The first difference between the Lundberg model and our model, is that we classify the aggregate claims $S(t)$ in two types and we consider them as two different processes for the stochastic modelling. Observe that if $\widehat{S}(t)$ and $\overline{S}(t)$ are equally distributed, we have the Lundberg model. As we remember, $\widehat{N}(t)$ and $\overline{N}(t)$ are compound Poisson processes with rates $\widehat{\lambda} = (1 - \alpha_3)(1 - \alpha_2)\lambda$ and $\overline{\lambda} = (\alpha_2 + \alpha_3 - \alpha_2\alpha_3)\lambda$. The parameter of $N(t)$ is $\lambda = \widehat{\lambda} + \overline{\lambda}$. From the independency of the arrival processes $\widehat{N}(t)$ and $\overline{N}(t)$, the aggregated claim processes $\widehat{S}(t)$ and $\overline{S}(t)$ are also independent.

However, the most important difference is that, by construction, this variant makes it possible to quantify and compare the impact in the risk reserve of early warning systems with different performance indicators.

8. GOVERNMENTAL FUND'S MODEL

The lack of actuarial models from a governmental perspective forced us to look for a real governmental fund for natural disasters to develop our model. Based on an analysis of Mexico's Fund for Natural Disasters (FONDEN) functioning and history, we conceived the actuarial model for a governmental fund for natural disasters here presented. Our model, however, can also be useful for other countries.

8.1 Expenditure process

A special feature of Mexico's Fund for Natural Disasters is that it not only considers damage ex-post but also resources for prevention. For this reason, we concluded that we should include two types of expenditures in our mathematical model: ex-ante and ex-post.

Ex-ante expenditures include only resources assigned during alert stages. For example, money provided for temporary shelters after a hurricane-warning. A fund's disbursement after a natural disaster is an ex-post expenditure.

After issuing a warning, whatever the result, we disburse a constant amount a_1. In case of a false alarm, the quantity a_2 should be returned to the fund at the end of the emergency phase.

Of course, in the real world a_1 is not constant and a_2 also varies. Nevertheless, the size of ex-ante expenditures is much easier to calculate than in the ex-post case. In practice, we can use mean observed values to calculate the constants a_1 and a_2 that we will use. The results should be adjusted according to the experience regarding the variability of ex-ante expenditures.

In our model, expenditures of size a_1 have the same arrival process as the warnings: $\kappa(t)$. The reimbursement a_2 has the same arrival process as false warnings $\breve{\kappa}(t)$. Both processes are dependent, but not the arrival processes of false warnings ($\breve{\kappa}(t)$) and working warnings ($\kappa^*(t)$). Hence, it is mathematically

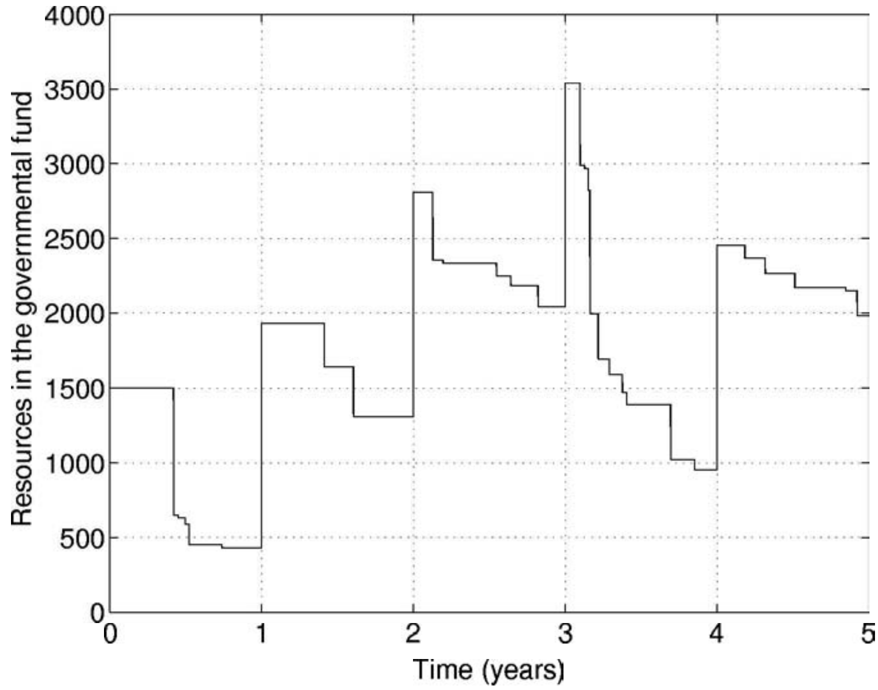

Fig. 8.1: Simulation of the governmental fund

more convenient to work with the arrival processes of the disbursements a_1 and $a_1 - a_2$ than with the arrival processes of a_1 and a_2.

A summary of results is in Table 8.1.

8.2 Fund's Model

Assume that we have an unlimited XL-reinsurance contract for year n with fixed retention level $\alpha^{(n)} > 0$. If there is no reinsurance contract this year, then $\alpha^{(n)} = \infty$.

Consider that the reinsurer uses the expected value principle with safety loading $\theta > 0$ for premium calculation. In this case,

$$C^{(n)} = (1+\theta)\left\{\mathbb{E}\left[\sum_{i=1}^{\widehat{N}(1)} (\widehat{S}_i - \alpha^{(n)})^+\right]\right.$$

Event	Expenditure	Arrival process	Poisson parameter
Technically-successful warning	a_1	$\kappa^*(s)$	σ^*
False warning	$a_1 - a_2$	$\check{\kappa}(s)$	$\check{\sigma}$
Claim ex-post (optimal emergency management)	$\widehat{S}_i$	$\widehat{N}(s)$	$\widehat{\lambda}$
Claim ex-post (deficient emergency management or non-warned disaster)	$\overline{S}_i$	$\overline{N}(s)$	$\overline{\lambda}$

Tab. 8.1: Classification of expenditures.

$$+ \quad \mathbb{E}\left[\sum_{i=1}^{\overline{N}(1)} (\overline{S}_i - \alpha^{(n)})^+\right]\Bigg\}, \tag{8.1}$$

$\alpha^{(n)} < \infty$. $C^{(n)}$ is the annual premium to be paid at the beginning of the year n. If $x_0^{(n)}$ are the initial resources for the year n, it is clear that only contracts with $C^{(n)} < x_0^{(n)}$ are viable, $x_0^{(n)}$ is the sum of the budget for year n and the surplus (if not zero) of the previous year.

In the above formula, we show that it is possible to quantify the effect of risk reduction in the risk premium. A risk premium calculated considering the effects of warnings can represent an economic incentive for risk-averse governments to invest in early warning systems and purchase more reinsurance.

Let the process $(R^{(n)}(s))_{s\in[0,1]}$ be the level of the fund at time $t = s+n-1$, $n \in \mathbb{N}$. The initial value of $(R^{(n)}(s))_{s\in[0,1]}$ is $b_0^{(n)} = x_0^{(n)} - C^{(n)}$.

The model for the governmental fund at time s for the n-year is

$$R^{(n)}(s) \quad = \quad b_0^{(n)} - \Pi(s), \tag{8.2}$$

where

$$\begin{aligned} \Pi(s) \quad := \quad & \sum_{i=1}^{\widehat{N}(s)} (a_1 + \min\{\alpha^{(n)}, \widehat{S}_i\}) + \sum_{i=1}^{\widetilde{N}(s)} (a_1 + \min\{\alpha^{(n)}, \overline{S}_i\}) \\ + \quad & \sum_{i=1}^{\check{N}(s)} \min\{\alpha^{(n)}, \overline{S}_i\} - (a_1 - a_2)\,\check{\kappa}(s). \end{aligned} \tag{8.3}$$

$\Pi(s)$ is a random variable that represents the aggregated expenditures up to time s. The process $R^{(n)}(s)$ considers ex-ante and ex-post economic resources together. As we mentioned before, in Mexico ex-ante and ex-post economic resources are administrated independently. We joined them for the mathematical formulation because they share the same initial budget.

The expectation and the variance of $\Pi(s)$ are given by

$$\begin{aligned}
\mathbb{E}[\Pi(s)] &= a_1\lambda^* s + (a_1 - a_2)\breve{\sigma} s \\
&+ \widehat{\lambda} s \mathbb{E}\left[\min\{\alpha^{(n)}, \widehat{S}_i\}\right] + \overline{\lambda} s \mathbb{E}\left[\min\{\alpha^{(n)}, \overline{S}_i\}\right] \qquad (8.4) \\
&= (1-\alpha_2)\lambda s \left(\frac{a_1 - a_2\alpha_1}{1-\alpha_1} + (1-\alpha_3)\mathbb{E}[\min\{\alpha^{(n)}, \hat{S}_i\}]\right) \\
&+ (\alpha_2 + \alpha_3(1-\alpha_2))\lambda s\, \mathbb{E}[\min\{\alpha^{(n)}, \bar{S}_i\}], \qquad (8.5)
\end{aligned}$$

and

$$\begin{aligned}
\text{Var}[\Pi(s)] &= a_1^2\lambda^* s + (a_1 - a_2)^2\breve{\sigma} s + \widehat{\lambda} s\, \mathbb{E}[(\min\{\alpha^{(n)}, \widehat{S}_i\})^2] \\
&+ \overline{\lambda} s\, \mathbb{E}[(\min\{\alpha^{(n)}, \overline{S}_i\})^2] \qquad (8.6) \\
&= \left(a_1^2 + (a_1 - a_2)^2 \frac{\alpha_1}{1-\alpha_1}\right)(1-\alpha_2)\lambda s \\
&+ \left((1-\alpha_3)\mathbb{E}\left[(\min\{\alpha^{(n)}, \hat{S}_i\})^2\right]\right)(1-\alpha_2)\lambda s \\
&+ \left((\alpha_2 + \alpha_3(1-\alpha_2))\mathbb{E}\left[(\min\{\alpha^{(n)}, \bar{S}_i\})^2\right]\right)\lambda s, \qquad (8.7)
\end{aligned}$$

respectively.

For the case $\alpha^{(n)} = \infty$ (no reinsurance), we have

$$\mathbb{E}[\Pi(s)] = (\widehat{\lambda}\mathbb{E}[\widehat{S}_i] + \overline{\lambda}\mathbb{E}[\overline{S}_i] + a_1\lambda^* s + (a_1 - a_2)\breve{\sigma})s \qquad (8.8)$$

and

$$\text{Var}[\Pi(s)] = (a_1^2\lambda^* + (a_1 - a_2)^2\breve{\sigma} + \widehat{\lambda}\, \mathbb{E}[\widehat{S}_i^2] + \overline{\lambda}\, \mathbb{E}[\overline{S}_i^2])s. \qquad (8.9)$$

In Chapter 12, we use the model for the cumulated expenditures $\Pi(s)$ considering an XL-reinsurance contract in order to find an optimal management strategy.

9. GENERALIZED-PARETO CLAIMS

In this chapter, we make some calculations assuming Generalized-Pareto Claims (see Def. 9.1). Finally, we present a numerical example.

Let us first introduce the definition of Generalized Pareto Distribution:

Definition 9.1: (Generalized Pareto Distribution ([KM01]))
Define the density function (df) $G_{\xi;\nu,\beta}$, $\xi, \nu \in \mathbb{R}$, $\beta > 0$, by

$$G_{\xi;\nu,\beta}(x) = \begin{cases} 1 - \left(1 + \frac{\xi(x-\nu)}{\beta}\right)^{-\frac{1}{\xi}} & if \quad \xi \neq 0, \\ 1 - \exp\left\{-\frac{x-\nu}{\beta}\right\} & if \quad \xi = 0. \end{cases} \tag{9.1}$$

where

$$\begin{array}{ll} x \geq \nu & if\ \xi \geq 0, \\ 0 \leq x \leq \nu - \frac{\beta}{\xi} & if\ \xi < 0. \end{array}$$

$G_{\xi;\nu,\beta}$ is called a standard generalized Pareto distribution (GPD).

If $\widehat{\xi} = 0$ or $\overline{\xi} = 0$, the respective claims have exponential distribution. For this reason, we restrict ourselves to the sub-exponential case, i.e. $\widehat{\xi} \neq 0$, $\overline{\xi} \neq 0$. Additionally, given that the claims ex-post, $\widehat{S}_t$ and $\overline{S}_t$, have values in $(0, \infty)$ and finite mean and variance, we set $\widehat{S}_s \sim G_{\widehat{\xi};\widehat{\nu},\widehat{\beta}}$, $\overline{S}_s \sim G_{\overline{\xi};\overline{\nu},\overline{\beta}}$ with $\widehat{\xi}, \overline{\xi} \in \left[0, \frac{1}{2}\right)$. In order to simplify the output, we consider $\widehat{\nu} = 0$ and $\overline{\nu} = 0$. We can easily generalize the results to other cases.

We have

$$\mathbb{E}[\widehat{S}_i] = \frac{\widehat{\beta}}{1 - \widehat{\xi}}, \tag{9.2}$$

$$\mathbb{E}[\widehat{S}_i^2] = \frac{2\widehat{\beta}^2}{(1 - \widehat{\xi})(1 - 2\widehat{\xi})} \quad \text{and} \tag{9.3}$$

$$\mathrm{Var}[\widehat{S}_i] = \frac{\widehat{\beta}^2}{(1-\widehat{\xi})^2(1-2\widehat{\xi})}. \tag{9.4}$$

$\mathbb{E}[\overline{S}_i]$, $\mathbb{E}[\overline{S}_i^2]$ and $\mathrm{Var}[\overline{S}_i]$ are defined in analogy to Eqs. (9.2), (9.3) and (9.4), respectively.

The XL-premium (see Eq. 8.1) that the government should pay is in this case

$$\begin{aligned} C^{(n)} &= (1+\theta)\left[\widehat{\lambda}\frac{\widehat{\beta}+\widehat{\xi}\alpha^{(n)}}{1-\widehat{\xi}}\left(1+\frac{\widehat{\xi}\alpha^{(n)}}{\widehat{\beta}}\right)^{-\frac{1}{\widehat{\xi}}}\right. \\ &+ \left.\overline{\lambda}\frac{\overline{\beta}+\overline{\xi}\alpha^{(n)}}{1-\overline{\xi}}\left(1+\frac{\overline{\xi}\alpha^{(n)}}{\overline{\beta}}\right)^{-\frac{1}{\overline{\xi}}}\right], \end{aligned} \tag{9.5}$$

where $\alpha^{(n)}$ is the retention level.

The mean ex-post expenditure per disaster, considering an XL-reinsurance, is

$$\mathbb{E}[\min\{\alpha^{(n)}, \widehat{S}_i\}] = \frac{\widehat{\beta}}{1-\widehat{\xi}} - \frac{\widehat{\beta}+\widehat{\xi}\alpha^{(n)}}{1-\widehat{\xi}}\left(1+\frac{\widehat{\xi}}{\widehat{\beta}}\alpha^{(n)}\right)^{-\frac{1}{\widehat{\xi}}}. \tag{9.6}$$

The second moment of the expenditure considering an XL-reinsurance is

$$\begin{aligned} \mathbb{E}\left[(\min\{\alpha^{(n)}, \widehat{S}_i\})^2\right] &= -2\left[\frac{\alpha^{(n)}(\widehat{\beta}+\widehat{\xi}\alpha^{(n)})}{1-\widehat{\xi}} + \frac{(\widehat{\beta}+\widehat{\xi}\alpha^{(n)})^2}{(1-\widehat{\xi})(1-2\widehat{\xi})}\right] \\ &\quad \ldots \left(1+\frac{\widehat{\xi}}{\widehat{\beta}}\alpha^{(n)}\right)^{-\frac{1}{\widehat{\xi}}} \\ &+ \frac{2\beta^2}{(1-\widehat{\xi})(1-2\widehat{\xi})}. \end{aligned} \tag{9.7}$$

$\mathbb{E}[\min\{\alpha^{(n)}, \overline{S}_i\}]$ and $\mathbb{E}[(\min\{\alpha^{(n)}, \overline{S}_i\})^2]$ are defined in analogy to Eqs. (9.6) and (9.7).

Substituting the equations for the mean and the second moment of the expenditures considering an XL-reinsurance contract in Eqs. (8.4) and (8.6), we obtain formulas for the calculation of the mean and the variance of the total aggregated outcome up to time s.

9.0.1 Example

Let the number of periods be $n = 1$. Assume we have a warning system with performance indicators $\alpha_1 = 0.2$ (error type I), $\alpha_2 = 0.3$ (error type II) and $\alpha_3 = 0.4$ (error type III). We will make an example based on the assumption that the planning is made considering a mean of 5 natural disasters per year. Remember that the incidence of natural disasters is variable on a yearly basis. Actually, we consider that this variability is already a good reason to build reserves.

We classify claims accordingly in two groups:

1. a warning was issued and it was technically and sociologically effective,

2. the rest of the disasters.

The next step would be to fit in a distribution for every group of data and to set the corresponding parameters. If the available information is not enough, then we need to make some assumptions according to our experience.

Assume that we adjust a generalized Pareto distribution for both types of claims and we obtain $\widehat{\xi} = 0.3$, $\widehat{\beta} = 50$, $\overline{\xi} = 0.4$ and $\overline{\beta} = 100$. The expenditures and the reimbursement for emergency management are $a_1 = 60$ and $a_2 = 40$, respectively. Consider a XL-reinsurance contract with retention level $\alpha^{(n)} = 1000$ and safety loading $\theta = 2$.

Our calculations yield $\eta = 5.87$, $\sigma = 4.37$, $\widehat{\lambda} = 2.10$ and $\overline{\lambda} = 2.90$. The expectation and variance of $\widehat{S}_i$ (optimal emergency management) and $\overline{S}_i$ (deficient emergency management) are $E[\widehat{S}_i] = 71.43$, Var$[\widehat{S}_i] = 12,755.10$, $E[\overline{S}_i] = 166.67$ and Var$[\overline{S}_i] = 138,888.89$. The corresponding premium, as defined in Eq. (8.1), is $C^{(n)} = 134.49$.

Moreover, $\mathbb{E}[\Pi(1)] = 816.00$, Var$[\Pi(1)] = 225,170.00$, $\mathbb{E}[\min\{\alpha^{(n)}, \widehat{S}_i\}] = 70.67$ and $\mathbb{E}[\min\{\alpha^{(n)}, \overline{S}_i\}] = 151.76$.

The influence of the warning system should be explicitly reflected in the difference in the results for both types of claims and implicitly in the premium and statistics for the cumulated expenditures at the end of the fiscal year $\Pi(1)$. Note, that if we consider that an early warning system has an effect on the claim sizes, the benefit of an effective risk mitigation is translated into a premium reduction. The more effective the early warning system is, the lower the premium.

The effects of the XL-reinsurance contract can be identified in the statistics of $\Pi(1)$ with and without reinsurance. If there is no reinsurance contract, $\mathbb{E}[\Pi(1)] = 860.85$ and Var$[\Pi(1)] = 533,783.33$.

Finally, we calculate the mean and the variance of the sum of all claims: $\mathbb{E}[\widehat{S}(1) + \overline{S}(1)] = 633.35$ and Var$[\widehat{S}(1) + \overline{S}(1)] = 520,833.33$.

Certainly, we can also make a variety of comparative analysis changing the XL-contract conditions, the performance indicators, the claim parameters, etc.

In Figs. 8.1 and 7.1, we illustrate a simulation of the governmental fund and the risk reserve during 5 years, respectively. With the help of these figures, we can appreciate the main differences between both processes. The governmental fund has an income once a year (budget), expenditures and reimbursements (or negative expenditures) for emergency management as well as post-disaster expenditures. The risk-reserve of the insurance company has a continuous income for premiums and claims post-disaster.

9.1 Final comments

The results of Parts I and II evidence that building reserves is justified in the framework of a risk-averse government. The reserves are important because they enable a better budget planning and they reduce economic vulnerability in the long-term.

The implementation of a natural disasters fund by itself is not enough to reduce substantially the economic vulnerability of a risk-averse country like Mexico if we are not able to take advantage of it in the long-term planning.

A better budget planning for a fund for natural disasters like FONDEN is important to reduce the disruptions to the budget process caused by unforeseeable expenditures from natural disasters. Another benefit of improving management for natural disasters funds is that risk-averse governments can implement them in a sustainable way.

For some countries, a better budget planning and reserve management using ad hoc actuarial technics can enable the possibility to stabilize also the budget for diverse social programs, like poverty mitigation. In some countries, the budget for social programs is shortened in order to cover natural disaster losses.

In the next part of the thesis, we use the actuarial model for a governmental fund for natural disasters here developed to find an investment strategy for the management of a natural disasters fund from a governmental perspective.

Part III

MANAGEMENT STRATEGY FROM A GOVERNMENTAL PERSPECTIVE

10. MARKET MODEL

The market model that we use for the optimization problem is the classical Black-Scholes. We have a bank account paying interest rate r and a risky asset Z in which the fund's manager can invest. The model can be generalized to consider a finite number of risky assets. We use the classical Samuelson model for the dynamics of the asset price $Z(s)$:

$$dZ(s) = Z(s)(\mu ds + bdB(s)),\ Z(0) > 0,\ \mu > 0,\ b > 0. \tag{10.1}$$

Let $B(s)$ be a standard Wiener process. $\mathbb{F}^{B,\Pi}$ denotes the $\mathbb{P}$-augmentation of the filtration generated by $B(s)$ and the process $\Pi(s)$. Consider a probability space $(\Omega, \mathcal{F}, \mathbb{F}, \mathbb{P})$ with a filtration $\mathbb{F} = (\mathcal{F}_s)_{0\le s\le 1} \supseteq \mathbb{F}^{B,\Pi}$ satisfying the usual conditions and $\mathcal{F} = \mathcal{F}_1$.

10.1 Market assumptions

We work in the framework of incomplete markets and no-arbitrage.

Denote by

$$\begin{aligned} \mathbf{M}^e(\mathbb{P}) \quad = \quad & \{\tilde{\mathbb{P}} \equiv \mathbb{P} : \tilde{\mathbb{P}} \text{ is a probability measure and} \\ & Y \text{ is a } \tilde{\mathbb{P}}\text{-local martingale}\} \end{aligned}$$

the set of all probability measures $\tilde{\mathbb{P}}$ on $\mathcal{F}$ which are equivalent to $\mathbb{P}$ in $[0, 1]$.

If there is no possibility of arbitrage, we can assume $\mathbf{M}^e(\mathbb{P}) \neq \phi$ ([HK79]).

Incompleteness implies that we can not replicate the contingent outcome with the instruments available in the market without risk. The total contingent expenditures of the fund ($\Pi(1)$) depend on a source of randomness which does not influence the market's coefficients μ, r and b.

11. INVESTMENT PORTFOLIO

Our aim is to find whether we can combine a risk free instrument (bank account) with risky investment (asset Z) to hedge the contingent total outcome $\Pi(1)$ of the fund for natural disasters.

With development purposes, we assume Pareto-distributed claims. The effect of an XL-reinsurance contract is considered in the model for $\Pi(1)$. In this chapter, we explain the model for the investment portfolio that we use to explore the possibility of managing risk using investment.

From the reserve available at the beginning of the year n ($R^{(n)}(0)$), we subtract the XL-premium ($C^{(n)}$) and other payments to be made at the beginning of the year. We denote the total amount to be subtracted as P, where $P \geq C^{(n)} \geq 0$. If the reserve suffices (i.e. $R^{(n)}(0) > P$), we assign an amount $x \in (0, R^{(n)}(0) - P)$ for the risk management strategy based on investment.

Define a real-valued process $X^{(n)}(s)$ with $X^{(n)}(0) = x$ representing the current wealth at time $t = s + n - 1$. Let $\pi(s)$ be the number of shares $Z(s)$ held at time t. At each point in time t, the amount $\pi(s)Z(s)$ is invested into the risky asset. The difference $X^{(n)}(s) - \pi(s)Z(s)$ is left in a bank account earning interest r. We deduce that the dynamics of the investment portfolio $X^{(n)}(s)$ during the year n is given by

$$dX^{(n)}(s) = rX^{(n)}(s)ds - r\pi(s)Z(s)ds + \pi(s)dZ(s), \tag{11.1}$$

$X^{(n)}(0) = x, x \geq 0, 0 \leq s \leq 1.$

Rewriting Eq. (11.1),

$$dX^{(n)}(s) = rX^{(n)}(s)ds + \pi(s)Z(s)((\mu - r)ds + bdB(s)), \tag{11.2}$$

where $B(s)$ is a standard linear Brownian motion.

All processes considered in this part of the thesis are indexed in $[0, 1]$. We calculate the optimal strategy for a time-horizon of one year. In order to simplify the notation, from now on we will write $X(s)$ instead of $X^{(n)}(s)$.

For our purposes, it is mathematically convenient to work with the discounted prices and portfolio values and to make a change of measure that eliminates the drift term $(\mu - r)ds$ in Eq. (11.2) (above) using Girsanov's Theorem.

Let $\tilde{Z}(s) = e^{-rs}Z(s)$ and $\tilde{X}(s) = e^{-rs}X(s)$ be the process of discounted asset prices and the discounted wealth process, respectively. If the process

$$\int_0^s \pi(u)d\tilde{Z}(u) \tag{11.3}$$

is a $\mathbb{Q}$-local martingale, the discounted process $(\tilde{X}(s))_{0\leq s\leq 1}$ is also a $\mathbb{Q}$-local martingale.

We can easily verify that $\tilde{Z}(s)$ is a $\mathbb{Q}$-local martingale. Applying Itô Calculus and substituting Eq. (10.1), we obtain

$$d\tilde{Z}(s) \quad = \quad \tilde{Z}(s)((\mu - r)ds + bdB(s)). \tag{11.4}$$

Consider the process

$$W(s) := B(s) + \frac{\mu - r}{b}s, \ W(0) = 0 \ a.s. \tag{11.5}$$

The process $W \in \mathcal{S}^2_{loc}$ is the sum of a local martingale $B(s)$ and a predictable process A that satisfies $A = \int_0^s \frac{\mu - r}{b} d\langle B \rangle$. Actually, the Doob-Meyer decomposition of W is $W = W(0) + B + A$.

$W(s)$ satisfies

$$dW(s) = dB(s) + \frac{\mu - r}{b}ds. \tag{11.6}$$

Put

$$\mathrm{M}_s = \exp\left\{-\frac{\mu - r}{b}B(s) - \frac{1}{2}\left(\frac{\mu - r}{b}\right)^2 s\right\}; \ s \in [0, 1]. \tag{11.7}$$

The process $\frac{\mu - r}{b}$ is constant, and thus, progressively measurable. It obviously satisfies Novikov's condition

$$\mathbb{E}\left[\exp\left(\frac{1}{2}\int_0^1 \left(\frac{\mu - r}{b}\right)^2 du\right)\right] < \infty, \tag{11.8}$$

where $\mathbb{E}$ is the expectation with respect to $\mathbb{P}$. Define the measure $\mathbb{Q}$ on $(\Omega, \mathcal{F}_1)$ by $\frac{d\mathbb{Q}}{d\mathbb{P}} = \mathrm{M}_1$ on $\mathcal{F}_1$. By Girsanov's theorem, we know that $(W(s))_{0\leq s\leq 1}$ is a standard Brownian motion with respect to $\mathbb{Q}$. This implies that W is a semimartingale under the basic measure $\mathbb{P}$.

It is easy to verify that the discounted process $\tilde{Z}(s)$ is a $\mathbb{Q}$-local martingale. Substituting Eq. (11.6) in Eq. (11.4), we obtain

$$d\tilde{Z}(s) = b\tilde{Z}(s)dW(s). \tag{11.9}$$

It is well-known that the solution of Eq. (11.9) with respect to $\mathbb{Q}$ is a geometric Brownian motion:

$$\tilde{Z}(s) = \tilde{Z}(0)\exp\left(bW(s) - \frac{b^2 s}{2}\right). \tag{11.10}$$

Now we will verify that the discounted process $\tilde{X}(s)$ is also a local $\mathbb{Q}$-martingale. Considering $\tilde{X}(s) = e^{-rs}X(s)$ and applying Itô Calculus, we have

$$d\tilde{X}(s) \;=\; -re^{-rs}X(s)ds + e^{-rs}dX(s). \tag{11.11}$$

Substituting $dX(s)$ (Eq. (11.1)) in the above equation,

$$d\tilde{X}(s) \;=\; e^{-rs}\pi(s)Z(s)((\mu - r)ds + bdB(s)). \tag{11.12}$$

It follows that the dynamics of the process under $\mathbb{Q}$ is given by

$$d\tilde{X}(s) \;=\; \pi(s)d\tilde{Z}(s). \tag{11.13}$$

Then $\tilde{X}(s)$ is a $\mathbb{Q}$-local martingale and admits the representation

$$\tilde{X}(s) \;=\; \tilde{X}(0) + \int_0^s \pi(u)\, b\, \tilde{Z}(u)\, dW(u). \tag{11.14}$$

From now on, we will work with the discounted processes $\tilde{Z}(s)$ and $\tilde{X}(s)$.

The equivalent martingale measure $\mathbb{Q}$ is not unique in the framework of incomplete markets. There are two widely extended criteria to choose an element of $\mathbf{M}^e(\mathbb{P})$ for the calculations: the minimal martingale measure (Def. 11.1) and the variance-optimal measure (Def. 11.3).

11.1 The minimal martingale measure

Definition 11.1: Let $M \in \mathcal{M}_2$. A martingale measure $\mathbb{P}^{\min} \equiv \mathbb{P}$ is called minimal if

$$\mathbb{P}^{\min} \equiv \mathbb{P} \text{ on } \mathcal{F}_0, \tag{11.15}$$

and if any square-integrable $\mathbb{P}$-martingale which is orthogonal to M under $\mathbb{P}$ remains a martingale under $\mathbb{P}^{\min}$:

$$L \in \mathcal{M}_2 \text{ and } \langle L, M\rangle = 0 \;\Rightarrow\; L \text{ is a martingale under } \mathbb{P}^{\min} \tag{11.16}$$

([FS91]).

From the Doob-Meyer decomposition of W, we know that the minimal martingale measure should be determined by

$$\mathrm{G}_s \;=\; \exp\left\{-\int_0^s \frac{\mu - r}{b} dB(s) - \frac{1}{2}\int_0^s \left(\frac{\mu - r}{b}\right)^2 d\langle W\rangle_s\right\}, \tag{11.17}$$

$s \in [0,1]$ (see [FS91]). The existence of the minimal martingale measure is ensured by the square integrability of G_s and $\mathbb{P}^{\min}$ is defined by the Radon-Nykodým derivative

$$\frac{d\mathbb{P}^{\min}}{d\mathbb{P}} = \mathrm{G}_1 = \exp\left\{-\frac{\mu - r}{b} B(1) - \frac{1}{2}\left(\frac{\mu - r}{b}\right)^2\right\} \tag{11.18}$$

(see [FS91]). Observe that $\mathrm{G}_s = \mathrm{M}_s$. That is, the minimal martingale measure is $\mathbb{Q}$ ($\mathbb{P}^{\min} = \mathbb{Q}$).

11.2 The variance optimal martingale measure

Let us first introduce the following definition:

Definition 11.2: The Hilbert space with scalar product $(\Lambda_1, \Lambda_2) = \mathbb{E}[\Lambda_1 \Lambda_2]$ and norm $||\Lambda_1|| = \sqrt{\mathbb{E}[\Lambda_1^2]}$ is the space of all square-integrable real random variables and we denote it by $\mathcal{L}^2$.

We define the variance-optimal martingale measure as follows:

Definition 11.3: The equivalent measure $\mathbb{P}_v \in \mathbf{M}^e(\mathbb{P})$ whose density with respect to $\mathbb{P}$ has minimal $\mathcal{L}^2$-norm is called the variance-optimal martingale measure ([DS96]).

Let Θ be the space of all $\mathbb{R}$-valued predictable W-integrable processes ϑ such that $G_s(\vartheta) = \int_0^s \vartheta dW$ is in the space $\mathcal{S}^2$ of semimartingales.

Remark 11.1: In our case, a random variable $\Lambda \in \mathcal{L}^2$ admits a strong F-S decomposition if Λ can be written as

$$\Lambda = \Lambda_0 + \int_0^1 \vartheta_s^\Lambda dW_s + L_1^\Lambda,\ \mathbb{P} - \text{a.s.}, \tag{11.19}$$

where $\Lambda_0 \in \mathbb{R}$ is a constant, $\vartheta^\Lambda \in \Theta$ and $L^\Lambda = (L_s^\Lambda)_{0\leq s\leq 1}$ is a square-integrable martingale, i.e., $L^\Lambda \in \mathcal{M}_2$, with $\mathbb{E}[L_0^\Lambda] = 0$ and strongly orthogonal to $\int \vartheta dB(s)$ for every $\vartheta \in \Theta$ ([Sch94]).

Let

$$\hat{K}_s := \left\langle \int_0^s \frac{\mu - r}{b} dW(s) \right\rangle = \left(\frac{\mu - r}{b}\right)^2 s. \tag{11.20}$$

$\hat{K}_s$ is the so-called mean-variance tradeoff (MVT) process. $\hat{K}$ is in our case deterministic and, obviously, continuous and bounded. If the MVT process is deterministic, it is known that the space $G_1(\Theta)$ is closed in $\mathcal{L}^2$ ([MS95], [RS98]).

From the closeness of $\tilde{G}_T(\Theta)$ in $\mathcal{L}^2$, we know that every r.v. in $\mathcal{L}^2$ has a F-S decomposition.

If the MVT process $\hat{K}$ is bounded, the Radon-Nykodým derivative M_1 is in $\mathcal{L}^2$ and it admits a F-S decomposition of the form

$$\mathrm{M}_1 \quad = \quad \mathbb{E}\left[\mathrm{M}_1^2\right] - \mathbb{E}\left[\mathrm{M}_1 \hat{L}_1\right] + \int_0^1 \hat{\psi}(u) dW(u) + \hat{L}_1 \tag{11.21}$$

([RS98]). If $\hat{L}_1 = 0$, we know from the results of [RS98] that the minimal and the variance-optimal martingale measures should coincide. This is precisely our case.

We find the F-S decomposition of M_1 as follows:

We have

$$\mathrm{M}_1 \quad = \quad \mathcal{E}\left(-\frac{\mu - r}{b} B(1)\right). \tag{11.22}$$

We first rewrite M_1 in terms of W. Substituting Eq. (11.5) in Eq. (11.22),

$$\mathrm{M}_1 \quad = \quad e^{\hat{K}_1} \mathcal{E}\left(-\frac{\mu - r}{b} W(1)\right). \tag{11.23}$$

From the continuity of the MVT process $\hat{K}$ and applying Yor's Formula we obtain

$$\mathrm{M}_1 = e^{\hat{K}_1} - \int_0^1 e^{\hat{K}_1} \mathcal{E}\left(-\frac{\mu - r}{b} W(u)\right) \frac{\mu - r}{b} dW(u) \tag{11.24}$$

([RS98]). Therefore, the process that is integrated with respect to $W(s)$ in the F-S decomposition of the measure M_1 (see Eq. (11.21)) is

$$\hat{\psi}(s) = -e^{\hat{K}_1} \mathcal{E}\left(-\frac{\mu - r}{b} W(s)\right) \frac{\mu - r}{b}, \; \hat{\psi}(s) \in \Theta. \tag{11.25}$$

The constant parameters μ, r and b are clearly independent of the standard Brownian motion $B(s)$ and we know that $B(s)$ is equal in distribution with a normal variable with mean 0 and variance s. So, we calculate

$$\mathbb{E}[\mathrm{M}_1^2] = e^{\hat{K}_1}. \tag{11.26}$$

Summarizing, the F-S decomposition of M_1 is

$$\mathrm{M}_1 = e^{\hat{K}_1} - \int_0^1 e^{\hat{K}_1} \mathcal{E}\left(-\frac{\mu - r}{b} W(u)\right) \frac{\mu - r}{b} dW(u). \tag{11.27}$$

That is, $\hat{L}_1 = 0$. Thus, the minimal martingale measure $\mathbb{Q}$ is also variance-optimal ($\mathbb{P}^{\min} = \mathbb{P}_v = \mathbb{Q}$).

12. MANAGEMENT STRATEGY FOR THE RISK RESERVE

In Chapter 8, we developed an actuarial model for a governmental fund for natural disasters. We defined the process

$$\begin{aligned}\Pi(s) &= \sum_{i=1}^{\widehat{N}(s)} (a_1 + \min\{\alpha^{(n)}, \widehat{S}_i\}) + \sum_{i=1}^{\widetilde{N}(s)} (a_1 + \min\{\alpha^{(n)}, \overline{S}_i\}) \\ &+ \sum_{i=1}^{\check{N}(s)} \min\{\alpha^{(n)}, \overline{S}_i\} - (a_1 - a_2)\,\check{\kappa}(s).\end{aligned}$$

$\Pi(s)$ is a non-decreasing process representing the aggregated expenditures up to time $s \in [0, 1]$. The total accumulated expenditures at the end of the fiscal year is $\Pi(1)$.

In order to develop an adequate optimal management strategy to hedge $\Pi(1)$ from the perspective of a risk-averse government, we should outline an adequate optimization problem. We investigated different possibilities and the resulting strategy comes from the solution of Problem 12.4.

The formulation and solution of the *main optimization problem* (Problem 12.4) is closely related with other problem, which we will call *basic optimization problem* (Problem 12.1).

12.1 Formulation of the basic optimization problem

Define $\tilde{H}(s) := \pi(s)\, b\, \tilde{Z}(s)$, $s \in [0, 1]$, where $\pi(s)$ is the number of shares to be held at s and $\tilde{Z}(s)$ is the discounted process of prices. Let $\tilde{G}_s(\tilde{H})$ be the cumulative gain process associated to the discounted wealth process $\tilde{X}(s)$. We have

$$\tilde{G}_s(\tilde{H}) = \int_0^s d\tilde{X}(u) = \int_0^s \tilde{H}(u) dW(u), \tag{12.1}$$

$0 \leq s \leq 1$.

Now we define the basic optimization problem.

Problem 12.1: Let Θ be the space of all investment strategies $\tilde{H}$ such that $\tilde{G}_1(\tilde{H})$ is in the space $\mathcal{S}^2$ of semimartingales.

The basic optimization problem is

$$\min \mathbb{E}\left[\left(\Pi(1) - c - \tilde{G}_1(\tilde{H})\right)^2\right], \; c \in \mathbb{R}, \text{ over all } \tilde{H} \in \Theta. \tag{12.2}$$

12.2 Solution of the basic optimization problem

We denote the strategy that solves Problem 12.1 as $\tilde{H}^{(c)}$. This strategy has the property to be mean-variance optimal. This type of problems has been often discussed in the literature in various forms of generality in both discrete and continuous settings.

As we mentioned before, from the closeness of $\tilde{G}_1(\Theta)$ in $\mathcal{L}^2$, we know that every r.v. in $\mathcal{L}^2$ has a F-S decomposition. $\Pi(1) \in \mathcal{L}^2$ implies that there is a solution $\tilde{H}^{(c)} \in \Theta$ for all c.

The first step is to find the intrinsic value process. We define the intrinsic value process V_s as a square-integrable process with right-continuous paths satisfying $V_0 = \mathbb{E}[\Pi(1)]$ and $V_1 = \Pi(1)$ $\mathbb{P}$-a.s. (see [FS91]).

The intrinsic value process for our problem is

$$V_s := \mathbb{E}[\Pi(1)|\mathcal{F}_s] = \Pi(s) + \mathbb{E}\left[\Pi(1-s)\right], \tag{12.3}$$

where

$$\begin{aligned} \mathbb{E}\left[\Pi(s)\right] \;&:=\; a_1\lambda^* s + (a_1 - a_2)\breve{\sigma} s \\ &+\; \hat{\lambda} s \mathbb{E}\left[\min\{\alpha^{(n)}, \hat{S}_i\}\right] + \bar{\lambda} s \mathbb{E}\left[\min\{\alpha^{(n)}, \bar{S}_i\}\right]. \end{aligned} \tag{12.4}$$

We wish to stress that the value of $\Pi(s)$ in Eq. (12.3) depends only on historical information.

If the minimal martingale measure is also variance-optimal, as it is our case, the solution of Problem 12.1 is given in feedback form as

$$\tilde{H}_s^{(c)} \;=\; \frac{\mu - r}{b}\left[V_{s-} - c - \int_0^s \tilde{H}_u^{(c)} dW(u)\right]. \tag{12.5}$$

Controlling every moment the amount invested in the asset $\tilde{Z}(s)$ using the solution of Problem 12.1, we influence the path of the portfolio value $\tilde{X}(s)$. However, it should be noticed that the solution of the basic problem is nonsense from an economic point of view. If the cumulated expenditures fall short, the discounted value of the portfolio will be pulled down. We should not apply the solution of Problem 12.1 in practice. Nevertheless, this problem is useful as a starting point. Before showing the main optimization problem, let us introduce two closely-related problems.

12.3 Optimal choice for the initial capital

Problem 12.2: Let Θ be the space of all investment strategies $\tilde{H}$ such that $\tilde{G}_1(\tilde{H})$ is in the space $\mathcal{S}^2$ of semimartingales.

We consider the following optimization problem

$$\min \mathbb{E}\left[\left(\Pi(1) - c - \tilde{G}_1(\tilde{H})\right)^2\right], \text{ over all pairs } (c, \tilde{H}) \in \Theta. \quad (12.6)$$

[Sch93] showed that the solution of Problem 12.2 is given by $c^* = \Pi_0$ and $\tilde{H}^{(c^*)}$. In our case, the optimal choice for the initial capital in Problem 12.1 is

$$c^* = \mathbb{E}[\Pi(1)]. \quad (12.7)$$

12.4 Variance-minimizing strategy

Problem 12.3: Let Θ be the space of all investment strategies $\tilde{H}$ such that $\tilde{G}_1(\tilde{H})$ is in the space $\mathcal{S}^2$ of semimartingales.

We consider the following optimization problem

$$\min \mathrm{Var}\left[\left(\Pi(1) - c - \tilde{G}_1(\tilde{H})\right)^2\right], \text{ over all } \tilde{H} \in \Theta. \quad (12.8)$$

This type of problem was solved by [Ric89], [DR91] and [Sch93] at different levels of generality. The solution of Problem 12.3 is given by the strategy $\tilde{H}^{(c^*)}$ (see [Sch93]).

12.5 Main optimization problem

Outgoing from the solution of Problem 12.1, we worked on the formulation of a related problem that leads to a more realistic investment strategy, feasible from the governmental perspective.

To explain the main idea for the formulation of the problem, let us consider the following citation from [WP02], p. 35, about reserve funds as governmental ex-ante financing tool:

> Reserve funds involve setting aside funds in highly liquid accounts held either domestically or abroad. In theory the annual contribution to that fund should be equal to the annual expected loss of the risk the fund is designed to cover. The cost of these funds is primarily the **opportunity cost** of not investing the funds elsewhere: highly liquid accounts offer only a 5-6% rate of return compared to the 16% rate of return frequently attributed to investment in development projects.

Our idea for the mathematical formulation is to diminish this opportunity cost through investment in the market. We renounce to absolute high liquidity allocating some resources for investment, but we reduce risk to its intrinsic value using an investment strategy. Our goal is to find an investment strategy that allocates the amount of investment resources in the market strictly necessary to hedge the maximum between the cumulated expenditures $\Pi(1)$ and the capital resulting from investing $c^* = \mathbb{E}[\Pi(1)]$ in a bank account earning r during the fiscal year.

Problem 12.4: Let Θ be the space of all investment strategies $\tilde{Q}$ such that $\tilde{G}_1(\tilde{Q})$ is in the space $\mathcal{S}^2$ of semimartingales.

The optimization problem is

$$\min \mathbb{E}\left[\left(\Pi^*(1) - k - \tilde{G}_1(\tilde{Q})\right)^2\right], \; k \in \mathbb{R}, \text{ over all } \tilde{Q}^* \in \Theta, \tag{12.9}$$

where

$$\Pi^*(1) = \max\{c^* e^r, \Pi(1)\}. \tag{12.10}$$

$c^* e^r$ represents the amount of capital that we would have in the fund if we would invest 100% of an initial capital $c^* = \mathbb{E}[\Pi(1)]$ in the bank account earning interest rate r. We have chosen the constant c^* for the formulation of the main problem because it is the optimal starting point to hedge the cumulated expenditures $\Pi(1)$.

12.6 Solution of the main optimization problem

The solution of Problem 12.4 will be denoted as $\tilde{Q}^{(k)}$. We solve this problem in an analogous way to Problem 12.1. We should find the intrinsic value process V_s^* that satisfies $V_0^* = \mathbb{E}[\Pi^*(1)]$ and $V_1^* = \Pi^*(1)$ $\mathbb{P}$-a.s., where $\Pi^*(s) = \max\{c^* e^r, \Pi(s)\}$, $s \in [0, 1]$.

We define the intrinsic value process V_s^* as follows:

$$V_s^* \quad = \quad \Pi^*(s) + \mathbb{E}[\Pi^*(1) - \Pi^*(s)]. \tag{12.11}$$

Equation (12.11) (above) satisfies the conditions $V_0 = \mathbb{E}[\Pi^*(1)]$ and $V_1 = \Pi^*(1)$.

Finally, the explicit solution of the main optimization problem (Problem 12.4) in feedback form is

$$\tilde{Q}_s^{(k)} \quad = \quad \frac{\mu - r}{b}\left[V_{s-}^* - k - \int_0^s \tilde{Q}_u^{(k)} dW(u)\right]. \tag{12.12}$$

The optimal choice for k in Problem 12.4 is $k^* = \mathbb{E}[\Pi^*(1)]$. From $\mathbb{E}[\Pi^*(1)] > \mathbb{E}[\Pi(1)]$, we know that the optimal starting capital k^* is higher than c^*. Although Problem 12.4 has a solution for all $k \in \mathbb{R}$, from an economical perspective, c^* can be interpreted as the minimal acceptable value of k.

We have conceived Problem 12.4 to be adequate from the public administration point of view. This mathematical model is useful when analyzing quantitatively the feasibility of the established goals at the end of every fiscal year.

12.7 The suboptimal strategy

The solution of Problem 12.4 ($\tilde{Q}^{(k)}(s)$) has the following disadvantages:

1. It can take negative values.

2. It can demand more resources than we have in our portfolio.

Therefrom, we suggest the use of the following (suboptimal) strategy:

$$\tilde{I}_s^{(k)} \quad := \quad \min\{\max\{\tilde{Q}_s^{(k)}, 0\}, \tilde{X}^*(s^-)\}. \tag{12.13}$$

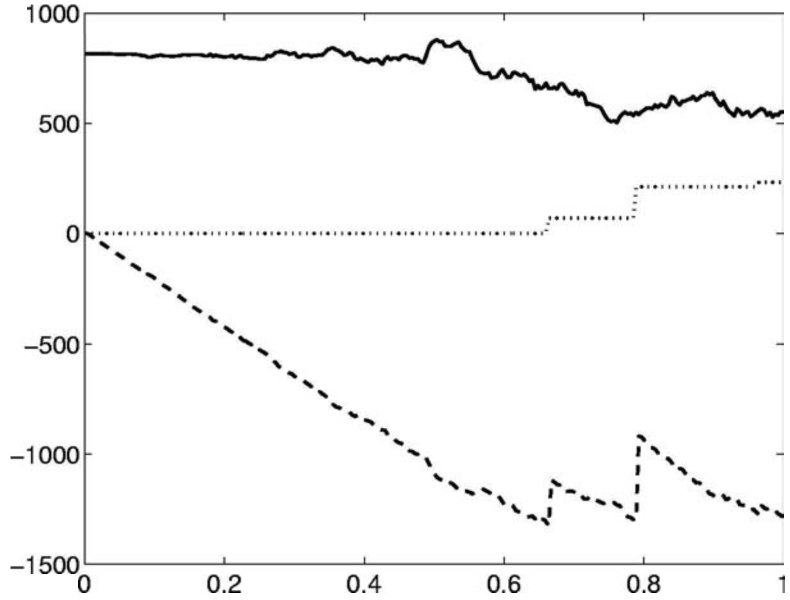

Fig. 12.1: Portfolio value $X(s)$ resulting from applying the optimal strategy of the basic problem (solid line), optimal amount to be invested $H^{(c)}(s)$ (dashed line) and cumulated expenditures $\Pi(s)$ (dotted line).

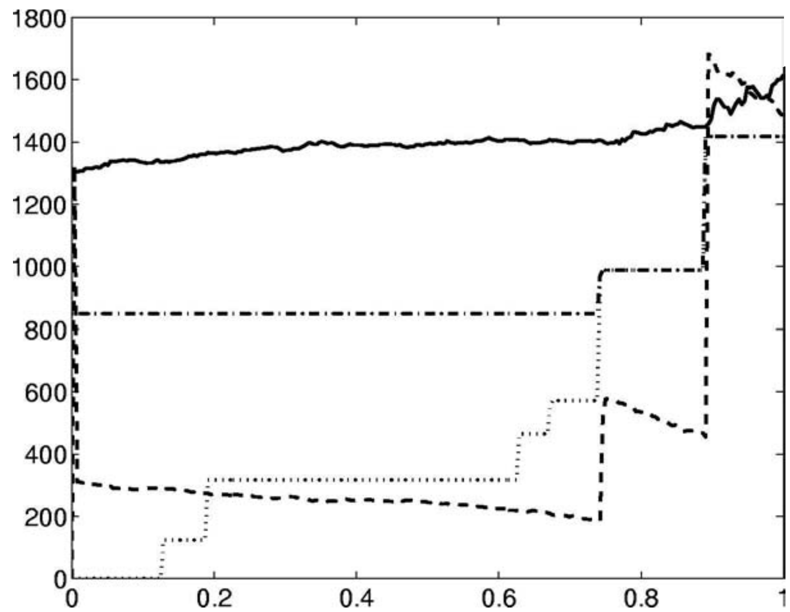

Fig. 12.2: Portfolio value $X^*(s)$ with initial capital $k = k^*$ resulting from applying the optimal strategy (solid line), optimal amount to be invested $Q^{(k)}(s)$ (dashed line), cumulated expenditures $\Pi(s)$ (dotted line), and $\Pi^*(s) = \min\{\max\{\Pi(s), 0\}, \tilde{X}^*(s^-)\}$ (dash-dot line).

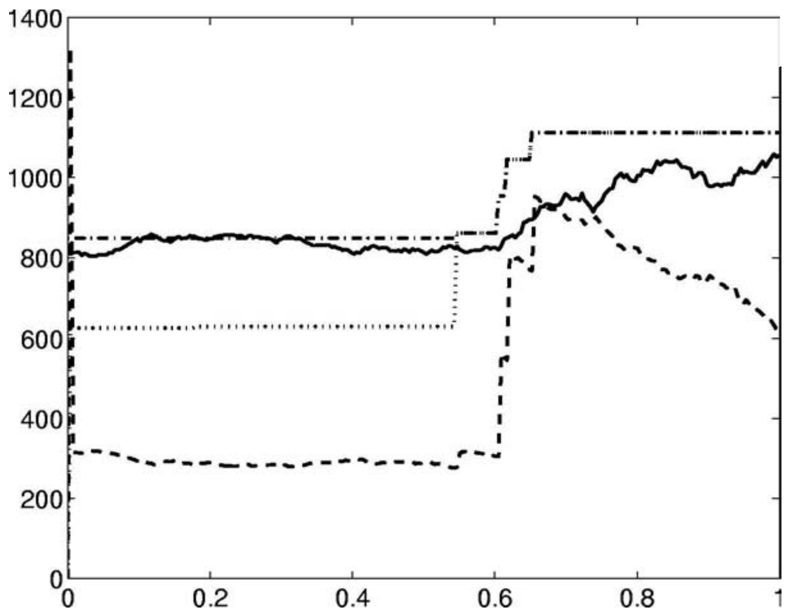

Fig. 12.3: Portfolio value $X^*(s)$ with initial capital $k = c^*$ resulting from applying the optimal strategy (solid line), optimal amount to be invested $Q^{(k)}(s)$ (dashed line), cumulated expenditures $\Pi(s)$ (dotted line) and $\Pi^*(s) = \min\{\max\{\Pi(s), 0\}, \tilde{X}^*(s^-)\}$ (dash-dot line).

12.8 Examples

In this section, we show some simulations that will help us visualize the functioning of the strategies solving the basic problem and the main optimization problem. Finally, we give an example of suboptimal strategy and we compare it with the corresponding optimal strategy.

We programmed the solution of the basic problem and of the main optimization problem using Matlab. For the simulations, we retake the settings of Sec. 9.0.1. The market parameters are $r = 0.4$, $\mu = 0.15$ and $b = 0.2$.

With illustration purposes, all the graphics of this section show the simulated present value processes.

12.8.1 Example A: the solution of the basic problem

The solution of Problem 12.1 is valid for all $c \in \mathbb{R}$. For the simulation, we used the optimal value for c ($c^* = E[\Pi(1)] = 816$) as initial capital to calculate the optimal strategy.

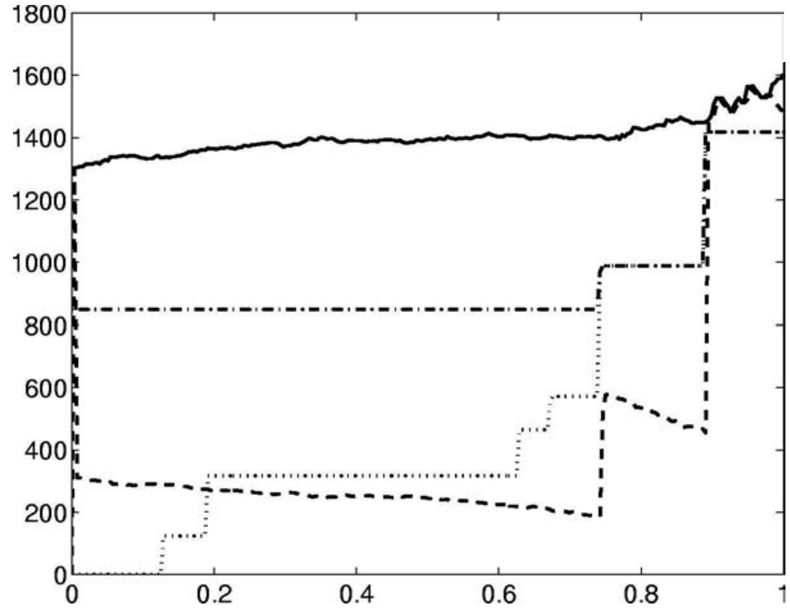

Fig. 12.4: Portfolio value $X^{**}(s)$ with initial capital $k = k^*$ resulting from applying the suboptimal strategy (solid line), suboptimal amount to be invested $I^{(k)}(s)$ (dashed line), cumulated expenditures $\Pi(s)$ (dotted line) and $\Pi^*(s) = \min\{\max\{\Pi(s), 0\}, \tilde{X}^{**}(s^-)\}$ (dash-dot line).

The simulation plotted in Fig. 12.1 evidences the economic nonsense of the basic problem. The optimal amount to be invested at time s is given by $H(s) = e^{rs}b\tilde{H}^{(c^*)}(s)$. Observe that the amount to be invested at moment s is always negative in this example. We can appreciate how the portfolio value $X(s) = e^{rs}\tilde{X}(s)$ is pulled down.

12.8.2 Example B: the solution of the main optimization problem

We calculated the expectation of $\Pi^*(s), 0 \leq s \leq 1$, numerically. The estimation of $\mathbb{E}[\Pi^*(1)]$ after 50,000 simulations is 1298.2.

The solution of the main optimization problem (Problem 12.4) is valid for all $k \in \mathbb{R}$. For the simulation, we first used the optimal value for k ($k^* = E[\Pi^*(1)] = 1298.2$) as initial capital to calculate the optimal strategy (see Fig. 12.2) and then we tried with $k = c^*$ (see Fig. 12.3).

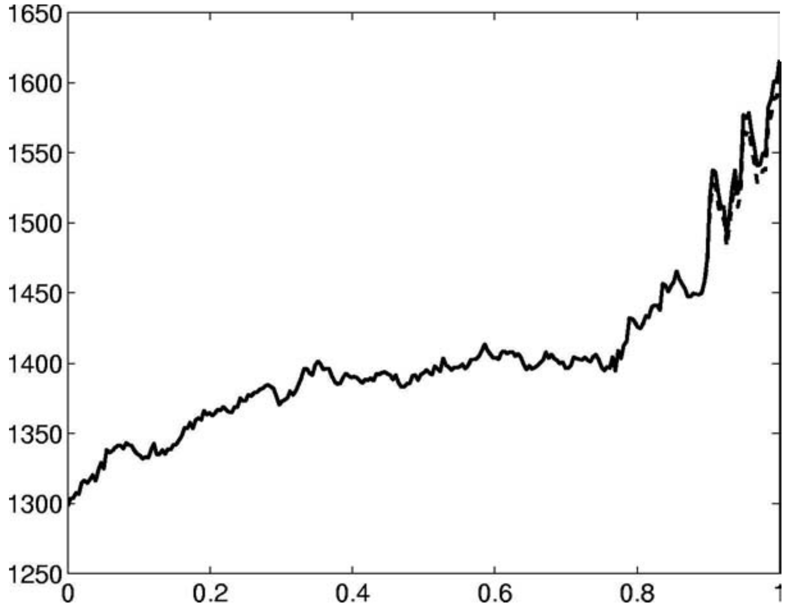

Fig. 12.5: Comparison of the suboptimal portfolio $X^{**}(s)$ with initial capital $k = k^*$ of Example C (dashed line) vs. the optimal portfolio $X^*(s)$ with initial capital $k = k^*$ (solid line) of Example B.

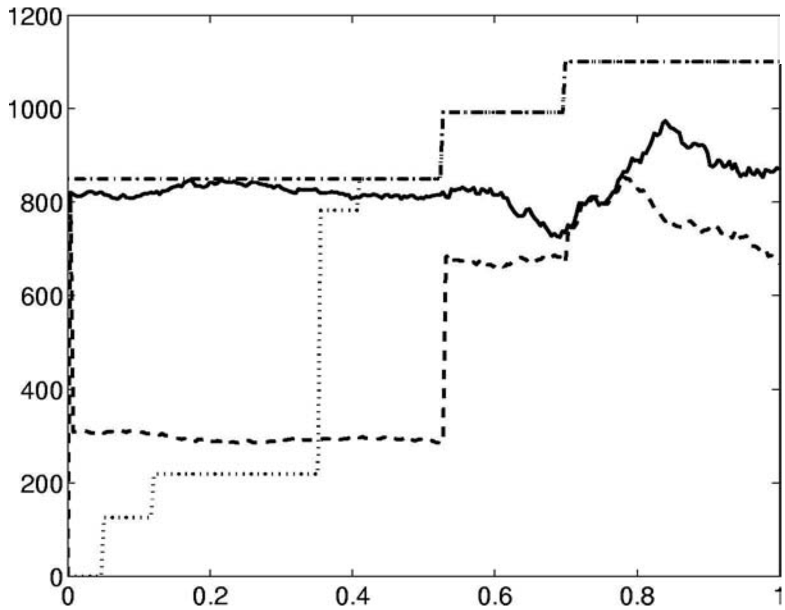

Fig. 12.6: Portfolio value $X^{**}(s)$ with initial capital $k = c^*$ resulting from applying the suboptimal strategy (solid line), suboptimal amount to be invested $I^{(k)}(s)$ (dashed line), cumulated expenditures $\Pi(s)$ (dotted line) and $\Pi^*(s) = \min\{\max\{\Pi(s), 0\}, \tilde{X}^{**}(s^-)\}$ (dash-dot line).

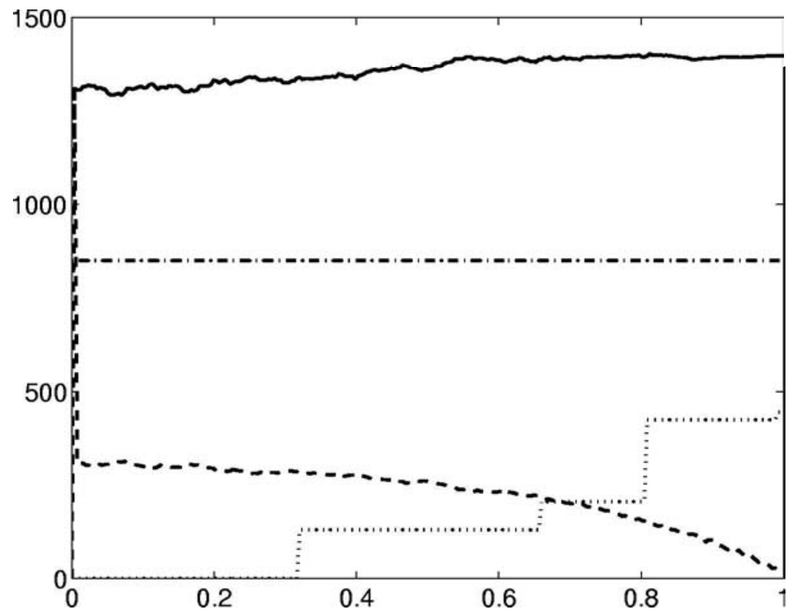

Fig. 12.7: Portfolio value with initial capital $k = k^*$ resulting from applying the optimal strategy (solid line), optimal amount to be invested (dashed line), cumulated expenditures $\Pi(s)$ (dotted line) and $\Pi^*(s) = \min\{\max\{\Pi(s), 0\}, \tilde{X}^*(s^-)\}$ (dash-dot line). The optimal and the suboptimal strategies coincide.

12.8.3 Example C: the suboptimal strategy

In this section, we retake the same simulation for the market and the expenditures of Example B and we calculate the suboptimal strategy. Compare Fig. 12.2 vs. Fig. 12.4, and Fig. 12.3 vs. Fig. 12.6. In these examples, the optimal strategy demanded an investment superior to the portfolio value. The suboptimal strategy does not allow an investment higher than the portfolio value.

In Fig. 12.5, we can appreciate the suboptimal and the optimal strategies of Fig. 12.2 (Example B) and Fig. 12.4 (Example C) together.

Finally, we present an example of the case when both strategies coincide (see Fig. 12.7) and a case with low cumulated expenditures and initial capital $k = c^*$.

12.9 Final comments

In this part of the thesis, we developed an optimal management strategy for the wealth $X(s)$ in order to hedge the total accumulated expenditure at the end of the fiscal year $\Pi(1)$. We showed that investment combined with XL-reinsurance is a

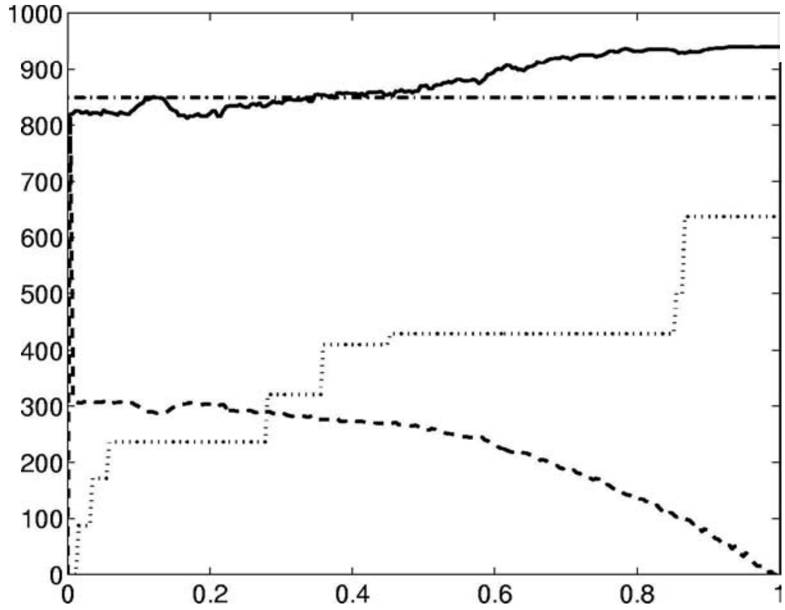

Fig. 12.8: Portfolio value with initial capital $k = c^*$ resulting from applying the suboptimal strategy (solid line), suboptimal amount to be invested (dashed line), cumulated expenditures $\Pi(s)$ (dotted line) and $\Pi^*(s) = \min\{\max\{\Pi(s), 0\}, \tilde{X}^*(s^-)\}$ (dash-dot line).

plausible alternative for risk-averse governments to improve the risk management of natural disasters funds and, therefore, improve long-term planning.

A topic for further research is to solve the optimization problem at different levels of generalization and to incorporate other alternatives for risk management in the modelling. We can also calculate optimal strategies for the reinsurance company and investigate the interaction of the governmental strategy with the strategy of a reinsurance company.

Nevertheless, we should remember that every model needs parameters. In the case of natural disasters, we do not usually have enough data or data bases are incomplete and imprecise.

In our opinion, the stochastic analysis of the underlying natural processes involved in natural disasters should be an important component for an integrated risk management. We could use this knowledge to generate realistic synthetic data bases and historical sequences.

However, the difficulty of this kind of research is that natural disasters are the result of the interaction of many processes. In which case, we need to begin with the study of the components before we intend to model any form of interaction.

For the beginning of our research, we should choose and concentrate our efforts in only one geophysical process. Considering that hydro-meteorological disasters have caused most of the expenditures of FONDEN and that rain is a fundamental variable of observation for many hydro-meteorological disasters, we focused our research in the rain process and its stochastic properties.

We are convinced that for a valuable analysis of the stochastic properties of *rainfall*, a purely mathematical analysis of data in the form of time-series is not enough. We strongly believe that rainfall behavior in space and time is so complex, that we should take geophysical sciences into consideration for the stochastic modelling.

In our opinion, the future of actuarial mathematics applied to natural disasters is the incorporation of geophysics. This perspective can also be extended for financial mathematics, because nowadays we have financial instruments that are indexed to some geophysical processes.

Now let's consider the following citation:

> "In Sweden, precipitation is rarely extreme in character, but there are severe disturbances from time to time and considerable variations on a yearly basis. The last 15 years have been remarkable because of an unusually high frequency of weather-related disaster events. The year 2000 featured the highest ever recorded precipitation levels, with some major floods." ([SS03])

Whether disturbances in Sweden and all around the world are a consequence of global climate changes or natural climate variability, it forces us to use stochastic models which are able to capture changes in weather over several time scales. Our approach here is the application of multifractal models.

Actually, several multifractal representations of rainfall have been proposed in the literature. For example, pulse-based models (e.g. [VI02], [BS99] and [Dei00]); non pulse-based models using wavelet decompositions (e.g. [PF96]) or non pulse-based models using discrete or continuous multiplicative cascades. For this research project, we restricted ourselves to non pulse-based multifractal representations using multiplicative cascades. Nevertheless, this does not mean that we suggest leaving out other representations.

From [GW93]:

> "It is clear that the analysis of intermittency and extremes in rainfall is particularly amenable to the cascade theory. Given the geometric

> and physical identity of quantities that have appeared in previous spatial hierarchial models of the type discussed in section 1, it is natural to explore how a cascade theory might explain the hierarchial or clustering structures."

With this motivation, we began to study multiplicative cascade models for rain.

The next part of our research is focused in placing some standard hydrological models for rain in the framework of multifractal theory and analyzing the potential application of multiplicative cascade models for rain in risk management. Part IV begins with three introductory chapters. We present our results in Chapters 16 and 17. We do not keep the notation from previous chapters.

Part IV

MULTIPLICATIVE CASCADE MODELS FOR RAIN IN RISK MANAGEMENT

13. FRACTAL GEOMETRY AND MULTIFRACTAL THEORY

Multifractal theory is a very young discipline, which includes fractal geometry. On account of this, we begin Part IV with two introductory chapters.

In this chapter, we introduce fractal geometry, and then multifractal theory. In the next chapter, we place stochastic processes with simple scaling behavior in the framework of multifractal theory and we introduce the topic of multiple scaling.

Fractal geometry, as defined in [Fal97], is the discipline that provides a general framework for the study of *irregular sets* (Def. 13.4).

We define multifractal theory as the discipline that:

1. aims to study the scaling behavior of measures (Def. 13.8),
2. integrates simple scaling stochastic models in a more general framework and
3. provides stochastic models for phenomena in which scaling occurs with a range of different power laws.

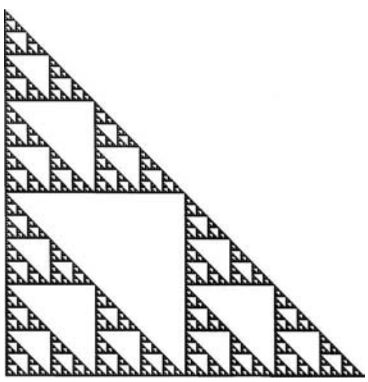

Fig. 13.1: Sierpinski triangle, conceived by Wracłav Sierpiński (1882-1969)

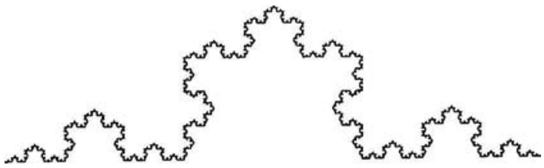

Fig. 13.2: Koch curve, conceived by Niels Fabian Helge von Koch (1870-1924) in 1904. To construct this curve we begin from a line segment. Then we replace the central third of this line by two lines of its own length, placed continuously as in an equivalent triangle. This process is continued for any segment, always on the same side of the curve. The Koch curve is infinite in length and its intersection with the original line corresponds to the Cantor set (Def. 13.3).

Multifractal theory is rooted in measure theory and stochastic analysis, and retakes some concepts of fractal geometry. Most of the theory and its applications are being developed in the frameworks of different natural sciences. For this reason, the available literature is written using different technical vocabulary, scientific methodology, notation and mathematical rigor. Hence, at its actual stage of development, a multidisciplinary level of understanding is required to decode and interrelate the scientific progresses in this young research field.

Definition 13.1: Let $A \subset \mathbb{R}^n$, $A \neq \emptyset$. We will denote the set of the countable ϵ-covers of A as $\mathcal{A}(\epsilon, A)$, where $\epsilon > 0$. For $s > 0$, let

$$h^s_\epsilon(A) := \inf \left\{ \sum_{i=1}^{\infty} |A_i|^s \,\middle|\, A_i \in \mathcal{A}(\epsilon, A) \right\}. \tag{13.1}$$

We define the s-dimensional Hausdorff measure as

$$h^s(A) = \lim_{\epsilon \to 0} h^s_\epsilon(A). \tag{13.2}$$

Definition 13.2: We define the Hausdorff dimension of a set A ($\dim_h(A)$) as

$$\dim_h(A) = \inf\{s : h^s(A) = 0\} = \sup\{s : h^s(A) = \infty\} \tag{13.3}$$

Remark 13.1: It is important to distinguish, that a dimension is a property of a set and it is not a measure.

Definition 13.3: Let

$$\begin{aligned} \Upsilon_0 &:= \bigcup_{k\in\mathbb{Z}} [2k, 2k+1], \\ \Upsilon_n &:= \Upsilon_0 \left(\frac{1}{3}\right)^n, \; n \in \mathbb{N}, \\ C_n &:= \Upsilon_0 \cap \ldots \cap \Upsilon_n \cap [0,1] \end{aligned}$$

(observe that Υ_0 and $\bigcap_{n=0}^{\infty} \Upsilon_n$ are closed).
The compact set

$$C = \bigcap_{n=0}^{\infty} C_n$$

was conceived by Georg Cantor (1845-1918) and is known as the Cantor set.

Example (Hausdorff dimension): Let $C = \bigcap_{n=0}^{\infty} C_n$ be the Cantor set (Def. 13.3) and $\mathcal{C}_\delta(C)$ be the smallest number of δ-covers required to cover the set C.

$$\dim_h(C) = \lim_{n\to\infty} \dim_h(C_n) \tag{13.4}$$

We observe, that $\forall\, n$ at least 2^n intervals of length $\delta_n = \left(\frac{1}{3}\right)^n$ are required to cover C_n. Therefore the Hausdorff dimension of a Cantor set is

$$\dim_h(C) = \frac{\ln \mathcal{C}_{\delta_n}(C)}{-\ln \delta_n} = \frac{\ln 2^n}{-\ln 3^{-n}} = \frac{\ln 2}{\ln 3} \approx 0.63. \tag{13.5}$$

Definition 13.4: Let A be a s-set (Def. 13.5). We say that A is an irregular set, if h^s-almost all of its points are irregular (Def. 13.6).

Definition 13.5: A is called a s-set if it is a Borel set $A \subset \mathbb{R}^n$ of Hausdorff dimension s, $s = dim_h A$, (Def. 13.2) and has positive finite s-dimensional Hausdorff measure (Def. 13.1), $0 < h^s(A) < \infty$.

Definition 13.6: Let A be a s-set. A point $x \in \mathbb{R}^n$ is called a regular point of A, if the lower and the upper densities of A at x (Def. 13.7) are equal to 1. That is, if

$$\underline{D}^s(A,x) = \overline{D}^s(A,x) = 1. \tag{13.6}$$

Otherwise, the point $x \in \mathbb{R}^n$ is called irregular.

Definition 13.7: Let A be a s-set. The lower and upper densities of A at a point $x \in \mathbb{R}^n$ are defined as

$$\underline{D}^s(A, x) = \underline{\lim}_{r \to 0} \frac{h^s(A \cap B_r(x))}{(2r)^s} \tag{13.7}$$

and

$$\overline{D}^s(A, x) = \overline{\lim}_{r \to 0} \frac{h^s(A \cap B_r(x))}{(2r)^s}, \tag{13.8}$$

where $B_r(x)$ is the closed disc of radius r and center x.

Definition 13.8: Let μ be a set function on a field $\mathcal{M}$ in the space Θ, where $\Theta \in \mathcal{M}$ and $\Theta^c = \emptyset$. If

1. (non-negativity) $\mu(A) \in [0, \infty]$ for $A \in \mathcal{M}$, and
2. (countable additivity) for a sequence $\{A_k\}_{k=1}^{\infty}$ of disjoint elements of $\mathcal{M}$,

$$\mu\left(\bigcup_{i=1}^{\infty} A_i\right) = \sum_{i=1}^{\infty} \mu(A_i);$$

then μ is a measure.

13.1 Self-similarity and self affinity

Both notions, self-similarity and self-affinity, can be applied to sets (fractal geometry) or measures (multifractal theory). Actually, there is no standard definition for "self-affinity" and "self-similarity" among disciplines.

Historically, the development of the notion of self-affinity began as a generalization of the notion of self-similarity. In the beginning, the notion of a self-similar structure was simply that it should look roughly the same on every scale. In time, it was observed that there are different types of scale invariance. A step forward in the development of the theory was reached with the introduction of the notions of isotropy and anisotropy to classify scale-invariant structures. The terms self-similarity and self-affinity were coined by Mandelbrot.

Self-similar objects are isotropic, in a deterministic or a statistical sense. Self-similarity is a particular case of self-affinity in the sense that self-affine objects may also be anisotropic or statistically anisotropic.

Fig. 13.3: Barnsley fern, code conceived by Michael Fielding Barnsley and presented at the congress SIGGRAPH-85. To obtain this figure, we first need a starting point (x_0, y_0) in the cartesian plane. Then we apply the corresponding creation rule to (x_0, y_0) to find a second image point (x_1, y_1). We repeat the process and we plot every resulting point. When several points have been plotted, we find the familiar shape.

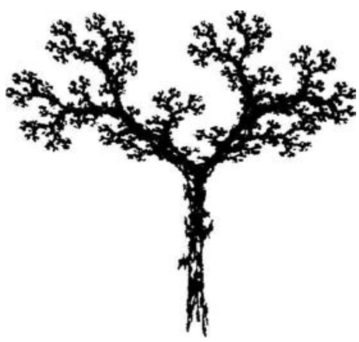

Fig. 13.4: Oak tree, its code is a slight variation of the Barnsley fern code.

Fractal sets can be isotropic, statistically isotropic, anisotropic or statistically anisotropic. The treatment of this topic is out of the scope of this research. We limit ourselves to mention some examples of self-similar and self-affine fractal sets. If the reader has special interest in fractal geometry, we recommend [Fal90] and [Fal97].

Some well-known examples of self-similar sets are the Cantor Set (Def. 13.3), the Sierpinski triangle (Fig. 13.1) and the Koch curve (Fig. 13.2). The Barnsley fern (Fig. 13.3) and the oak tree (Fig. 13.4) are self-affine sets that result from iterating linear equations in the two-dimensional cartesian plane. For further details about these fractal sets and their algorithms see e.g, [Bar93] and [Her94].

In the real world, we only find "approximate" fractals or multifractals that we can model with "exact" fractals or multifractals. For example, segments of coastline, snowflakes, fern leaves and oak trees are approximately self-affine. In particular, the segments of coastline and snow flakes are approximately self-similar.

14. STOCHASTIC PROCESSES WITH SIMPLE SCALING BEHAVIOR

Multiscaling stochastic models arise from simple scaling stochastic models. For this reason, we devote a chapter to place stochastic processes with simple scaling behavior in the framework of multifractal theory. We also emphasize the historical development of the theory.

14.1 Self-similar stochastic processes

In the context of multifractal theory, the proper name for what in stochastic analysis we usually call "self-similar stochastic processes" is "*self-affine stochastic processes*". The reason for this is that they are not isotropic processes in all cases.

For clarity purposes, we keep the terminology used in the cited references but we add * to stress when the generalization to self-affinity is valid.

Definition 14.1: ([ST94], p. 311) The real-valued stochastic process $\{X(t), t \in T\}$ with index set $T \in \{\mathbb{R}, \mathbb{R}^+, [0, \infty)\}$ is said to be self-similar* with index $H > 0$ (H-ss) if its finite-dimensional distributions satisfy the relation

$$(X(at_1), \ldots, X(at_m)) \stackrel{d}{=} a^H (X(t_1), \ldots, X(t_m)) \tag{14.1}$$

for any choice of values $t_1, \ldots, t_m \in T$, $a \in \mathbb{R}^+$.

Definition 14.1 can be extended to the cases:

1. $(X(t))$ is complex-valued ($\{\text{Re}\, X(t), \text{Im}\, X(t), t \in T\}$), [ST94], p. 311, and

2. $(X(t))$ is a random field ($\{X(t), t \in \mathbb{R}^n\}$, $n \geq 1$), [ST94], p. 392.

Remark 14.1: Lamperti [Lam62] was the first to establish the connection of stochastic self-similar⋆ processes to limit theorems. He called "semi-stable" to the class of processes "that can occur as limits upon subjecting a fixed stochastic process to infinite contractions of its time and space scales".

Let $\{X(t),\ t > 0\}$ be a d-dimensional stochastic processes with non-degenerate distribution. In [Lam62], $(X(t))$ is called a semi-stable process if it obeys the continuity condition

$$\lim_{h \to 0} \mathbb{P}(||X(t+h) - X(t)|| > \epsilon) = 0,\ \forall\, t \geq 0,\ \epsilon > 0, \tag{14.2}$$

and, keeping the notation of [Lam62],

$$\{X(at)\} \sim \{X(t)\}. \tag{14.3}$$

This means, if $(X(t))$ satisfies Eq. (14.2) and

$$\{X(at)\} \stackrel{d}{=} \{b(a)X(t) + c(a)\},\ a > 0, \tag{14.4}$$

where $b(a)$ is a positive function and $c(a) \in \mathbb{R}^d$, then $(X(t))$ is self-similar⋆. If $X(t)$ is self-similar⋆ and $X(0) = 0$, then $c(a) = 0$ and $b(a) = a^H$, $H > 0$ ([Lam62]). The term semi-stable was replaced by self-similarity⋆ in later literature.

Let us introduce the definition of isotropic process.

Definition 14.2: Let $\{X(t), t \in T\}$ with index set $T \in \{\mathbb{R}, \mathbb{R}^+, [0, \infty)\}$ be a stochastic process satisfying

$$\{X(st+h) - X(h)\} \stackrel{d}{=} \{s^H(X(t+h) - X(h))\}. \tag{14.5}$$

$(X(t))$ is said to be isotropic if

$$\{X(t) - X(s)\} \stackrel{d}{=} \{X(|t-s|)\}. \tag{14.6}$$

We wish to stress that if the process $(X(t))$ is self-affine and isotropic, $(X(t))$ is self-similar.

It is easy to verify that if the isotropic condition holds (see Eq. (14.6)), then

$$\mathbb{E}[X(t)^2] = |t|^{2H}\mathbb{E}[X(1)] \tag{14.7}$$

and

$$\mathbb{E}[X(t)X(s)] = \frac{1}{2}\{|s|^{2H} + |t|^{2H} - |t-s|^{2H}\}\mathbb{E}[X^2(1)]. \tag{14.8}$$

Definition 14.3: Let $\{X(t), t \in T\}$ with index set $T \in \{\mathbb{R}, \mathbb{R}^+, [0,\infty)\}$ be a self-affine stochastic process that does not satisfy the condition of isotropy (see Eq. (14.6)). In this case, we say that $(X(t))$ is anisotropic.

Definition 14.4: Let $\{X(t), t \in T\}$ be a H-ss stochastic process with index set $T \in \{\mathbb{R}, \mathbb{R}^+, [0,\infty)\}$. If $(X(t))$ has stationary increments, i.e. if

$$\{X(t+h) - X(h), t \in T\} \stackrel{d}{=} \{X(t) - X(0), t \in T\}, \forall\, h \in T, \tag{14.9}$$

we say that it is H-sssi ([ST94]).

Consider the following definition:

Definition 14.5: Let $\{Y_j, j = 1, 2, \ldots\}$ be a stationary sequence with zero mean. We say that Y_j belongs to the domain of attraction of a process $\{X(t), t \geq 0\}$, if the finite dimensional distributions of

$$X_N(t) = \frac{1}{d_N} \sum_{j=1}^{\lfloor Nt \rfloor} Y_j,\ t \geq 0. \tag{14.10}$$

Lamperti (1962) showed that self-similar* stochastic processes results from limits of normalized sums: the limit process $(X(t))$ of Def. 14.5 should be self-similar*. d_N in Eq. (14.10) is any positive normalising factor satisfying

$$\lim_{N\to\infty} d_N = \infty, \tag{14.11}$$

converges as $N \to \infty$ to the finite-dimensional distribution of $(X(t))$. Specifically, d_N must have the form $N^H L(N)$, where $L(\cdot)$ is a slowly varying function at infinity. It means, $L(\cdot)$ is positive and satisfies

$$\lim_{N\to\infty} \frac{L(kN)}{L(N)} = 1,\ \forall\, k > 0. \tag{14.12}$$

Definition 14.6: Let $\{X(t), t \in T\}$ be a stochastic process with index set $T \in \{\mathbb{R}, \mathbb{R}^+, [0,\infty)\}$. If

$$\{X(t+h), t \in T\} \stackrel{d}{=} \{X(t), t \in T\}, \forall\, h \in T, \tag{14.13}$$

we say that $\{X(t), t \in T\}$ is a stationary process.

Let $(X(t))$ be a non-degenerate H-ss process. Observe that $(X(t))$ can not be stationary. If it were, we would have for any $a > 0$ and $t > 0$,

$$X(t) \stackrel{d}{=} X(at) \stackrel{d}{=} a^H X(t) \tag{14.14}$$

and we would obtain a contradiction because $a^H X(t) \to \infty$ as $a \to \infty$ ([ST94], p.312).

The relation of H-self-similarity* to stationarity is described by Theorem 14.1.

Theorem 14.1: If $\{X(t),\ t > 0\}$ is H-ss then

$$Y_t = e^{-Ht} X_{e^t},\ t \in \mathbb{R} \tag{14.15}$$

is stationary. Conversely, if $\{Y(t),\ t \in \mathbb{R}\}$ is stationary, then

$$X(t) = t^H Y_{\ln t},\ t > 0, \tag{14.16}$$

is H-ss. ([KM01], p. 547)

14.1.1 Examples and its historical development

One of the best-known examples of a stochastic self-similar* process is the Brownian motion. This is also a canonical example of a Markov process and a martingale.

The biologist Robert Brown discovered it in 1827, when studying the microscopical movement of pollen particles in water. The stochastic model for Brownian motion and its stochastic calculus were developed much later. In 1900, Louis Bachelier published the first mathematical study of Brownian motion in his doctoral dissertation *Théorie de la spéculation*, where he proposed to describe the evolution of quotes in the stock market. Albert Einstein and Robert Wiener were also pioneers in the development of the theory of Brownian motion. The stochastic model of Brownian motion is also known as Wiener process.

More than one century after Bachelier's visionary work, the Brownian motion has become a standard tool in mathematical finance. In Chapter 12, for example, we model the risky asset based on Brownian motion (Samuelson model) and, using stochastic calculus for Brownian motion, we find a projection of the random variables $\Pi(1), \Pi^*(1) \in \mathcal{L}^2$ into a probability space $(\Omega, \mathcal{F}, \mathbb{F}, \mathbb{P})$ provided with a filtration $\mathbb{F}$ that contains the $\mathbb{P}$-augmentation of the filtration generated by a Brownian motion and the process of cumulated expenditures $\Pi(s)$.

Despite of its complexity, Brownian motion is too simple for the modelling of some natural processes that play an important role in natural disasters. In the case of river flows, an important empirical evidence was provided by the hydrologist Harold Edwin Hurst. After decades of research in Egypt, he discovered that cumulative yearly flows of the Nile River do not obey a power law with $H = 0.5$, as expected from the classical central limit theorem, but with $H \cong 0.7$ ([Hur51]). Actually, the index of self-similarity* H is also known as *Hurst coefficient*. Based on Hurst's work, Mandelbrot (1965) proposed *fractional Brownian motion* (Def. 14.7), a process discovered by Andrei Nikolaevich Kolmogorov in 1940, to model the yearly flow levels of the Nile River ([Man65]). Nevertheless, since recent years we know that even fractional Brownian motion (FBM) is too simple for the stochastic modelling of processes like river flows and rainfall. FBM has the disadvantage that its increments have symmetrical distributions (isotropy); therefore this model is not appropriate for cases evidencing asymmetrical distributions ([Man97]) as it is our case.

Definition 14.7: A Gaussian H-sssi process $\{B_H(t), t \in T\}$ with index set $T \in \{\mathbb{R}, \mathbb{R}^+, [0,\infty)\}$, $\mathbb{E}[B_H(t)] = 0$ and autocovariance function

$$\text{Cov}(B_H(t_1), B_H(t_2)) = \frac{1}{2}\{|t_1|^{2H} + |t_2|^{2H} - |t_1 - t_2|^{2H}\}\text{Var}X(1), \quad (14.17)$$

where $0 < H \leq 1$, $t_1, t_2 \in \mathbb{R}$, is called fractional Brownian motion (FBM). If $\text{Var}X(1) = 1$, we say that $(B_H(t))$ is a standard fractional Brownian motion. Brownian motion is a particular case of fractional Brownian motion ($H = 0.5$).

It should be stressed that fractional Brownian motion is isotropic, and hence self-similar, if $B_H(0) = 0$ a.s.

Finally, define the process $\{Y(t),\ t \in \mathbb{R}\}$ as

$$Y(t) = e^{-0.5t} W(e^t), \quad (14.18)$$

where $W(t)$ is a standard linear Brownian motion ($\{B_{0.5}(t),\ t \geq 0\}$, $B_{0.5}(0) = 0$ a.s.). This scaled and time-transformed Wiener process is an Orstein-Uhlenbeck process. $(Y(t))$ is an example of a stationary process obtained from a H-ss process using Theorem 14.1.

14.2 Symmetric α-stable Lévy processes

Consider the following definition:

Definition 14.8: A r.v. Y is stable if, $\forall k$, there are i.r.v's $Y_1 \ldots Y_k$ with the same distribution as Y and constants $a_k > 0$, b_k, such that

$$\sum_{i=1}^{k} Y_i \overset{(d)}{=} a_k Y + b_k. \tag{14.19}$$

This equality forces $a_k = k^{\frac{1}{\alpha}}$ where $0 < \alpha \leq 2$ ([RY91], p. 110). The number α is called the index of the stable distribution. For $\alpha = 2$ we get the Gaussian random variables. Among the infinitely divisible r.v.'s, the so-called stable r.v.'s form a subclass.

If $\{Y(t), t \geq 0\}$ is a real-valued Lévy process, then any r.v. $Y(t)$ is infinitely divisible. Conversely, Lévy proved that for any infinitely divisible r.v. X there is a Lévy process $(Y(t))$ such that $Y(1) \overset{d}{=} X$ (see [RY91]).

Theorem 14.2: Consider the Lévy-Khintchine formula

$$\psi(u) = iMu - \frac{\sigma^2 u^2}{2} + \int \left(e^{iux - 1 - \frac{iux}{1+x^2}} \right) \nu(dx), \tag{14.20}$$

where $M \in \mathbb{R}$, $\sigma > 0$ and ν a Radon measure on $\mathbb{R} - \{0\}$ such that

$$\int \frac{x^2}{1+x^2} \nu(dx) < \infty. \tag{14.21}$$

If the r.v. Y is stable with index $\alpha \in (0, 2]$, then $\sigma = 0$ and the Lévy measure ν has the density

$$(m_1 \mathbf{1}_{(x<0)} + m_2 \mathbf{1}_{(x>0)})|x|^{-(1+\alpha)}, \tag{14.22}$$

with m_1 and $m_2 \geq 0$ ([RY91]).

Remark 14.2: Consider Theorem 14.2. Let $\{Y(t), t \geq 0\}$ be a real-valued Lévy process. If $M = 0$ and $m_1 = m_2$, $(Y(t))$ is a symmetric stable process of order α and Eq. (14.20) is $\psi(u) = -c|u|^\alpha$, where c is a positive parameter ([RY91]).

$\{Y(t), t \geq 0\}$ satisfies the following conditions:

1. $Y(0) = 0$ a.s.,

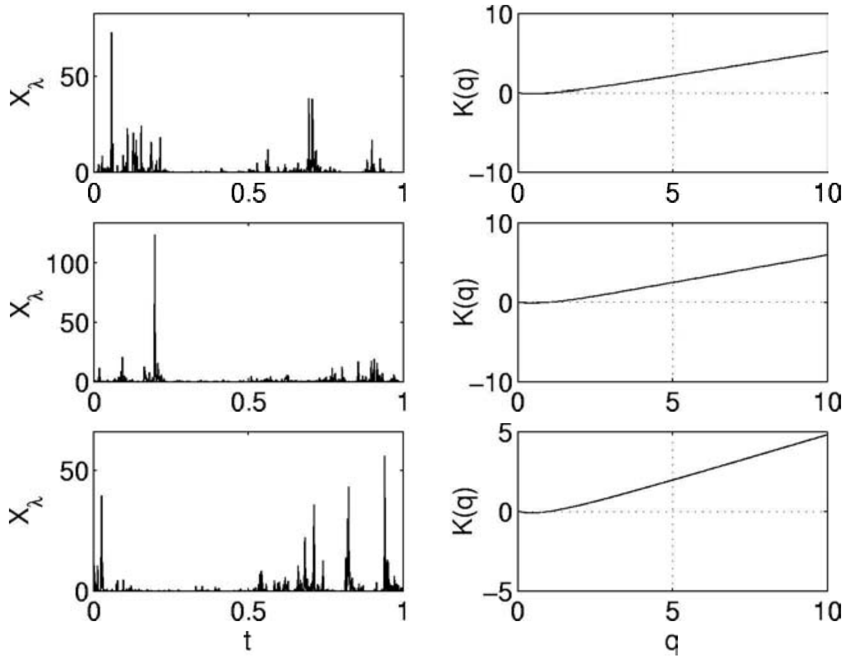

Fig. 14.1: Three simulations of the same multiscaling process in the interval $[0, 1]$ at scale $\Delta t = 2^{-10}$, scale ratio $\lambda = 2^{10}$, (left column) and the corresponding moment scaling functions $K(q)$ (right column), see Ap. A

2. $(Y(t))$ has independent increments,
3. $Y(t) - Y(s) \stackrel{d}{=} Y(t - s), t > s$, and
4. $Y(t)$ is symmetric α-stable $\forall\, t$

[KM01].

A symmetric stable process $\{Y(t), t \geq 0\}$ has the scale invariance property

$$Y(t) \stackrel{d}{=} c^{-1} Y(c^{\alpha} t) \tag{14.23}$$

([RY91]). Actually, symmetric α-stable processes are H-sssi with $H = \alpha^{-1} \in (0, \infty)$. The standard linear Brownian motion is a symmetric stable process ($\alpha = 2$). Another example is the Cauchy process ($\alpha = 1$, $\psi(u) = -t|u|$).

14.3 Final comments

In geophysics, we make inferences based on *measurements*. We should not confuse the samplings with the true process. Multifractal approaches take into account the possible changing behavior of processes across scales. Multiplicative cascade models are a special type of multifractal models.

All self-affine processes mentioned in the precedent sections of this chapter are simple scaling processes. This means that they have the same behavior at all scales. This is reflected in the fact that the scaling exponent H is a constant. If we want to model a stochastic process with multiscaling behavior, we should allow the existence of different scaling exponents. In some cases, scaling exponents take the form of a smooth function. This is the so-called codimension function. The multiplicative cascades of our interest have a convex codimension function. Simple scaling processes are defined in the context of multiscaling processes as having constant codimension.

Let X_λ be the sample of a process $X(t)$ in the interval $t \in [0, O_p]$, $O_p \in \mathbb{R}^+$, at scale $\Delta = O_p\lambda^{-1}$. That is, $t = 0, \lambda^{-1}, 2\lambda^{-1}, \ldots$ are the sampling times. Define the function

$$K(q) = \frac{\log(\mathbb{E}[|X_\lambda|^q])}{\log(\lambda)}. \tag{14.24}$$

Remark 14.3: $\mathbb{E}[|X_\lambda|^q]$ is not conceptually the same as $\mathbb{E}[|X|^q]$. The point-process X and the sample process X_λ are not necessarily equal in distribution.

We call $K(q)$ the moment scaling function. Estimating and plotting $K(q)$ is useful as a first approach to identify presumable multiscaling processes.

In Fig. 14.1, we present three simulations of a stationary multiscaling process generated from a multiplicative cascade and we plot the corresponding moment scaling function $K(q)$ in each case. Observe that $K(q)$ is convex. Its shape is the same for every simulation. The algorithm to simulate this process is given in Appendix A.

The same procedure, but using a standard linear Brownian motion ($B(t)$), is illustrated in Fig.14.2. As we know, standard Brownian motion is not a stationary process but has stationary increments ($dB(t)$) (see Fig. 14.3).

Multiscaling processes are characterized by their behavior among scales. It means, their random variables can be defined as being functions of the scale. If Δt is the scale and X is a random variable with multiscaling behavior, then we write $X(\Delta t)$. Alternatively, we can also represent X as a function of a scale ratio λ ($X_\lambda \equiv X(\Delta t)$).

The basic idea of multifractal approaches is the inference of the stochastic behavior of the process at small-scales using sample processes. Let $\mathcal{B}(\mathcal{X})$ be the

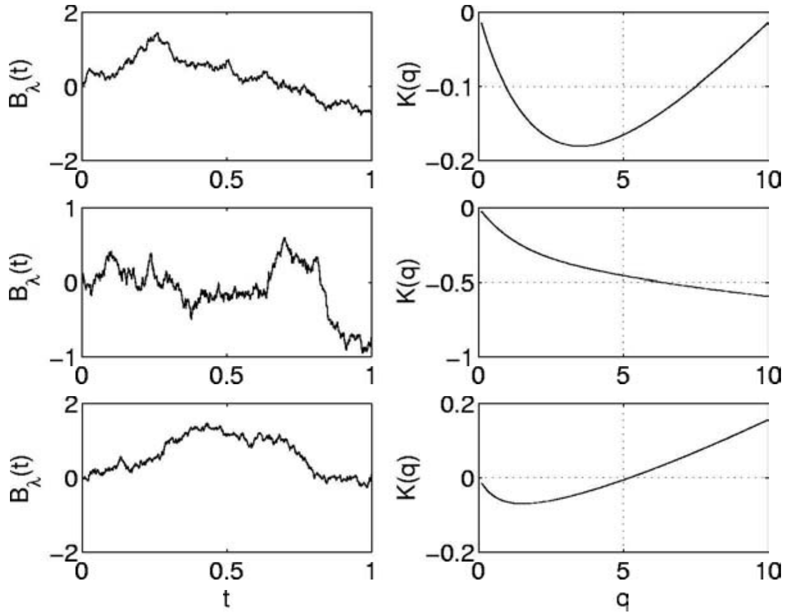

Fig. 14.2: Three simulations (samples) of a linear Brownian motion ($B_\lambda(t)$ in the interval $[0, 1]$ at scale $\Delta t = 0.001$, scale ratio $\lambda = 1000$, (left column) and the corresponding moment scaling functions $K(q)$ (right column)

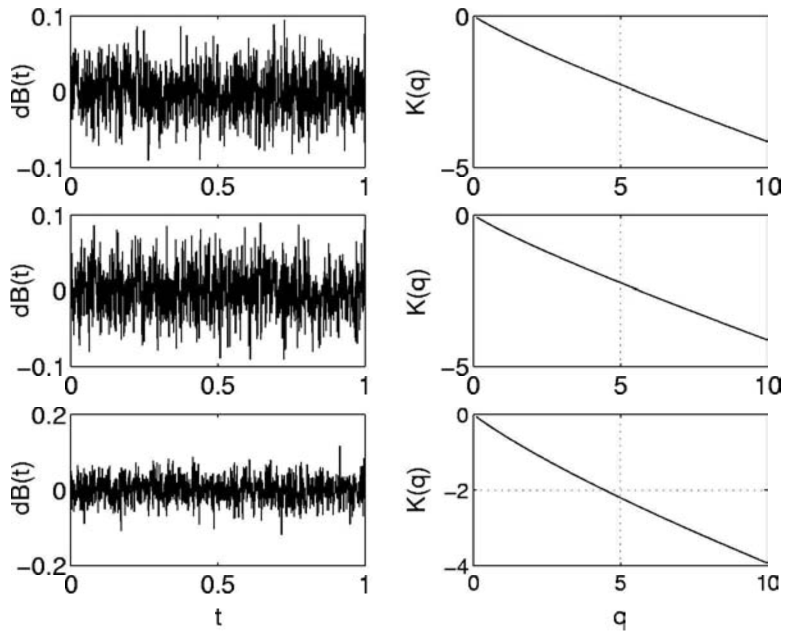

Fig. 14.3: Three simulations of the increments of linear Brownian motion in the interval $[0, 1]$ at scale $\Delta t = 0.001$ (left column) and the corresponding moment scaling functions $K(q)$ (right column) ($dB(t) := B(t) - B(t + \Delta t) \sim N(0, \sqrt{\Delta t})$)

Borel sets of $\mathcal{X}$, where $\mathcal{X} \subseteq \mathbb{R}^d$. Define the measure space $(\mathcal{X}, \mathcal{B}(\mathcal{X}), \mu^{(\delta)})$, where $\mu^{(\delta)}$ is a sampling measure changing with the scale δ. The multiscaling random variables $X(\delta)$ of our interest for this research are defined in $(\mathcal{X}, \mathcal{B}(\mathcal{X}), \mu^{(\delta)})\ \forall\, \delta$. We are interested in the limit of $\mu^{(\delta)}$ at small scales.

The limiting measure μ is not trivial. In Chapter 13, we explained the basics of multifractal theory and fractal geometry. Making an analogy, the limit measure μ represents for multifractal theory what an irregular set (Def. 13.4) for fractal geometry.

In subsequent chapters, we discuss the scale problem present in rain-intensity time series and the stochastic modelling of rainfall intensity[1] with further detail.

[1] The scale problem is also present in river-flow time series.

15. FUNDAMENTALS OF HYDROLOGY AND METEOROLOGY

In this chapter, we explain the fundamental concepts in hydrology and meteorology that we need in order to understand the scale problem in rain processes. An important setback for multidisciplinary research is the lack of a common language among disciplines. The same words can have different meanings among specialists in each field. For this reason, we adapted the technical language and usual notation of hydrology and meteorology to make this chapter accessible for mathematicians, actuaries and economists.

15.1 Rainfall measurement

We understand the term "rain" as falling water drops with a diameter of at least 0.5 mm (to observe is the difference from fog or drizzle). A large part of the water present in rainfall comes in drops with a diameter around 2 mm ([BC01]). Although rain is, strictly speaking, only one form of atmospheric precipitation, in this research we use the term rainfall interchangeably with precipitation.

We have two fundamental records of rainfall at a site:

1. rainfall depth (h) and

2. amount of precipitation (m).

Both are associated with an observation period of length d and a reference point (i.e. site location). d is called *duration*. When we are working within the multifractal framework, we refer to the duration d as *scale of observation*.

We wish to stress that measured m and h are only physical *estimates*, because of the many possible sources of error in the readings. Examples of them are the gauge height, large- and small-scale turbulence in the air flow, splash-in and evaporation ([BC01]). Actually, there are different methodologies for quality assurance of the data in meteorology (see e.g. [Fok03]). Further treatment of this topic is out of the scope of this research. In theory, we assume that the quality of all measurements has already been controlled and, where applicable, corrected.

The amount of precipitation (m) collected during d is a volume over a horizontal surface and it is given in liter per square meter (l/m^2).

The rainfall depth (h) is numerically equivalent to the amount of precipitation (m) but the former is normalized by area. Rainfall depth (also called rainfall height) also measures the rainfall collected over an horizontal surface during d but h is the height that corresponds to the water level in a column with a base of 1 m^2. The unit of measure is usually millimeters or inches. 1 mm of rainfall depth over a duration d is equivalent to 1 l/m^2 of rain water collected over the same duration d.

15.2 Rainfall intensity

The concept of rainfall intensity is of particular importance for the stochastic modelling of rain using multiplicative cascades.

Rainfall intensity (I) is defined as rainfall depth (h) per unit of time. I is usually given in mm/hr or in/hr. As far as estimation is concerned, there are different mathematical relationships to obtain rainfall intensity from rainfall data in the technical literature. For the purposes of this research, we work with time-average intensities. We define the rainfall time-average intensity as

$$I = \frac{h}{d},\ d > 0. \tag{15.1}$$

Usually, the measurement of the time-average intensity I for the interval $[t, t+d]$ is related to the instant in time $t + d/2$ for theoretical purposes.

In hydrology and meteorology, the *time-average intensity of a rainfall event* $(\bar{I})$ occurred during the time interval $[t, t + D]$, $t \geq 0$, in a given site location is defined as

$$\bar{I} = \frac{h}{D}, \tag{15.2}$$

where h is the total depth (mm or in) and D is the total duration of the rainfall event (usually in *hr*). The difference between $\bar{I}$ and I is that $\bar{I}$ is related to an event and I is not.

We wish to stress that the measurement of the duration of a rainfall event is influenced by the resolution of the record. For example, if we take measurements every 6 hours, a rainfall event of 25.17 hr can be perceived as having a duration of 24 hr or 30 hr.

Once we know the nature of the available data, we are able to understand the essence of the *scale problem* present in rain-rate time series: the characteristics of the intensity process markedly varies depending on the scale of observation. For example, consider the time series illustrated in Fig. 15.1. The records were taken every 10 seconds using an optical rain gauge (the technical details about the obtention of this data are in [SC94]). Usually, measurements are taken with lower resolution. Suppose that we would have obtained the records every hour. In this case, we would perceive the intensity process as shown in Fig. 15.2.

Actually, the scale problem in rain-rate time series has motivated a number of studies about the relationships between intensity, duration and frequency since the beginning of the XX century. Certainly, it is true that most of these studies are based rather on empirical evidence than on statistical theory, but the mathematical theory to deal with this type of statistical problems is of recent development and not trivial.

We conclude this section introducing some concepts and notation that will be of relevance in further chapters.

Let $O_p > 0$ be the total length of the period within which the measurements were made. We define the scale-ratio λ as

$$\lambda = \frac{O_p}{d}. \tag{15.3}$$

In particular, if d is the scale of observation in years, $O_p = 1$ and $\lambda = d^{-1}$ is the scale-ratio on a yearly basis.

We define

$$i_\lambda = i_0 \lambda^\gamma. \tag{15.4}$$

i_λ is the time-average intensity at time t associated with the scale-ratio λ and $i_0 > 0$ is some *constant rainfall intensity*. To simplify the output, we can also work with $i_0 = 1$. We will use Eq. (15.4) for rainfall intensity when talking about asymptotic expressions for $\mathbb{P}(I_\lambda > i_\lambda)$. In this context, γ is called *order of singularity*.

15.3 Intensity-duration-frequency (IDF) curves

An efficient, purpose-oriented way in hydrology and meteorology of representing some of the information contained in both marginal and joint probability distri-

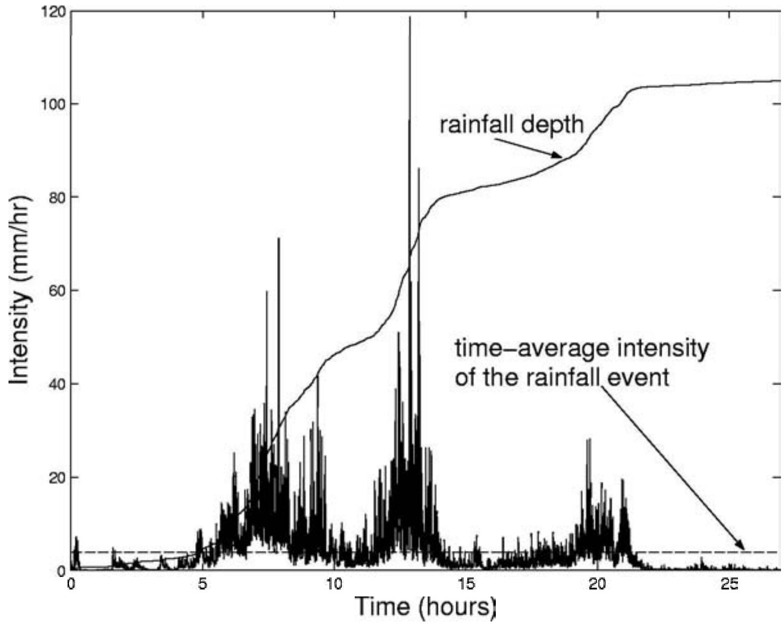

Fig. 15.1: Rain-rate time series with observations every 10 sec, data collected on December 2nd, 1990, in Iowa City by an optical rain gauge at the Hydrometeorology Lab of the Iowa Institute of Hydraulic Research

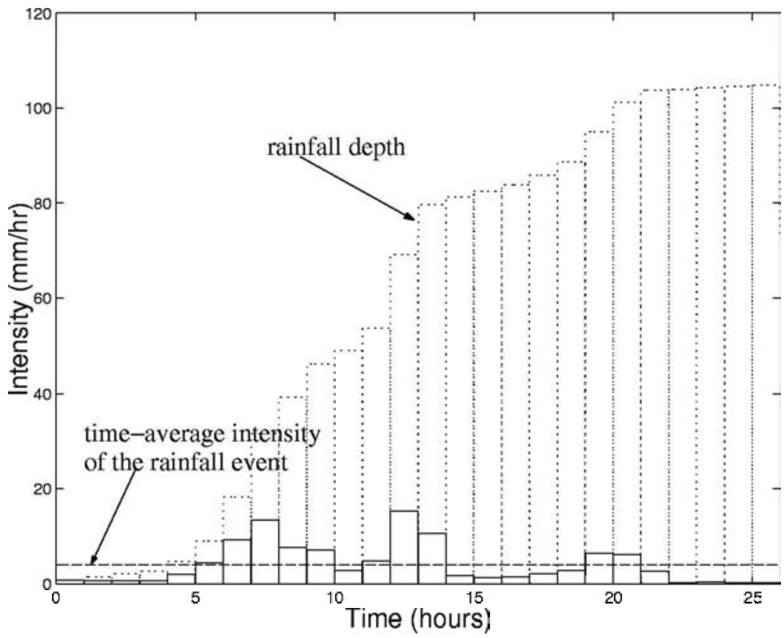

Fig. 15.2: Rain-rate time series with observations every hour, same rainfall event as in Fig. 15.1

butions of hydro-meteorological variables, such as rainfall intensities or river discharges, are the so-called exceedance probability nomograms (see e.g. [Eag70], [BH88]). Among them, we find the intensity-duration-frequency (IDF) curves.

IDF curves are models that were conceived to describe how the probability distribution of the intensity of *rainfall* changes with respect to different sampling event durations d. There are several ways to obtain these plots proposed in the literature and all of them are called IDF curves. We can adjust IDF curves from the intensities averaged over time periods d, annual maxima of intensities averaged over d or d-averaged intensities over a threshold (see e.g. [VF02a]).

Let $\mathcal{I}$ be a random variable representing the time-averaged rainfall intensity. From Eq. (15.2), we have that the r.v. $\mathcal{I}$ is a function of the total duration d, so that we write $\mathcal{I}(d)$. A common practice in hydrology is to use the so-called *relative* return period $T > 0$ to calculate IDF curves. The mathematical definition of T comes from the following expression:

$$\frac{d}{T} := \mathbb{P}(\mathcal{I}(d) > i) = 1 - F_{\mathcal{I}(d)},\ i \geq 0,\ d > 0. \tag{15.5}$$

In Eq. (15.5), we assume at least ergodicity of marginals at all durations d. The parameter i represents an intensity threshold.

The scale-parameter d should be included in the definition of the return period T (Eq. (15.5)) because the stochastic process $\mathcal{I}(d)$ is scale-dependent. Measurements are spaced along time and the sampled intensity process $\mathcal{I}(d)$ depends on the scale of observation d (Eq. (15.1)).

Observe that the probability $\mathbb{P}(\mathcal{I}(d) > i)$ not only depends on the threshold i but also on the scale d. Therefrom, finding equivalent thresholds i for the process $\mathcal{I}(d)$ at different scales d becomes an interesting problem. Therefore, the notation $i = I(d, T)$ is often used in technical literature. In hydrology, the return period T will be used for calculations rather than $\mathbb{P}(\mathcal{I}(d) > i)$. In the context of IDF curves, T is sometimes expressed as a function of the intensity and the duration ($T := T(i, d)$). In order to avoid confusions, in Chapter 17, where the area A will also be involved, we will use the notation $T_{(\mathcal{I}(d,A)>i)}$ instead of the more usual notation $T(I(d, A), d)$.

Remark 15.1: In our case, the notation $\mathbb{P}(\mathcal{I}(d) > i)$ is more appropriate than $\mathbb{P}(\mathcal{I}(\mathcal{D}) > i|\mathcal{D} = d)$, where $\mathcal{D}$ is a r.v. representing the total event duration, because within the multifractal framework our interest is focused in modelling the stochastic behavior of the rain-rate process as a function of the scale. Hence, we consider the duration d as the scale of observation and the intensity as a r.v. varying with the scale of observation d.

Throughout this research, we use IDF curves calculated as in Eq. (15.5). In hydrology T is often measured in years. Sometimes the relative return period T is simply called *return period*. The value of T given by the curve may be adjusted (for the graphic), if the scale (i.e. the duration) d is not expressed in years.

Given that rain is a process with seasonality, practitioners sometimes use the curves for the annual maxima of intensities. In this case, independence for the $\mathcal{I}_{\max}$ of different years is assumed, and an extreme-value-type probability distribution function is fitted to the data for each duration. Finally, T' is estimated in years for every duration group using

$$T' := \frac{1}{\mathbb{P}(\mathcal{I}_{\max}(d) > i)}, \; i \geq 0, \tag{15.6}$$

where $\mathcal{I}_{\max}(d)$ is a random variable representing the annual maximum intensity among rainfall events of duration d. One disadvantage of using T' is that it only holds for scales equal or greater than one year [VF02a].

As anticipated, using the annual maximum intensities and Eq. (15.6) or the intensities and Eq. (15.5) leads to different results. Nevertheless, both curves are practically the same for $T' > 10$ years ([MM88]). [VF02a] validates through simulations, that we can convert IDF curves from T-based into T'-based for large values of T', based on:

$$\lim_{T' \to \infty} \frac{T}{T'} = 1. \tag{15.7}$$

By inverting the function $T(i, d)$, we can obtain the intensity threshold $i(T, d)$ for a duration d, to be exceeded at average intervals T, and an empirical relationship for it has been historically given by:

$$i(T, d) = K \frac{T^m}{d^n}, \tag{15.8}$$

where K, m, n are positive real-valued parameters to be adjusted from point rainfall data at the site of interest.

It is common practice to estimate the parameters K, m and n by multiple regression using

$$\log i = m \log T - n \log d + \log K. \tag{15.9}$$

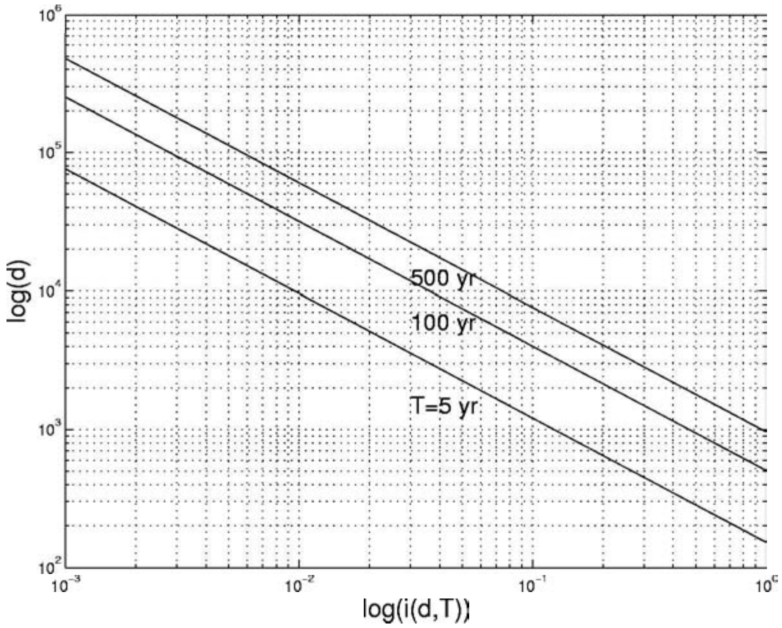

Fig. 15.3: Example of IDF curves (Eq. (15.8))

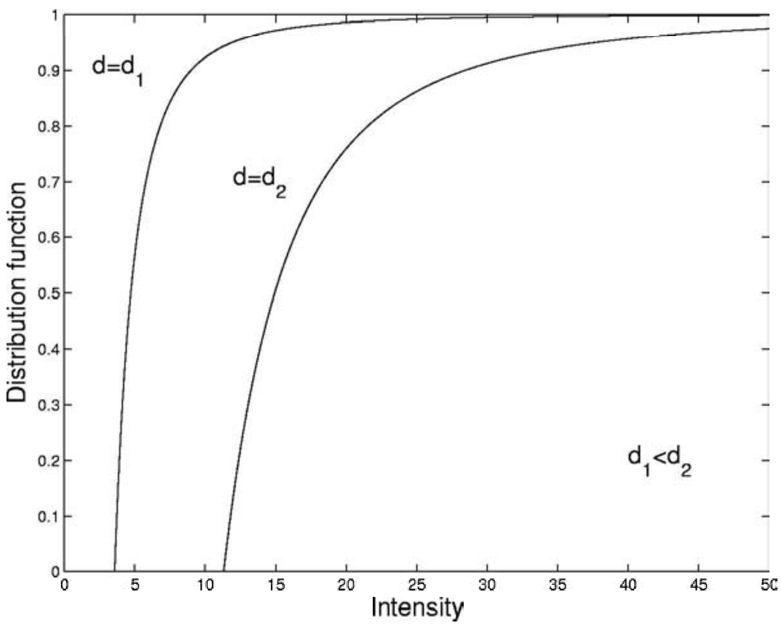

Fig. 15.4: Two level curves of the distribution function for the intensity as a function of the duration $F_{\mathcal{I}(d)}(i)$ implicit in IDF curves (Eq. (15.8))

We are dealing with equations of surfaces, on which the IDF curves are T=constant level curves for different values of T. In fact, speaking about IDF surfaces instead of IDF curves would be more adequate.

Substituting Eq. (15.8) into Eq. (15.5), we calculate

$$1 - F_{\mathcal{I}(d)}(i) := \mathbb{P}(\mathcal{I}(d) > i) \quad = \quad \left(\frac{i\, d^{n-m}}{K}\right)^{-\frac{1}{m}}, \tag{15.10}$$

$i := I(T, d)$.

If we consider $F_{\mathcal{I}(d)}(i) \in [0, 1]$, the next inequality should hold:

$$i \quad \geq \quad K d^{n-m}, \tag{15.11}$$

where $d, m, n, K > 0$. This is to say that this type of empirical relationships may hold for large intensities, which will actually show to be the case for multifractal fields.

Now consider the following (hypothetical) IDF curve:

$$i(T, d) = 80\, T^{0.4} d^{-0.9}, \tag{15.12}$$

$i(T, d)$ in mm/hr, d in hours.

If we draw the IDF curves as traditionally, in log-log coordinates, they will appear as parallel straight lines with a negative slope. In Fig. 15.3, we present an example of IDF curves drawn from Eq. (15.12) as it is usually done in hydrology. Each level curve is associated with a value of T. In hydrology, T is measured in years. If necessary, units are adjusted accordingly.

We can rewrite Eq. (15.12) as

$$F_{\mathcal{I}(d)}(i) \quad = \quad 1 - 80^{2.5} d^{-1.25} i^{-2.5},\ i \geq 80 d^{0.5}. \tag{15.13}$$

We plot two level curves of this equation in Fig. 15.4.

15.4 Final comments

The Eq. (15.1) is relevant for the stochastic modelling of rainfall using multifractals. Observe that whereas the shape of the rainfall intensity process drastically changes with the scale of observation, the rainfall depth is conserved and redistributed across the observation period. Rainfall depth is defined in hydrology as being the integral of the rainfall intensity.

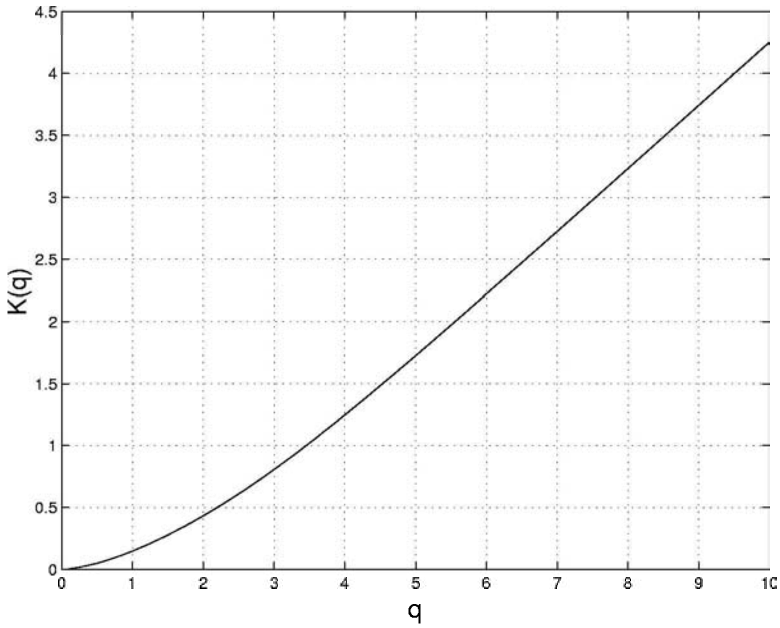

Fig. 15.5: Moment scaling function $K(q)$ of the rain-rate time series of Fig. 15.1

If we include spatial scales for the stochastic modelling of rainfall using multifractals, the quantity that we redistribute across space-time scales is the water volume corresponding to an area A and a duration d. In this case, we should take the possible space-time scaling anisotropy into account. Heuristically speaking, this means that the water volume is redistributed across space scales in a different way than among time scales. We discuss this topic with further detail in Chapter 17.

The distribution along scales of rainfall depth in the case of time series (or water volume if we include space scales) is modelled in this research using random multifractal measures. There are different ways to generate such measures, but we focus our attention on those generated by random multiplicative cascades.

As a motivation for the next chapter, we calculated $K(q)$ (see Eq. (14.24)) for the time-series of Fig. 15.1. Compare Fig. 15.5 above with Figs. 14.1, 14.2 and 14.3. The nonlinear $K(q)$ function denotes a multifractal behavior, typical of the multiplicative cascade models proposed in the next chapter.

16. MULTIPLICATIVE CASCADE MODELS FOR RAIN IN HYDRO-METEOROLOGICAL DISASTERS RISK MANAGEMENT

It is our conviction that one should incorporate the information provided by geophysical sciences into insurance mathematics. The present research is conceived as a first step in this direction. In this chapter, we provide a review of key results for multifractal models of rain and discuss their potential and relevance for hydro-meteorological disaster risk management. As a main result, we obtained an asymptotic expression for the tail probability of the return period that we derived from intensity-duration-frequency curves under the assumption of multifractality.

16.1 Why multifractals in hydro-meteorological disasters risk management?

Regarding extreme precipitation, we find two widespread views. The first one relies on the phenomenological notion of the *probable maximum precipitation* (PMP). However, approaches from this perspective demand a sophisticated analysis of rainfall process in an attempt to address all its relevant physical aspects. Certainly, the existence of such a threshold is plausible, as far as the amount of rainfall over a surface is finite. Nevertheless, it is likely that this physical maximum is far larger than any rainfall intensity that has ever been registered, and has therefore little relevance for the probability distribution tails of rainfall intensities. Indeed, nowadays the physical foundations of rainfall generation are known to a certain extent. On the one hand, however, important aspects in the process of drop growth in convective clouds are still unknown, to the point that real growth occurs considerably faster, and can lead to more intense extremes than predicted by current models. On the other hand, the large number of degrees of freedom is currently by far prohibitive for direct numerical simulation (DNS) at any significant atmospheric scale. Various closure equations can be used to resolve the dynamical partial differential equations in larger-scale numerical schemes, but the simplifications that they introduce, combined with the relevance of drop-size scales in the rainfall production, result in ensemble statistics for these kind of models that differ considerably from natural statistics, a fact that makes them hardly useful for risk management of natural disasters.

Secondly, there are statistical models parameterized directly from natural statistics. In this case, we consider rainfall intensity as a random variable and the time series as realizations of a stochastic process. This perspective is usually applied for engineering design and risk assessment. The disadvantage is that we are fitting empirical data to ad hoc statistical laws with little or no knowledge about the rain process, which makes this approach unreliable when estimating extreme event probabilities, where the data is scarce. In the classical statistical approaches, the scale issue as such is ignored. Moreover, we assume that the behavior across scales is the same. We need this, because otherwise the fit would not be statistically significant. However, scale-by-scale parameterizations lead to an unacceptably high number of parameters to fit. As data for the statistical analysis, we have records of the rate of rainfall (hyetograms). As we explained in Chapter 15, our observations of the intensity process markedly vary with respect to the selected time scale. If we observe the same process with different resolutions, the empirical maximum values strongly vary (an analysis of the time series of Figs. 15.1 and 15.2 via classical statistical as well as fractal and chaotic dynamics methods is presented in [SC94] and [SS95]). This situation is also present in rainfall time series over longer observation periods (see e.g. [VF02a], [LS95]). The rainfall process has also a high spatial variability (see e.g [GW93]), so the same problem arises with spatial observations. Consequently, rainfall is a highly intermittent space-time variable process, and the scale plays a fundamental role in its stochastic description. This fact is particularly relevant for extreme rainfall events, especially in case of extremely high rainfall depth over a short space-time interval.

16.2 Introduction to multiplicative cascades

Multiplicative cascade models are mathematical constructs suitable to capture intermittent and highly irregular behavior. Actually, these models have a wide range of applications, such as the modelling of turbulence (e.g. [Kol41], [Man74], [FP85] and [MS87]), internet packet traffic (e.g. [RL97], [GW98]), stock prices (e.g. [Man97]), river flow (e.g [GW90]) and rainfall. They are capable of gener-

$$
\begin{array}{ccccccccc}
 & & & & m & & & & \\
 & & & \swarrow & & \searrow & & & \\
 & w_1^{(1)}m & & & & & & w_2^{(1)}m & \\
 & \swarrow \quad \searrow & & & & & & \swarrow \quad \searrow & \\
w_1^{(2)}w_1^{(1)}m & & w_2^{(2)}w_1^{(1)}m & & & & w_3^{(2)}w_2^{(1)}m & & w_4^{(2)}w_2^{(1)}m \\
\swarrow \quad \searrow & & \swarrow \quad \searrow & & & & \swarrow \quad \searrow & & \swarrow \quad \searrow \\
 & & & & \vdots & & & & \\
w_1^{(n)}\ldots w_1^{(1)}m & & & & \ldots & & & & w_2^{(n)}\ldots w_2^{(1)}m
\end{array}
$$

Tab. 16.1: Levels of a “bare” multiplicative cascade

$$
\begin{array}{cccc}
w_1^{(2)}w_1^{(1)}m & w_2^{(2)}w_1^{(1)}m & w_3^{(2)}w_2^{(1)}m & w_4^{(2)}w_2^{(1)}m \\
\searrow & \swarrow & \searrow & \swarrow \\
\multicolumn{2}{c}{(w_1^{(2)}+w_2^{(2)})w_1^{(1)}m} & \multicolumn{2}{c}{(w_3^{(2)}+w_4^{(2)})w_2^{(1)}m} \\
\multicolumn{2}{c}{\searrow} & \multicolumn{2}{c}{\swarrow} \\
\multicolumn{4}{c}{((w_1^{(2)}+w_2^{(2)})w_1^{(1)} \quad + \quad (w_3^{(2)}+w_4^{(2)})w_2^{(1)})m}
\end{array}
$$

Tab. 16.2: Levels of a “dressed” multiplicative cascade

ating measures with an asymptotically almost-everywhere singular, multifractal behavior.

Let us begin with the simplest case of a “bare” cascade. To reconstruct a multiplicative cascade, we begin with a given “measure” m uniformly distributed along a support (Fig. 16.1). Physically, the measure represents an extensive quantity, such as e.g. mass or energy.

As we can observe in Table 16.2, each subsequent step belonging to an interval of the cascade process splits the support, and the contained mass m is divided according to the respective weights of each level. The generated number of weights is the “branching number” (b) of the cascade generator. A binary cascade, for example, has $b = 2$. Subsequently, the resulting measure on the support can be described in terms of an infinite iterative construction.

When the resulting measure is then aggregated over nested intervals, see Tab. 16.2, we are talking about a "dressed" cascade. Note that the mass m is redistributed to each branch by multiplication with the respective weight $w_i^{(k)}$, see Fig. 16.1. The generator of a multiplicative cascade can be random and it is analogous to the weights in our example. Note that to achieve conservation in the ensemble average of the mass, the expected value of the sum of weights should be equal to unity. The process illustrated in Fig. 16.1 and described in the Tables 17.1 and 16.2, can be generalized to $\mathbb{R}^d$.

A multiplicative cascade is an iterative process that fragments a given subset of $\mathbb{R}^d$ into smaller and smaller pieces according to some geometric rule. The support of a multiplicative cascade can represent a surface or the time axis. Intertwined fractal sets of different singularity strengths of the measure result in multifractality. Monofractality is a particular case of multifractality, when only one singularity strength order appears.

The limiting measures of multiplicative cascades generally exhibit multifractal scale invariance. Let $\mathcal{B}(\mathcal{X})$ be the Borel sets of $\mathcal{X}$, where $\mathcal{X} \subseteq \mathbb{R}^d$. Define the measure space $(\mathcal{X}, \mathcal{B}(\mathcal{X}), \mu_n)$, where μ_n is the sampling measure from a cascade developed until level n. The sampling measures μ_n generated by certain multiplicative cascades have an a.s. limit at small scales, μ_∞, that is also defined in the measure space $(\mathcal{X}, \mathcal{B}(\mathcal{X}))$. Observe that the higher the level n the smaller the scale δ (the higher the scale-ratio $\lambda = \delta^{-1}$). The measures μ_n from cascade processes will not be probability measures, but we require their expected values to be one ([Har01]).

It is important to note that, whereas multifractals in general are measures, monofractals can be associated with the measure given by an indicator function of a set and hereby associated directly to a set of fractionary dimension (in other words, the now classical notion of a fractal).

16.3 Multifractal analysis of rain using multiplicative cascades

The fundamental idea of multiplicative cascade modelling is to try to capture the multiscaling behavior of a process when present. Certainly, there exists vast evidence of the multifractal scaling of rainfall up to planetary scales (see e.g. [SL87], [GW93]).

Let us introduce the following definition:

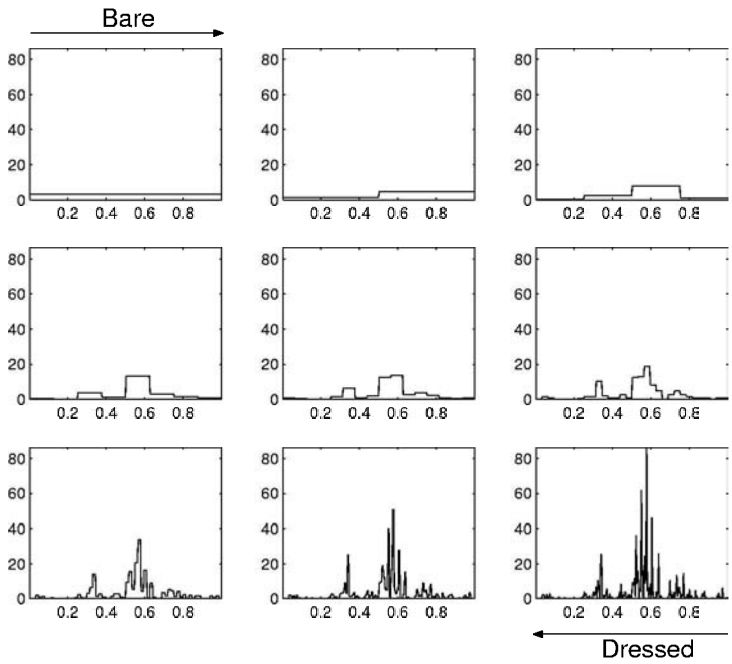

Fig. 16.1: Binary conservative multiplicative cascade with uniform generator ([Flo04]), see Ap. A

Definition 16.1: A non-negative cascaded variable W will be said to be strongly bounded below if $\mathbb{P}(W \geq a) = 1$ for some positive number a. W will be said to be strongly bounded above if $\mathbb{P}(W < b) = 1$, where $b \in \mathbb{N}$ is the cascade branching number. [HW92]

The Rényi spectrum of scaling exponents $\tau(q)$ of a field is a function defined from the scaling of moments of order q of the respective field

$$\langle |r(\Delta)|^q \rangle \propto \lambda^{\tau(q)}, \tag{16.1}$$

where $r(\Delta)$ is the integral of the quantity of interest over the scale Δ, λ is the scale-ratio and $\langle\,\rangle$ is the averaging operator.

We work under the hypothesis that rainfall depth is equal in distribution with a multifractal measure μ_∞ generated by a multiplicative cascade. In our case, $r(\Delta)$ is always non-negative and corresponds to the amount of precipitation caught over the scale Δ. If Δ is a time-scale, $r(\Delta)$ corresponds to the rainfall depth.

Multifractal scaling of a measure is defined as the measure having a curvilinear (strictly convex) $\tau(q)$, whose definition for the one-realization case under the assumption that the limit exists is:

$$\tau(q) = \lim_{\delta \to 0} -\frac{\ln \sum_{k=1}^{k=\lfloor T_{tot}/(\delta d) \rfloor} |r_k(\delta d)|^q}{\ln \delta}, \tag{16.2}$$

where d is the scale of observation, $r_k(\Delta)$ (amount of precipitation) is the integral of the quantity of interest (rainfall intensity) over the scale $\Delta := \delta d$, T_{tot} is the total length of the support and $\delta > 0$ represents a factor scale. In multiplicative cascade models, the function $\tau(q)$ is determined by the probability distribution of the weights in the cascade generator and it is also known as *multiscaling exponent* or *Rényi exponent*. In other words, the statistical moments of order q of $r(d/\lambda)$ are given by

$$\mathbb{E}[r(d/\lambda)^q] = \lambda^{\tau(q)}. \tag{16.3}$$

Estimating and plotting $\tau(q)$ is useful to identify multiscaling behavior in the data. However, it should be noticed that estimating $\tau(q) = 1 - K(q)$ using Eq. (14.24) (see Fig. 15.1) generally results in values different from Eq. (16.1), due to the non-ergodicity of the cascading process. For a more detailed treatment of the ensemble vs. realization estimation of scaling exponents, see also [OW00], [OW02] and [SL87].

The basic equation of multiplicative cascades is given by

$$P(r(d/\lambda) > \lambda^\gamma) \sim \lambda^{-c(\gamma)}, \tag{16.4}$$

where $r(d/\lambda)$ is the random variable of our interest (e.g. rainfall intensity), $\lambda := 1/\delta$ is the inverse scale factor, $c(\gamma)$ is the codimension function, γ is an order of singularity and "$\sim$" denotes asymptotic equality as $\lambda \to \infty$ (see [SL87], [GW93]).

We can rewrite Eq. (16.4) as

$$\lim_{\lambda \to \infty} \frac{\log(P(r(d/\lambda) > r_0 \lambda^\gamma))}{\log \lambda} = -c(\gamma). \tag{16.5}$$

If the codimension function $c(\gamma)$ is a closed convex function with is not identically ∞, $c(\gamma)$ is dual to $\tau(q)$ by the Legendre-Fenchel transform (see Def. 16.2). The fact that $c(\gamma)$ is a function of γ on an interval of strictly positive length, rather than a single point, is the origin of the term *multifractality*.

Definition 16.2: Let $C(q) : \mathbb{R}^d \to \mathbb{R} \cup \{\infty\}$ be a closed convex function which is not identically ∞. The function $I : \mathbb{R}^d \to \mathbb{R} \cup \{\infty\}$ defined by

$$I(y) = \sup_{q \in \mathbb{R}^d} \{ \langle q, y \rangle - C(q) \} , \ y \in \mathbb{R}^d, \tag{16.6}$$

is the Legendre-Fenchel Transform of $C(q)$.

The modelling of rain processes using multiplicative cascades with log-Lévy generator is often found in the literature of multifractal models for rain. Log-stable distributions with skewness parameter $\beta = -1$ are used in modelling multifractals, partly because of the finiteness of their moments ([ST94], p. 52).

16.3.1 Discrete multiplicative cascades

This approach relies on the statistical inference for multiplicatively generated multifractals, and rainfall modelling is only one of its applications. [OW02], [GW93] and [GW97] point out that the precise nature of the cascade generator is not a central issue in the case of rainfall modelling. From a single realization of the cascade process, we try to infer statistically the distribution of the cascade generator that presumably generated the sample. The probability distribution of the cascade generators represents here a hidden parameter which is reflected in the fine-scale limiting behavior of certain scaling exponents calculated from a single sample realization ([OW02]). Some relevant works on discrete multiplicative cascades are [HW92], [OW00] and [OW02]. Examples of discrete multiplicative cascades applied to rainfall modelling can be found in [GW90], [GW93], [VF02a], [VF02b] and [Ven02].

As we explained before, this is only a review of key results that can be of our interest. A compilation of fundamental results in discrete multiplicative cascades can be found e.g. in [Har01], Chapter 6. For an introduction to the mathematical foundations of the random cascade theory, see e.g. [GW93]. Further mathematical treatment of this topic is in [HW92], [OW00] and [OW02].

[GW93], p. 253, emphasized that the first foundational results for the development of statistical cascade theory were obtained by [Kah74], [Pey74], [KP76] and [Man74]:

> “They proved the existence and nontriviality of the limiting statistical cascades of a probability distribution carried by a random variable W, called the generator, and branching number b. In particular,

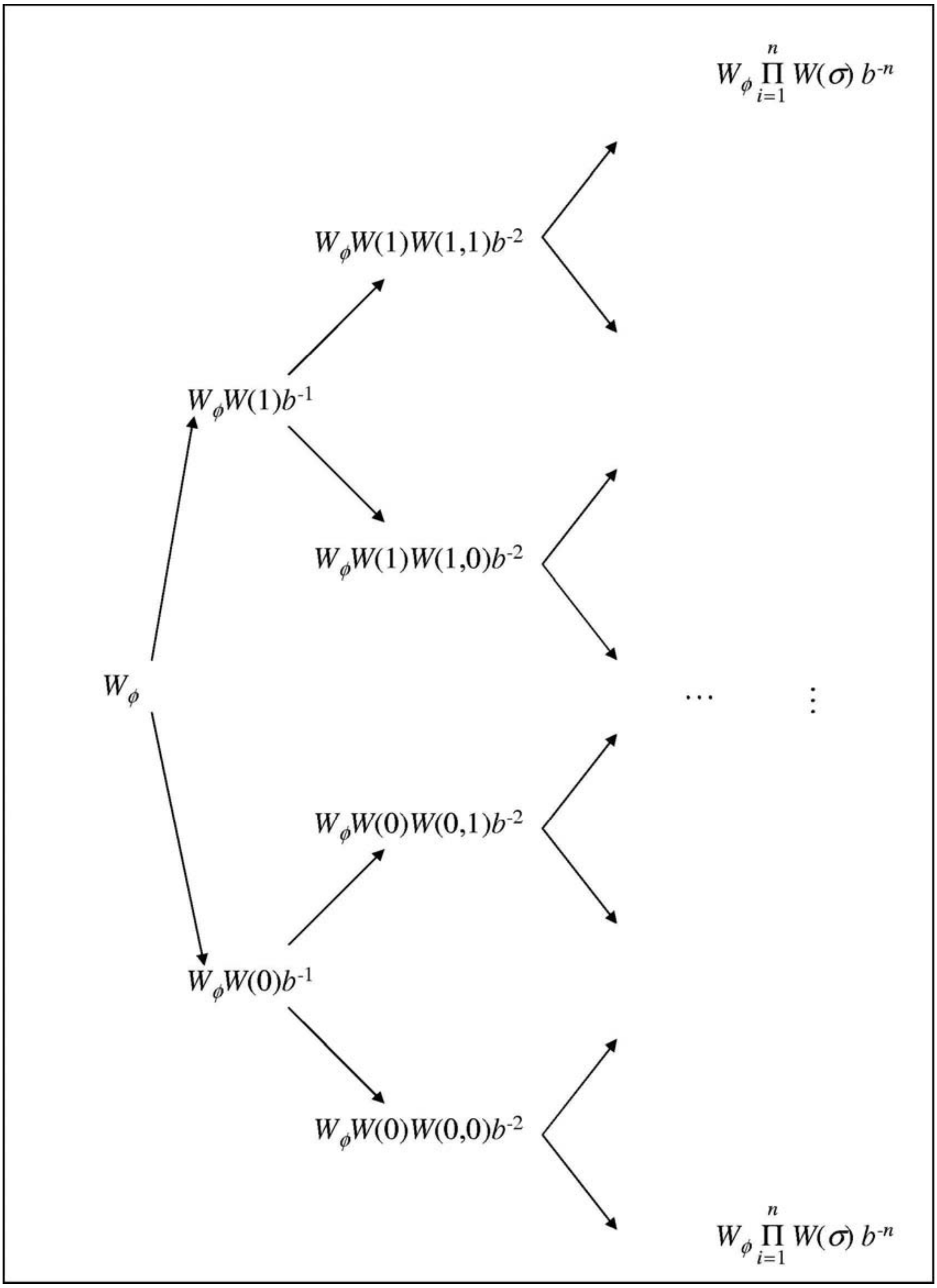

Fig. 16.2: Example of (discrete) random cascade with support in $[0, 1]$ and branching number $b = 2$

these authors found that the nontriviality of the resulting limit measure (mass distribution) and the Hausdorff dimension of its support can be determined completely from the modified cumulant generating function $\chi_b(h)$ of the probability distribution of the generator W."

$\chi_b(q)$ is the so-called MKP (Mandelbrot-Kahane-Peyrière) function,

$$\chi_b(q) := \log_b \mathbb{E}\left[W^q \mathbf{1}_{\{W>0\}}\right] - (q-1). \tag{16.7}$$

Rain intensity and river flow are non-negative processes. For this reason, we will focus on multiplicative cascades with nonnegative cascaded random variable W.

The following fundamental theorem was stated in [KP76]:

Theorem 16.1: Let

$$\mathcal{X} := \{0, 1, \ldots, b-1\}^{\mathbb{N}} \tag{16.8}$$

be a product topology. Denote by

$$\sigma := (\sigma_1, \sigma_2, \ldots) \in \mathcal{X},\ \sigma_i \in \{0, 1, 2, \ldots, b-1\}, \tag{16.9}$$

the successive vertices of a random tree rooted at the vertex ϕ with branching number $b \geq 2$, $b \in \mathbb{N}$ (see Fig. 16.2). $\mathcal{X}$ has metric $\rho(\sigma, \eta) = b^{-\mathbf{a}(\sigma,\eta)}$, where $\mathbf{a}(\sigma, \eta)$ is defined as the number of vertices common to σ, η. Let W denote a random variable which has the common distribution of the $W(\sigma)$'s and MKP-function $\chi_b(q)$.

I. (Nondegeneracy) If $-D = \chi_b'(1-) \equiv \mathbb{E}[W] \log_b W - 1 < 0$, then $\mathbb{E}\mu_\infty([0,1]) > 0$, and conversely.

II. (Divergence of moments) Let $q > 1$. Then $Z_\infty := \mu_\infty([0,1])$ has a finite moment of order q if and only if $q < q_c = \sup\{q \geq 1 : \chi_b(q) < 0\}$. Moreover, $\mathbb{E}[Z_\infty^q] < \infty$ for all $q > 0$, if and only if W is essentially bounded by b and $\mathbb{P}(W = b) < b^{-1}$.

III. (Support dimension) Assume that $\mathbb{E}[Z_\infty^q \log Z_\infty] < \infty$. Then μ_∞ is a.s. supported by the random set

$$\begin{aligned} \text{supp}(\mu_\infty) &= \{\sigma \in \mathcal{X} : \lim_{n\to\infty} n^{-1} \log_b \mu_\infty \left(B_{b^{-n}}(\sigma)\right) \\ &\quad = \mathbb{E}[W] \log_b W - 1\}, \end{aligned} \tag{16.10}$$

where

$$B_{b^{-n}}(\sigma) = \left[\sum_{j=1}^{n} \sigma_j b^{-j}, \sum_{j=1}^{n} \sigma_j b^{-j} + b^{-n}\right) \tag{16.11}$$

is a closed ball of radius $b^{-n} > 0$ located at $\sigma \in \mathcal{X}$, of Hausdorff dimension

$$D = -\chi_b(1) = 1 - \mathbb{E}[W] \log_b W. \tag{16.12}$$

Under the assumption that the measure μ_∞ is non-degenerate, i.e. $\mathbb{E}[W \log_b W] = 1$, the Rényi exponent $\tau(q)$ for a multiplicative cascade with branching number b is

$$\tau(q) := \lim_{n\to\infty} \frac{\log M_n(q)}{n \log b} = \lim_{\delta\to 0} -\frac{\log M_n(q)}{\log \delta}, \tag{16.13}$$

where

$$M_n(q) := \sum_{i=1}^{b^n} \mu_\infty^q(\Delta_n^i) \tag{16.14}$$

and Δ_k^i, $i = 1, 2, \ldots, b^k$ are the b-adic intervals at the k^{th} generation (level) of the cascade (see [HW92]).

The following theorem is important, because it relates the Rényi exponent $\tau(q)$ for a multiplicative cascade defined in Eq. (16.14) with the MKP function and thus with $\log_b \mathbb{E}[W^q]$.

Theorem 16.2: Assume that the non-negative cascaded variable W is strongly bounded above and below and that

$$\frac{\mathbb{E}[W^{2q}]}{(\mathbb{E}[W^q])^2} < b, \tag{16.15}$$

where $b > 0$ is the branching number. Then, with probability 1, we have

$$\tau(q) = \chi_b(q) \tag{16.16}$$

([HW92]).

If the cascaded r.v. W satisfies the boundedness conditions and Eq. (16.15) holds, the Legendre transform formalism is

$$c(\gamma) = \max_q \{q\gamma - \tau(q)\} \quad (16.17)$$

$$\tau(q) = \max|_{\gamma=\gamma(q)} \{q\gamma - c(\gamma)\} \quad (16.18)$$

$$\gamma(q) = \frac{d\tau(q)}{dq} \quad (16.19)$$

([HW92]).

If we assume that the multifractal measure μ_∞ was generated by a discrete multiplicative cascade with log-Lévy generator, we have $W = e^{-X}$, where X is a Lévy-stable random variable (see Theorem B.1). X depends on the following parameters: the Lévy index $\alpha \in (0, 2]$, the location parameter $l \in \mathbb{R}$, the scale parameter $\sigma > 0$ and a skewness parameter $\beta \in [-1, 1]$. If $\mathbb{E}[W] = 1$ (mean conservation condition) and $\mathbb{E}[W^q] < \infty$, the values of β and l are determined. Therefore, in this case only α and σ are free parameters.

For applications, we can statistically estimate $\tau(q)$ from the data ([TV99]). From the obtained $\hat{\tau}(q)$, we can estimate the codimension function $c(\gamma)$. However, obtaining criteria for the choice of W is an important statistical problem.

[Ven02] considered various cases involving discrete multiplicative cascades with dependent or independent generator and he proposes a technique to estimate the codimension function $c(\gamma)$. However, we realized that the observation of a critical value for q (q^*) and thus a critical value for γ (γ^*) does not contradict the results for all γ obtained by applying Chernoff's theorem of large deviations ([Bil95], p. 147) in [GW93], p. 260, as pointed out in [Ven02], p. 119. That is, because when estimating $\tau(q)$ a critical interval for q exists ([OW02], p. 330).

Remark 16.1: We wish to stress that when $W \geq 0$ is not essentially bounded by b or $\mathbb{P}(W = b) \geq b^{-1}$, the existence of a critical order of moments is well established in the theory (see Theorem 16.1). This case should be distinguished from the problems related to the estimation of $\tau(q)$.

[RW03] used wavelet–based statistical techniques for inference about the cascade generator —in the case of conservative cascades— to obtain estimators of the structure function.

16.3.2 Universal multifractals

In this case, it is considered that multifractals arise when cascade processes concentrate energy, water, or other fluxes into smaller and smaller regions.

The notion of universality in physics corresponds to the fact that among the many parameters of a theoretical model, it may be possible that only a few of them are relevant in the sense of capturing the essence of the process. The concepts of *universal multifractals* and *continuous multiplicative cascades* were introduced in [SL87]. For a debate about universality in multifractals for rain, see e.g. [GW93], [SL97] and [GW97].

If the results of [SL87] hold, the limiting measure of continuous multiplicative cascades produces generators with weights whose distribution is attracted to Lévy-stable distributions.

Let $r(d/\lambda)$ be the intensity of the rain field at scale ratio $\lambda > 0$. In the universality class of Lévy-stable processes, we have from the theory of continuous multiplicative cascades that, under the assumption of conservation, the asymptotic behavior of the tail probability of $r(d/\lambda)$ is given by

$$\mathbb{P}(r(d/\lambda) > \lambda^{\gamma}) = A(\lambda)\,\lambda^{-c(\gamma)} \qquad (16.20)$$

([SL87], [SL89]), where $\lambda = O_p/d$ is the scale ratio in time series of length O_p divided in elementary time-periods d ($d \to 0$), γ is an order of singularity, $c(\gamma)$ is the codimension function of the singularities dual to $\tau(q)$ by the Legendre-Fenchel transform and $A(\lambda)$ is a slowly varying function at infinity. It means,

$$\lim_{\lambda\to\infty} \frac{A(a\lambda)}{A(\lambda)} = 1, \forall\, a > 0. \qquad (16.21)$$

Equation (16.20) shows how the probability distribution of singularities of order higher than a value γ is related to the fraction of the space they occupy as determined by the characterizing factor of scale invariance of the probability distribution.

In the context of [GW93], $\tau(q)$ arises through log-log plots of empirical moments of various orders q and the choice of discrete multiplicative cascades with log-Lévy generator was only a model assumption. For [SL87], multiplicative cascades with log-Lévy generator should be strongly universal in the context of continuous scales. A review to this model is that this class of generators does not satisfy the strong boundedness conditions (see e.g. [GW93], p. 260, [Har01], p. 102).

The codimension $c(\gamma)$ is a non-decreasing convex function of γ as in Sec. 16.3.1, but for the universal multifractals, $c(\gamma)$ is considered as belonging to the universality class of Lévy-stable processes as it is meant in [SL87]. $c(\gamma)$ depends in this context on two fundamental parameters: C_1 and α (universality). C_1 is the codimension of the mean field and it should satisfy the fixed point relation $C_1 = c(C_1)$. $\alpha \in (0, 2]$ is the Lévy index (in this context, α is meant as in Def. 14.8 but in a continuous setting) and it measures how fast the codimension changes with the singularity. If $\alpha = 2$, we set $\beta = 0$, so that the generator W is log-normal. For $\alpha \in (0, 2)$, we set $\beta = -1$.

To go from the conserved process (φ) to the observed non-conserved process (R), a parameter H is required. H specifies the exponent of the power law filter or order of fractional integration needed to obtain R from φ. That is, $\varphi : \langle|\Delta R_\lambda|\rangle \approx \lambda^H$. Thus, for the measured field R,

$$\mathbb{P}(\Delta R > \lambda^{\gamma - H}) = A(\lambda)\lambda^{-c(\gamma - H)}. \tag{16.22}$$

For a further explanation, see [LS95].

For the codimension $c(\gamma)$ of a log-Lévy (universal) multifractal, we have the following expression ([VD93]):

$$c(\gamma) = \begin{cases} C_1 \left(\frac{\gamma}{C_1 \alpha'} + \frac{1}{\alpha}\right)^{\alpha'} & \alpha \neq 1 \\ C_1 \exp\left(\frac{\gamma}{C_1} - 1\right) & \alpha = 1 \end{cases}, \tag{16.23}$$

where $\alpha'^{-1} + \alpha^{-1} = 1$, $C_1 \neq 0$.

According to Eq. (16.23), for $\alpha \in [1, 2]$, the orders of singularity are unbounded. If $\alpha \in (0, 1)$, a finite maximum order of singularity γ_0 does exist:

$$\gamma_0 = \frac{C_1}{1 - \alpha}. \tag{16.24}$$

Regarding the maximum order of singularity ($\gamma_{\max}$) used in [VD93] to estimate the maximum accumulation A_λ for a duration τ ($A_\lambda \propto \lambda^{\gamma_{\max} - 1} \propto \tau^{1 - \gamma_{\max}}$) in extreme rainfalls, [DB03] pointed out that even if the singularity γ is theoretically unbounded, the maximum order of singularity in a finite sample will always be bounded due to spurious scaling artifacts resulting from undersampling. Using the experimental setting for the small space-time scale presented in Chapter 17 we obtained different estimated values for $\gamma_{\max}$ from the samples, so that we can not conclude about the universality of $\gamma_{\max}$ from our results.

[SL91b] found that for spatial averages over observing sets with dimension D, a critical value q_D of the moment of order q exists, such that the estimated statistical moments diverge as soon as $q > q_D$. That is,

$$\langle \varphi_\lambda^q \rangle = \infty, \; q > q_D. \tag{16.25}$$

where

$$\tau(q_D) = (q_D - 1)D. \tag{16.26}$$

For time series, we have $D = 1$.

If the statements above mentioned hold, the probability of $\varphi_\lambda > \lambda^\gamma$ can be approximated by

$$P(\varphi_\lambda > \lambda^\gamma) \approx (\lambda^\gamma)^{-q_D} \tag{16.27}$$

for large enough values of γ. According to this result, for $q > q_D$ the tail of the distribution (Eq. (16.20)) decays algebraically ([SL92]).

According to the theory of universality, q_D should be a universal constant, but different studies have obtained values varying between 1.5 and 5. Some authors attribute this variability to differences in rainfall physics, orography, temporal resolution of the observations, and length of the time series (e.g. [Ols95], [SG01]). [DB03] point out that common values range from slightly below 2 to a little above 3.

Remark 16.2: We wish to emphasize that all multiplicative cascade models mentioned in this Chapter work under the assumption of stationarity.

16.4 IDF curves in a multifractal framework

Our hypothesis is that probabilistic frequencies of extreme events may be inferred by extrapolating these curves under the assumption of multifractality. It has been observed that these empirical curves are traditionally modelled for rare events using power laws that are compatible with multifractal scaling. The models mentioned in Sec. 16.3 have the disadvantage that their phenomenology can not be extended to time scales of the orders of magnitude involved in the return periods of extreme events. However, good scaling is observed in empirical data and no scaling break has been found to date.

This working hypothesis is not new in geophysics literature, see [DL97], [VF02a]. [BR96] analyzed depth-duration-frequency (DDF) curves using multiplicative cascades. [KR02] and [CF04] (reprinted in Chapter 17) worked with intensity-duration-area-frequency (IDAF) curves.

We wish to emphasize that IDF curves are standard tools in hydrology and they were developed absolutely independently from the multifractal theory. The observed organization of the data gives empirical evidence of scale invariance. Actually, multifractal models of rainfall-depth process have been shown to lead to such power laws for their extremes ([BR96]).

However, a question of central importance to take advantage of IDF curves within the multifractal framework is the following: Which kind of mathematical relationship have IDF curves and multiplicative cascade models?

An answer to this question is a fundamental step for:

1. a precise interpretation of IDF curves under the assumption that rainfall intensity is multifractal,

2. improving methodologies for the parametrization of IDF curves or justifying the existent ones and

3. evaluating quantitatively in which cases IDF curves suffices as an approximation for the distribution function.

This explains why we concentrated our efforts in looking for relationships between IDF curves (in the form of Eq. (15.8)) and the multifractal representation of rain in form of a stationary multiplicative cascade. At the actual stage of development of the multifractal theory, looking for any kind of relationship is not a trivial task.

If we accept the evidence showing that rainfall intensity has multiscaling behavior, then IDF curves approximates a multiscaling process. Hence, it makes sense to consider $\mathbb{P}(\mathcal{I}(d) > i)$ and T from IDF curves as estimators under the multifractal ansatz.

We noticed that in all the reviewed literature IDF curves have never been treated from this perspective. This is also the case of flow-duration-frequency (QDF) curves, DDF curves, IDAF functions and flow-duration-area-frequency (QDAF) functions. Estimators from empirical curves have never been viewed as random variables. Therefore, the probability distribution of T (recall Eq. (15.5)) and $F_{\mathcal{I}(d)}$ (recall Eq. (15.10)) given by the IDF curves has never been explored. So, we studied these curves from this perspective and we obtained an asymptotic expression for the tail probability of the (relative) return period T here presented and previously published in [Flo04].

If we consider a yearly scale and d as our elementary time-period in years, then $\lambda = d^{-1}$. λ represents the ratio of the yearly scale with the scale of observation d. Let $\mathcal{T}$ be a random variable representing the estimator for the return period obtained from IDF curves. We are interested in computing the probability $\mathbb{P}(\mathcal{T} > t)$, $(\lambda t)^{-1} \in (0, 1]$.

We have

$$\mathbb{P}(\mathcal{T} > t) = \mathbb{P}\left(\left[\frac{\mathcal{I}(d)\, d^n}{K}\right]^{\frac{1}{m}} > t\right) \tag{16.28}$$

$$= \mathbb{P}\left(\mathcal{I}(d) > K\frac{t^m}{d^n}\right) \tag{16.29}$$

$$= \mathbb{P}\left(\mathcal{I}(d) > i_0\lambda^{\hat{\gamma}}\right), \tag{16.30}$$

where

$$\hat{\gamma} = -\frac{\log I(t,d) + C}{\log d}, \quad C = \text{constant}, \tag{16.31}$$

$$I(t,d) = K\frac{t^m}{d^n} \tag{16.32}$$

and $\lambda = 1/d$.

Remark 16.3: Observe that the structure of IDF curves (Eq. (15.8)) appears again in the exponent $\hat{\gamma}$ (Eq. (16.32)).

The limiting behavior of $\hat{\gamma}$ at small-scales is

$$\lim_{d\to 0} \hat{\gamma} = \lim_{d\to 0} -\frac{\log I(t,d) + C}{\log d} \tag{16.33}$$

$$= \lim_{d\to 0} \frac{n \log d}{\log d} \tag{16.34}$$

$$= n. \tag{16.35}$$

Therefore,

$$\mathbb{P}(\mathcal{T} > t) \sim \lambda^{-c(n)}. \tag{16.36}$$

The asymptotical expressions that we found recall multifractal behavior of rainfall time series and simple scaling in IDF curves as well. They reveal a link between the probability distribution of $\mathcal{T}$, the multiscaling behavior of rain intensity and the empirical parameter n. Our result shows that, viewed as estimators, IDF curves are consistent with the multifractality of rainfall time series. The underlying Hurst coefficient in IDF curves, meant as in Eq. (15.8), is then the codimension function of the multiplicative cascade model evaluated in n ($H = c(n)$). Our results (see Eq. (16.30)), recall IDF relationships that are established as asymptotically self-similar models.

We observe that Eq. (16.36) seems to be in concordance with the results of [VF02a]. They found that under limiting conditions (very short durations d or very long return periods T), the IDF values are simple scaling with a power law dependence on d and T.

Clearly, scale invariance of physical systems generally holds within a certain range of scales bounded by the inner cut-off and the outer cut-off and that different scaling exponents for the duration are found to characterize different ranges of scales.

Also, in our case the value of the parameter n only fits well over a certain range of durations, so that we can obtain a different value of n for every range of durations d. Calculating the small-scale limit behavior in the case of IDF curves that does not hold at small-scales is not misleading because Eq. (16.36) describes how much the approximation from IDF curves deviates from an underlying multiscaling process with codimension function $c(\gamma)$.

We can obtain different expressions for Eq. (16.30), depending on the multiplicative cascade model that we choose for the data.

16.5 Possible applications in risk management

As a result of our interdisciplinary adventure in hydrology and meteorology, we are convinced of the high potential of IDF curves within the multifractal framework. They can be exploited to calculate return periods of extreme events and they can also be useful for the generation of synthetic sequences of data. Although IDF curves are not multifractal models themselves, these models are compatible with the multifractality of rainfall intensity from a mathematical point of view. We can use them as estimators of the multiscaling process.

If we want to see an example of applying multiplicative cascades, we can begin studying the work of [VF02a]. There we can find an extended analysis of scaling properties of IDF curves for temporal rainfall. For their research, they used synthetic sequences of data generated using a β-lognormal multiplicative cascade as well as real data.

Multiplicative cascade models are stochastic models that can be applied to valuate heavy rain, flood and hail insurance policies and these models can also be useful for the development of innovative weather-related disaster insurance policies. Given that in the case of natural disasters in some countries, both the public and the private sectors share risks, stochastic models for rain are also important for the development of risk management strategies for governmental funds for natural disasters. We do not recommend these models in the case of rain insurance application, because they are not suitable for the valuation of short-term policies.

16.6 Final comments

In Secs. 16.1 and 16.2, we explained why multiplicative cascade models can be useful for hydro-meteorological disaster risk management. In Sec. 16.3, we explained the central idea of multiplicative cascade models. In Sec. 16.4, we provided a review of key results for multifractal models of rain. Subsequently, we introduced the reader to the topic of intensity-duration-frequency (IDF) curves in a multifractal framework. We think that they can lead to the applications that we are looking for. After that, we presented the asymptotic expression for the tail probability of the return period T that we found from IDF curves under the assumption of multifractality, and we commented its implications. Finally, we exposed our ideas about how we could apply multiplicative cascade models in hydro-meteorological disasters risk management.

Although much more empirical and theoretical research is needed, multifractals models in rain can already be considered as a real alternative for some applications in risk management. However, when applying multiplicative cascades, we should always remember that all models of Secs. 16.3 and 16.4 work under the assumption of stationarity. We also wish to emphasize, that in the multiplicative cascades framework, the study of the rain process at small-scales is of the highest importance for the future development of the theory and its applications.

In the next chapter, we explore the multifractality at small scales using an experimental setup and we parametrize an IDAF function for the small-scale considering anisotropic space-time scaling.

17. IDAF FUNCTIONS FOR PRECIPITATION IN A MULTIFRACTAL FRAMEWORK[1]

This chapter was a result from the team-work with Jorge Castro and Alin Andrei Cârsteanu. An intensity-duration-area-frequency (IDAF) function is derived for the small-scale, large-intensity limit of multifractal fields. A parameterization of the function from tropical rainfall, filmed with a digital camera in Mexico City, is being attempted. Implications of the formulae are being discussed.

17.1 *Intensity-duration-area-frequency (IDAF) functions*

Information from marginal and joint probability distributions of space-time rainfall intensities can be represented in a purpose-oriented manner using the exceedence probability of intensity $\mathcal{I}$ as a function of area A and duration d. Such a function can certainly not capture all the information contained in the joint probability distributions of point-instantaneous intensity, but it does capture all marginals corresponding to various space-time scales, which are indeed the functions that play an important role for the purpose of estimating the impact of rainfall, including its extreme events, in hydrological terms.

Let us note that the exceedence probability, which is the complement of the probability distribution function F, is in praxis most often replaced by its inverse, the *relative* return period T:

$$\mathbb{P}\left(\mathcal{I}\left(d,A\right) > i\right) \quad = \quad 1 - F_{\mathcal{I}(d,A)}\left(i\right) = \frac{d}{T}. \tag{17.1}$$

This identity between exceedance probability and inverse relative return period is based on a temporal ergodicity assumption, which in turn implies at

[1] REPRINTED FROM PHYSICA A, VOL 338, CASTRO, J., CÂRSTEANU, A., FLORES, C.-G., IDAF FUNCTIONS FOR PRECIPITATION IN A MULTIFRACTAL FRAMEWORK, PAGES 206-210, COPYRIGHT (2004), WITH PERMISSION FROM ELSEVIER

least first-order stationarity at all time scales d, a hypothesis that is not tenable due to the existence of hydro-meteorological cycles. However, as long as $d \ll 1\text{year} < T\,(d, A)$, at least the influence of the yearly cycle can be considered negligible. Another consequence of the yearly water cycle is that practitioners often prefer to use, instead of the process $\mathcal{I}(d, A)$, the process $\max_{1\text{year}} \mathcal{I}(d, A)$. Being a process of a non-additive nature (to be more precise, additive in L_∞ instead of L_1), this latter process exhibits a somewhat different scale-related behavior than the one previously defined, and will not make the object of the present article. The interested reader can find a comparison between the scaling behaviors of the two processes e.g. in [VF02a].

An observation concerning the representation of the exceedance probability $P\,(\mathcal{I}(d, A) > i)$, is that for historical reasons, mainly stemming from the absence of digital computers in the past, practitioners estimate the return period $T := T_{(\mathcal{I}(d,A)>i)}$ from nomograms called Intensity-Duration-Frequency curves, and multiply the obtained T with a function of the area A, called "areal reduction factor". Certainly, nowadays the fact that $P\,(\mathcal{I}\,(d, A) > i)$ and the corresponding $T_{(\mathcal{I}(d,A)>i)}$ are functions of the 3 variables d, A and i, does not impede in any way their convenient representation as such, and we shall not be concerned with this aspect any further. Moreover, the scaling properties of the rainfall process, for which evidence has accumulated for some two decades (see e.g. [SL87]), result in a rigorous expression for $T_{(\mathcal{I}(d,A)>i)}$, which is relatively simple to compute.

17.2 Scaling of IDAF Functions for Multifractal Rainfall Fields

The question, of whether the spatial and the temporal support of the $\mathcal{I}(d, A)$ process can be related in any way in terms of their scale-related behavior, has been another point of interest in scaling studies over the past few years. It should be noted that in another recent study ([DS03]), performed in a different climate and using a different experimental setting, results showing a remarkably accurate multifractal scaling have been reported for various rainfall events. Given the mounting empirical evidence in favor of multifractal scaling of rainfall in both space and time, it is natural to ask the question about space-time scaling, its characteristics and mechanisms, under this multifractal ansatz. As far as the mathematical description of space-time scaling is concerned, research was oriented towards finding either a unique anisotropy exponent for all existing moments of the probability distributions of $\mathcal{I}$, or an order-of-moment-dependent anisotropy exponent, or else another type of relationship. Various recent studies indicate that an anisotropy exponent independent of the order of moments is in good agreement with different data sets ([MS96], [FS99], [DC01], [Dei00]), although the exponent z does not seem to be universal:

$$d \propto A^{z/2}. \tag{17.2}$$

The terms used for this type of behavior have been "anisotropic space-time scaling" or "dynamic scaling".

In the context of the large-deviations property of multifractal fields (see e.g. [SL87], [VD93], [BR96])

$$\lim_{\lambda \to \infty} \frac{P\left(\mathcal{I}\left(\lambda^{-1} d, \lambda^{-2} A\right) > i_0 \lambda^{\gamma}\right)}{g(\lambda)\, \lambda^{-c_{2\times 1}(\gamma)} P\left(\mathcal{I}(d, A) > i_0 \lambda^{\gamma}\right)} = 1, \tag{17.3}$$

where λ is a scale factor, i_0 is some constant rainfall intensity, γ is an order of singularity, $c_{2\times 1}(\gamma)$ is the corresponding codimension function of the $2D \times 1D$ space-time multifractal field, and $g(\lambda)$ is a slowly-varying function of λ, in the sense that $\lim_{\lambda \to \infty} g(a\lambda)/\, g(\lambda) = 1, \forall\, a \in \mathbb{R}$, the space-time scaling property becomes:

$$\lim_{\lambda \to \infty} \frac{P\left(\mathcal{I}\left(\lambda^{-1} d, A\right) > i_0 \lambda^{\gamma}\right)}{P\left(\mathcal{I}\left(d, \lambda^{-2/z} A\right) > i_0 \lambda^{\gamma}\right)} = \lim_{\lambda \to \infty} \frac{g(\lambda)\, \lambda^{-c_{0\times 1}(\gamma)}}{g\left(\lambda^{2/z}\right) \lambda^{-2c_{2\times 1}(\gamma)/z}} = 1. \tag{17.4}$$

Denoting $i := i_0 \lambda^{\gamma}$, we obtain:

$$i \propto T_{(\mathcal{I}(d,A)>i)}^{(1-\gamma)/(1-c_{0\times 1}(\gamma))} d^{-1} A^{-z/2} \tag{17.5}$$

(compare also with [DL97] for the purely temporal case). Let us note that, while the exponent of the return period T seems to be a function of the order of singularity γ, in fact, due to the divergence of moments of the variable $\mathcal{I}(d, A)$, distributed according to $F_{\mathcal{I}(d,A)}(i)$, there exists a whole interval of orders of singularity where $c_{0\times 1}(\gamma)$, the temporal codimension function, is a linear function of γ, and $(1-\gamma)/\,(1-c_{0\times 1}(\gamma))$ is a constant. This interval corresponds precisely to the highest values of orders of singularity γ up to $\gamma_{\max}$, and as expected, the highest value of the exponent of T is reached over the aforementioned interval. This is to say that the worst-case scenario, in the sense of the highest rainfall intensity corresponding to a given return period, is reached over this interval, due to the fact that the highest orders of singularity dominate the field at small scales. This is, on the one hand, a non-trivial implication of multifractality (see e.g. [SL87]), which does not have a correspondent in non-singular

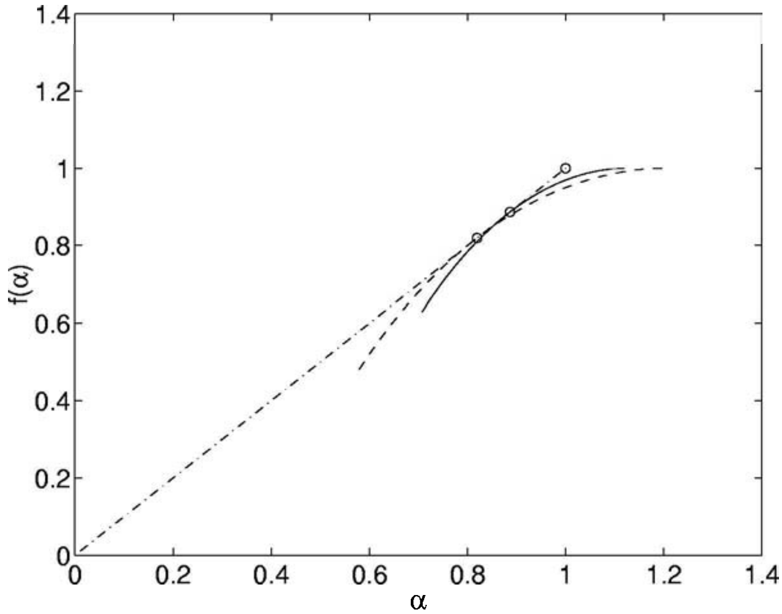

Fig. 17.1: Typical singularity spectrum of a Mexico City rainfall event, $\alpha \equiv 1-\gamma$, $f(\alpha) \equiv 1-c(\gamma)$, used to compute scaling exponents of the IDAF function. The temporal function is represented by the dotted line, the spatial function by the solid line, and both tangency points with the main diagonal, as well as the point at $(1,1)$, are marked for reference

(smooth) fields. On the other hand, this same property implies that if a given sample does not capture the linear interval of $c_{0\times 1}(\gamma)$, then the estimated values of γ and $\gamma_{\max}$, will not result in the true highest exponent of T, but rather in a lower value. However, even in this latter case, $(1-\gamma_{\max})/(1-c_{0\times 1}(\gamma_{\max}))$ is the highest exponent of T that can be obtained from the sample.

17.3 Experimental setting

Rainfall has been filmed in a spatial cube of $1.2\text{m}\times 1.2\text{m}\times 1.2\text{m}$, at a rate of 30 images/second, using a Sony DCR-TRV 130 camera with Digital 8 format tape. The camera has a 37mm lens with a focal length of 3.672mm, and is capable of an optical zoom of 20. All filming has been done with natural-light illumination, using black plates as background and bottom. The 30 bitmaps/second obtained from the digital film have 640×480 pixels each, resulting in a ratio of 2.5mm/pixel.

Drops have been detected as a trace representing their trajectory during one

CCD scan. Many raindrops that appear in more than one image can be matched between successive images, and hereby the CCD scanning time can be related to the interval of $1/30$s between images, and the drop velocities determined. Drop sizes have been inferred from vertical velocities, considering the latter as terminal. Possible sources of errors in this procedure are updrafts and drop interactions, however the proximity of the measurements to the Earth's surface limits the updraft scale, whereas changes in terminal velocity due to drop coalescence or break-off are being asymptotically reached within a few meters. The positions of the drops have been determined geometrically within the frontal plane, and approximated from their impact location in depth.

17.4 Results

Figure 17.1 shows a typical singularity spectrum of a Mexico City rainfall event. The resulting values are $\gamma_{\max} \cong 0.418$, $c_{0\times1}(\gamma_{\max}) \cong 0.524$ and $z \cong 1.161$, and several Mexico City storms like the one presented, show values of $0.3 \ldots 0.5$ for $\gamma_{\max}$, and of $0.4 \ldots 0.6$ for the respective $c_{0\times1}(\gamma_{\max})$. The estimated IDAF function in the presented case turns out to be

$$i \propto T^{1.227}_{(\mathcal{I}(d,A)>i)} d^{-1} A^{-0.581}. \tag{17.6}$$

It should be observed, however, that no clearly linear interval appears in the $c_{0\times1}(\gamma)$ curve, so we have to conclude that the true values of $\gamma_{\max}$ have not been reached. Also, the obtained values are valid in the small-scale limit, and should not be simply extrapolated to larger scales. It is nevertheless at these smallest scales where singularities are phenomenologically best captured.

Acknowledgments

The authors gratefully acknowledge CONACyT Grant 32495-T and SEMARNAT Grant C01-0306, as well as the organization of the conference "Frontier Science 2003" in Pavia, Italy.

Part V

CONCLUSIONS AND PROSPECTS

18. CONCLUSIONS AND PROSPECTS

In some developing countries, the government plays a fundamental role to absorb the losses of natural disasters. The low insurance density, the poverty and the macroeconomic problems are some causes of the low participation of private capitals in the risk management of natural disasters in these cases.

Mexico is a developing country with vast experience in natural disasters of almost all types. Furthermore, it is one of the few countries that has a natural disasters fund. For this reason, the case of Mexico is important to be analyzed. Some of its experience can be applied to improve the implementation and management of natural disaster funds in other countries.

The main goal of Mexico's Fund for Natural Disasters (FONDEN) is to mitigate the effects of natural disasters whose magnitude surpass the capacity of answer of local governments and public federal entities. FONDEN can provide economic resources for

- the reestablishment of the normal functioning of governmental entities,
- the reconstruction of non-insurable infrastructure,
- help for low-income victims,
- the acquisition of specialized equipment and
- the restoration of cultural and historical patrimony.

FONDEN's assistance should be provided within a budget established at the beginning of every fiscal year. In case of imminent danger or high probability of disaster, the Mexican Ministry of the Interior (SEGOB) can declare a situation of emergency and provide resources to attenuate the effects of the possible disaster.

FONDEN's rules of operation establish that in case of high probability of natural disaster or imminent danger, local governments can call a state of emergency to get resources faster from FONDEN. Hence, they can take measures in order to attenuate the effects of the possible disaster. For this reason, it becomes necessary the development of a mathematical model considering this type of outcome.

The problem of how to use information from a warning system was unexplored in actuarial sciences and the model here presented is, as far as we know, the first accomplished attempt to quantify the economic impact of an early warning system with a parsimonious stochastic model. Our models for a governmental fund for natural disasters and the risk-reserve of an (re)insurance company considering the existence of an early warning system serve as starting point to outline new mathematical problems in risk management of natural disasters. For example, risk-partnership models for the public and the private sector.

One difficulty for this part of our research was to identify the relevant information for the modelling in order to simplify the problem to its essence. Not necessarily "more" is "better". Our starting model for the governmental fund was much more complex as the one here presented. Step by step, as we were understanding the elements involved and its interaction, we were improving abstraction until capturing the very essence of our problem. One of our main results is that we discovered that we can use to our benefit the statistics of performance measurements of early warning systems to outline the problem using Markov processes. This representation is very convenient in order to take advantage of previous results that have been proven to be useful in the practice. In particular, our model for the risk-reserve is a generalization of the classical Lundberg model for the risk reserve. We didn't find other actuarial models for a governmental fund in the literature.

We decomposed the group of dependent and not simultaneous processes involved in our problem into independent processes. So, we conclude that for the quantification of the economic impact of early warning systems, the fundamental information is

- the claim sizes sorted with respect to the observed performance of the early warning system,
- the probabilities of error $(\alpha_1, \alpha_2, \alpha_3)$ and
- the mean number of claims (or outcomes in the case of the governmental fund) pro year.

This result is also useful as a justification for structuring data bases in such a way that we can at least obtain/estimate this information.

Our results make it possible to formulate different mathematical problems in risk management considering the existence of early warning systems that can shed light inside the financial planning of a governmental fund of natural disasters and of the risk-reserve of a reinsurance company from the perspective of actuarial sciences and financial mathematics.

In our case, we applied our model to formulate a stochastic optimization problem in order to make a first step to find an optimal management strategy for a governmental fund for natural disasters. For the modelling, we assumed that the government is risk-averse. We used the F-S strategy to solve the problem.

From the results of Part II, we conclude the following:

I. A premise of Mexican government is not investing financial resources for natural disasters in risky assets. We consider that this postulate should be reviewed, since any form of risk transfer is by definition expensive and contingent credits as basis for the management strategy is not desirable from a political point of view.

II. It is often argued that natural disasters losses can not be managed using traditional financial instruments, because they have less variability. Nevertheless, considering the established budget as the estimation of a random quantity with a deterministic value, as we do, we can improve budget's approximation using investment. That is, we can invest a part of the reserves in order to reduce the fund's deficit to its intrinsic value using traditional financial instruments, less expensive than CAT bonds.

III. Our results show that investment can help to reduce the amount of risk to be transferred to its intrinsic value. Introducing the possibility of investment, we can reduce the amount of risk to be transferred. Our model also considers the possibility of XL-reinsurance, so that we can explore the differences resulting from varying the retention level.

IV. The strategy that we propose consists basically in having budget resources and part of the reserves in high liquidity, low risk investments and the other part of the reserves in a portfolio investment. The concept is to facilitate self-financing and building of reserves in "good years". It should be noticed that this strategy requires a minimum level of reserves that should not be available until the end of the fiscal year. Nevertheless, this is not a disadvantage in the long-term planning.

	Investment of a part of the reserve fund in traditional risky assets
Cost before event	• A minimum level or reserves is required, but we only transfer intrinsic risks • We have market risk, but it does not necessarily surpass the cost of risk transfer
Benefit after event	It improves absorbing capacity of the government and it facilitates building reserves in the long term
Cost after event	The revenues as well as the invested capital are not immediately available after event and the investment strategy should be carried out the whole fiscal year
Incentive for mitigation	Yes, if the positive effect of warnings is also taken into account in this and the other strategies that interact and compose the whole management strategy

Tab. 18.1: Costs and benefits of the ex-ante investment strategy, viewed as part of an integrated risk management strategy

Summarizing, in spite of market risk, we found that, for risk-averse governments, investment as a part of an integrated risk-management strategy can improve considerably the performance of a governmental fund for natural disasters. In Tab. 18.1, we present a similar analysis of our strategy as that done in Tab. 4.1 for reserve funds[1], insurance and contingent credits. We wish to stress that every type of strategy interacts with the others, so that with integrated risk-management strategy we mean a system of strategies.

The last part of this research was devoted to the integration of geophysical models in risk management. As we mentioned at the beginning of this thesis, in the case of natural disasters we need multidisciplinary skills to make better use of available information. In this research we have explained the scale-problem present in some natural processes. We, the actuaries, have been completely ignoring it in the past.

The identified problem of missing information on rain (also present in run-off

[1] In this research, it is understood that reserve funds are highly-liquid.

data) should be considered (or at least remembered) in any case when using data bases, also when not applying IDF curves or calculating asymptotic tail probabilities. Multiplicative cascades can be used for generation of synthetic sequences that resemble the original data in terms of its scaling properties.

If not using multiplicative cascade models, the existent evidence of intermittency, long memory and multiscaling properties in rain processes provided by geophysical sciences is already helpful for the development of risk management techniques as well as for other applications.

The asymptotic expression for $\mathbb{P}(\mathcal{T} > t)$ that we found shows that IDF curves are consistent with the multifractality of rainfall time series and the limiting behavior of $\hat{\gamma}$ at small-scales widens the interpretation of the empirical scaling parameter n ($\hat{\gamma} \to n$). It is also possible to extend the results to include the area by means of empirical intensity-duration-area-frequency functions (IDAF), using the relationship $T \propto i^m d^k A^p$, where A is the area of observation, d is the scale of observation and m, k, p are parameters to be adjusted. The parameter p is the anisotropy exponent $p = -z/2$, where $z = \tau_{space}(q)/\tau_{time}(q)$.

The small-scale analysis of the multifractal behavior of the rainfall process has brought one more evidence of multifractal behavior, anisotropic between space and time. This leads us to validate the asymptotic small-scale, large-intensity behavior of multifractal fields for the case of rainfall. By means of a case study, we show how to parameterize IDAF curves corresponding to this limiting behavior.

In an internal meeting at the Mexican Ministry of Finance (SHCP) on January 2003, we noticed that our results can be useful for improving laws, budget planning as well as providing a technical justification for risk reserves in governmental funds. Nevertheless, our work is not only useful for governments, but also for the insurance industry and consulting firms.

APPENDIX

A. SIMULATION OF A MULTIPLICATIVE CASCADE

In this appendix we present the program made in Matlab language that we wrote to generate Figs. 14.1 and 16.1. Using this algorithm we can "bare" a multiplicative cascade in the sense of Tab. 16.2 until a finite level n, $n \in \mathbb{N}$.

This program simulates a binary multiplicative cascade with support in the interval $[0, T]$, $0<T<\infty$, complementary weights and uniform generator $w_i^{(n)} \sim U[0, 1]$. A graphic of the cascade at every level is produced. The algorithm can be adapted to simulate other discrete multiplicative cascades.

```
% Begin
m=4; % This is the mass to be distributed along the support.
n=8; % This is the number of levels of the cascade that we want to develop.
T=1; % This is the length of the support.
%The cascade has support in the interval [0,T].
branchn=2^n; % This is the branch number.
% In the last level (n) we will have 2^n branches.
% Now we generate a matrix with complementary weights (w).
w=zeros(n,branchn);
for i=1:n; % rows
    for j=1:2:2^i %columns;
        w(i,j)=rand(1,1); % The weights are uniformly distributed in [0,1].
        w(i,j+1)=1-w(i,j); % We have complementary weights.
    end;
end;
% In the matrix M, we store the weights in a convenient order.
M = ones(n+1,branchn);
% The first row of M will have ones, because the mass (m) is uniformly
% distributed along the support at the first level of the cascade,
% The cells of the other rows will store elements of the matrix of weights (w).
```

```
for i = 2:n+1 % i − 1 is the corresponding row in w
repeat = 2^(n-i+1);
    for k = 0:branchn/repeat-1;
        for j = k*repeat+1:(k+1)*repeat;
            if j <= 2^k*repeat;
                temp = k+1;
            else temp = k+2;
            end;
            M(i,j) = w(i-1,temp);
        end;
    end;
end;
% We calculate the values for every branch:
cascade = cumprod(M)*m;
% Every row of the matrix 'cascade' corresponds to a level of the cascade.
% For the graphics:
N = zeros(n+1,branchn);
for i=1:n+1; % We should consider the different scales for the graphic.
    N(i,:)=cascade(i,:)*2^(i-1)/T; % . i-1 is the level of the cascade.
% The calculated mass for every sub-interval of length T/2^(i−1) is distributed
% along it.
end;
graf=N';
t=T/branchn:T/branchn:T; % The matrix stores the support divided in the
% finest scale.
% This is to obtain a graphic of the simulated binary multiplicative cascade
figure(1);
for i=1:n+1;
    subplot(3,3,i); % n+1=9 graphics are generated and presented in a 3x3 array.
    plot(t,graf(:,i));
    axis([1/branchn,T,0,max(graf(:))]);
end;
% End
```

In Fig. 14.1, we plot three simulations of a binary multiplicative cascade developing 10 levels. This cascade has support in $[0, 1]$, $m = 1$, uniform generator and complementary weights.

BIBLIOGRAPHY

[AC03] Argüello, M.-Y. Aguayo Quezada, S. and Cabello, A., editors. *México a la mano*. Grijalbo, 2003.

[Bar93] M.-F. Barnsley. *Fractals Everywhere*. Morgan Kaufmann, second edition, 1993.

[BC01] Barry, R.-G. and Chorley, R.-J. *Atmosphere, weather and climate*. Routledge, seventh edition, 2001.

[BH88] Bedient, P.-B. and Huber, W.-C. *Hydrology and Foodplain Analysis*. Addison-Wesley, 1988.

[Bil95] Billingsley, P. *Probability and Measure*. John Wiley & Sons, second edition, 1995.

[BR96] Burlando, P. and Rosso, R. Scaling and multiscaling models of depth-duration-frequency curves for storm precipitation. *Journal of Hydrology*, 187, 1996.

[BS99] Deidda, R., Benzi, R. and Siccardi, F. Multifractal modeling of anomalous scaling laws in rainfall. *Water Resources Research*, 35, 1999.

[CEN01] CENAPRED. *Diagnóstico de peligros e identificación de riesgos de desastres en México. Atlas Nacional de Riesgos de la República Mexicana*. Centro Nacional de Prevención de Desastres (CENAPRED), Secretaría de Gobernación (SEGOB), 2001.

[Cen04] Centro de instrumentación y registro sísmico (CIRES). The seismic alert system of mexico city. Electronic publication, http://www.cires.org.mx, 2004.

[CF04] Castro, J., Cârsteanu, A.-A. and Flores, C.-G. Intensity-Duration-Area-Frequency Functions for Precipitation in a Multifractal Framework. *Physica - Section A*, 338(1):206—210, 2004.

[Con03] Consejo Nacional de Población (CONAPO). *Indices de Marginación, 2000*. CONAPO, 2003.

[Coo83] Coordinación General del Plan Nacional de Zonas Deprimidas y Grupos Marginados (Coplamar). *Geografía de la marginación. Necesidades esenciales en México.* Siglo veintiuno editores, 1983.

[DB03] Douglas, E.-M. and Barros, A.-P. Probable Maximum Precipitation Estimation Using Multifractals: Application in the Eastern United States. *Journal of Hydrometeorology*, 4(6), 2003.

[DC01] Venugopal, V., Deidda, R. and Cârsteanu, A.-A. Dynamic scaling in the context of multifractal rainfall modeling. *Seventh International Conference on Precipitation: Estimation and Prediction of Precipitation Variability at All Scales*, 2001. Rockport, Maine.

[DE91] Davis, M.-H.-A. and Elliot, R.-J., editors. *Applied Stochastic Analysis*, volume 5 of *Stochastics Monographs*. Gordon and Breach Science Publishers, 1991.

[Dei00] Deidda, R. Rainfall downscaling in a space-time multifractal framework. *Water Resources Research*, 36(7), 2000.

[dkv03] *Hochwasservorsorge in Deutschland: Lernen aus der Katastrophe 2002 im Elbegebiet*. Schriftenreihe des DKVV 29. Deutsches Komitee für Katastrophenvorsorge e.V. (DKVV), November 2003. ISBN: 3-933181-32-1.

[DL97] Bendjoudi, H., P. Hubert, D. Schertzer and Lovejoy, S. Interprétation multifractale des courbes intensité-duré-fréquence des précipitations. *Comptes Rendus de l'Academie des Sciences - Serie IIa - Sciences de la Terre et des Planetes*, 325(5), 1997.

[DR91] Duffie, D. and Richardson, H.-R. Mean-variance hedging in continuous time. *Annals of Applied Probability*, 1, 1991.

[DS96] Delbaen, F. and Schachermayer, W. The variance-optimal martingale measure for continuous processes. *Bernoulli*, 2(1), 1996.

[DS03] Lovejoy, S., Lilley, M., Desaulniers-Soucy, N. and Schertzer, D. Large particle number limit in rain. *Physical Review E*, 68, 2003.

[Eag70] Eagleson, P. *Dynamic Hydrology*. McGraw-Hill, 1970.

[ECL95] ECLAC. Family and future. a regional programme in latin america and the caribbean. United nations publication, Economic Comission for Latin America and the Caribbean (ECLAC), Chile, 1995.

[Fal90] Falconer, K. *Fractal geometry*. John Wiley & Sons, 1990.

[Fal97] Falconer, K. *Techniques in fractal geometry*. John Wiley & Sons, 1997.

[Flo03] Flores-González, C.-G. Risk Management of Natural Disasters in Mexico. *Proceedings of the 5th CENAT PhD Students' and Advisors' Meeting, October 5th-7th 2003 in Bad Schwarzsee/Fribourg, Switzerland*, 2003.

[Flo04] Flores, C.-G. Multiplicative cascade models for rain in hydrometeorological disasters risk management. *Proceedings of the XXXV ASTIN Colloquium*, 2004.

[FM01] Freeman, P. and Mechler, R. Public Sector Risk Management in Mexico for Natural Disaster Losses. Technical report, International Institute for Applied Systems Analysis (IIASA), Laxenburg, Austria, 2001.

[Fok03] Foken, T. *Angewandte Meteorologie, Mikrometeorologische Methoden*. Springer, 2003.

[FP85] Frisch, U. and Parisi, G. Fully developed turbulence and intermittancy. *In [Ghi85]*, 1985.

[Fre02] Freeman, P. Environmental Risk Management for Developing Countries. *The Geneva Papers on Risk and Insurance*, 27(2), 2002.

[FS91] Föllmer, H. and Schweizer, M. Hedging of Contingent Claims under Incomplete Information. *In: [DE91]*, 1991.

[FS99] Venugopal, V., Foufoula-Georgiou, E. and Sapozhnikov, V. Evidence of dynamic scaling in space-time rainfall. *Journal of Geophysical Research*, 104(D24), 1999.

[Ghi85] Ghil,M., editor. *Turbulence and Predictability in Geophysical Fluid Dynamics and Climate Dynamics (Proceedings of the International School of Physics)*. North-Holland, 1985.

[Guy00] Guy Carpenter & Co. Managing the financial impacts of natural disaster losses in Mexico. A World Bank report prepared for the Government of Mexico by Guy Carpenter & Co. Inc., in association with EQECAT, with contributions from IIASA, November 2000.

[GW90] Gupta, V.-K. and Waymire, E.-C. Multiscaling properties of spatial rainfall and river flow distributions. *Journal of Geophysical Research*, 95(D3), 1990.

[GW93] Gupta, V.-K. and Waymire, E.-C. A statistical analysis of mesoscale rainfall as a random cascade. *Journal of Applied Meteorology*, 32, 1993.

[GW97] Gupta, V.-K. and Waymire, E.-C. Reply - Universal Multifractals Do Exist!: Comments on “A Statistical Analysis of Mesoscale Rainfall as a Random Cascade”. *Journal of Applied Meteorology*, 36, 1997.

[GW98] Feldmann, A., Gilbert, A.-C. and Willinger, W. Data networks as cascades: Investigating the multi-fractal nature of internet WAN traffic. *In: ACM/SIGCOMM ’98 Proceedings: Applications, Technologies, Architectures, and Protocols for Computer Communication, Association for Computing Machinery*, 1998.

[Har01] Harte, D. *Multifractals*. Chapman & Hall/CRC, 2001.

[Her94] Herrmann, D. *Algorithmen für Chaos und Fraktale*. Addison-Wesley, 1994.

[HK79] Harrison, J.-M. and Kreps, D. Martingale and arbitrage in multiperiod securities markets. *Journal of Economic Theory*, 20, 1979.

[Hur51] Hurst, H.-E. Long-term storage capacity of reservoirs. *Transactions of the American Society of Civil Engineers*, 116:770–808, 1951.

[HW92] Holley, R. and Waymire, E. Multifractal dimensions and scaling exponents for strongly bounded random cascades. *Annals of Applied Probability*, 2(4), 1992.

[IMF03] IMF Statistics Department. International financial statistics. Institutional publication Vol. LVI, No. 12, International Monetary Fund, International Monetary Fund, Publication Services, December 2003.

[IMF04] IMF Statistics Department. International financial statistics. Institutional publication Vol. LVII, No. 3, International Monetary Fund, International Monetary Fund, Publication Services, March 2004.

[Ins03] Instituto Nacional de Estadística, Geografía e Informática (INEGI). Información estadística. Electronic publication, http://www.inegi.gob.mx/inegi/default.asp, June 2003.

[Kah74] Kahane, J.-P. Sur le modele de turbulence de Benoit Mandelbrot. *Comptes Rendus*, 278, 1974. Serie A.

[KM01] Embrechts, P., Klüppelberg, C. and Mikosch, T. *Modelling Extremal Events for Insurance and Finance*. Springer Berlin, Heidelberg, New York, third edition, 2001.

[Kol41] Kolmogorov, A.-N. The local structure of turbulence in an compressible liquid for very large reynolds numbers. *C.R. (Dokl.) Acad. Sci. URSS (N.S.)*, 30, 1941.

[KP76] Kahane, J.-P. and Peyrière, J. Sur certaines martingales de Benoit Mandelbrot. *Advances in Mathematics*, 22, 1976.

[KR02] De Michele, C., Kottegoda, N.-T. and Rosso, R. IDAF (Intensity-Duration-Area-Frequency) curves of extreme storm rainfall: a scaling approach. *Water Science and Technologie*, 45(2), 2002.

[Kun95] Kundzewicz, Z., editor. *New Uncertainty Concepts in Hydrology and Water Resources*. Cambridge University Press, 1995. Proceedings of the International Workshop on New Uncertainty Concepts in Hydrology and Water Concepts, held Sept. 24-28, 1990, in Madralin, near Warsaw, Poland.

[Lam62] Lamperti, J. Semi-stable stochastic processes. *Transactions of the American Mathematical Society*, 104:62–78, 1962.

[LS95] Lovejoy, S. and Schertzer, D. Multifractals and rain. *In Kundzewicz (1995)*, 1995.

[Man65] Mandelbrot, B.-B. Une classe de processus stochastiques homothétiques à soi; application à la loi climatologique de H. E. Hurst. *Comptes Rendus de l' Académie des Sciences de Paris*, 240:3274—3277, 1965.

[Man74] Mandelbrot, B.-B. Intermittant turbulence in self-similar cascades: Divergence of high moments and dimension of the carrier. *Journal of Fluid Mechanics*, 62, 1974.

[Man97] Mandelbrot, B.-B. *Fractals and Scaling in Finance: Discontinuity, Concentration, Risk.* Springer, 1997.

[Mex03] Mexican Ministry of Finance (SHCP). Fonden budgets versus utilization. Personal communication with Víctor Cárdenas Santiago, Dirección General de Seguros y Valores, Secretaría de Hacienda y Crédito Público (SHCP), August 2003.

[Min00a] Ministry of Finance and Public Credit (SHCP). Aclaración de adecuación a la Declaratoria de Emergencia que para efectos de las Reglas de Operación del FONDEN fue publicada el pasado 4 de octubre para el Estado de Quintana Roo. Diario Oficial de la Federación, November 30^{th} 2000. Estados Unidos Mexicanos.

[Min00b] Ministry of Finance and Public Credit (SHCP). ACUERDO que establece las Reglas de Operación del Fondo de Desastres Naturales (FONDEN). Diario Oficial de la Federación, February 29^{th} 2000. Estados Unidos Mexicanos.

[Min01] Ministry of Finance and Public Credit (SHCP). ACUERDO que modifica las Reglas de Operación del Fondo de Desastres Naturales (FONDEN), publicadas el 29 de febrero de 2000, y el Acuerdo que reforma y adiciona el diverso que establece las Reglas de Operación del Fondo de Desastres Naturales, publicado el 30 de noviembre de 2000. Diario Oficial de la Federación, March 31^{st} 2001. Estados Unidos Mexicanos.

[Min02] Ministry of Finance and Public Credit (SHCP). ACUERDO que establece las Reglas de Operación del Fondo de Desastres Naturales (FONDEN). Diario Oficial de la Federación, March 15^{th} 2002. Estados Unidos Mexicanos.

[Min03] Ministry of the Interior (SEGOB). ACUERDO que establece las Reglas de Operación del Fondo de Desastres Naturales (FONDEN). Diario Oficial de la Federación, May 23^{rd} 2003. Estados Unidos Mexicanos.

[MM88] Chow, V.-T., Maidment, D.-R. and Mays, L.-W. *Applied Hydrology*. Mc Graw Hill, New York, 1988.

[MP04] Malzahn, D. and Plapp, T., editors. *Disasters and Society - From Hazard Assessment to Risk Reduction*. Logos Verlag Berlin, 2004.

[MS87] Meneveau, C. and Sreenivasan, K.-R. Simple multifractal cascade model for fully developed turbulence. *Physical Review Letters*, 59, 1987.

[MS95] Monat, P. and Stricker, C. Föllmer-Schweizer decomposition and mean-variance hedging for general claims. *Annals of Probability*, 23:605–628, 1995.

[MS96] Marsan, D. and Schertzer, D. Causal space-time multifractal processes: Predictability and forecasting of rain fields. *Journal of Geophysical Research*, 101(D21), 1996.

[Mun00] Munich Reinsurance Company. World of natural hazards. CD Rom, 2000.

[MW04] Böse, M., Mustafa, E. and Wenzel, F. Near real-time estimation of ground shaking for earthquake early warning in Istanbul. *In [MP04]*, pages 175–182, 2004.

[Ols95] J. Olson. Limits and characteristics of the multifractal behaviour of a high-resolution rainfall time series. *Nonlinear Processes in Geophysics*, 2:23—29, 1995.

[OW00] Ossiander, M. and Waymire, E.-C. Statistical Estimation for Multiplicative Cascades. *The Annals of Statistics*, 28, 2000.

[OW02] Ossiander, M. and Waymire, E.-C. On Estimation Theory for Multiplicative Cascades. *The Indian Journal of Statistics*, 61, 2002. San Antonio Conference: selected articles.

[Pey74] J. Peyriere. Turbulence et dimension de Hausdorff. *Comptes Rendus, Serie A*, 278:567—569, 1974.

[PF96] Perica, S. and Foufoula-Georgiou, E. Model for multiscale disaggregation of spatial rainfall based on coupling meteorological and scaling descriptions. *Journal of Geophysical Research*, 101:26347—26361, 1996.

[Pie89] Pietronero, L., editor. *Fractals: Physical Origin and Consequences*. Plenum, New York, 1989.

[PM01] Plate, E.-J. and Merz, B., editors. *Naturkatastrophen: Ursachen, Auswirkungen, Vorsorge*. Schweizerbart, 2001.

[PV99] Kreimer, A., Arnold, M., Barham, C., Freeman, P, Gilbert, R., Krimgold, F., Lester, R., Pollner, J.-D. and Vogt, T. *Managing disaster risk in Mexico: market incentives for mitigation investment*. Disaster Risk Management Series. The World Bank, 1999.

[Ric89] Richardson, H.-R. A minimum variance result in continuous trading portfolio optimization. *Management Science*, 35, 1989.

[RL97] Riedi, R.-H. and Lévy-Véhel, J. Multifractal properties of TCP traffic: A numerical study. Technical Report 3129, INRIA, 1997.

[RS98] Pham, H., Rheinländer, T. and Schweizer, M. Mean-variance hedging for continuous processes: New proofs and examples. *Finance and Stochastics*, (2), 1998.

[RW03] Gilbert, A. Resnick, S., Samorodnitsky, G. and Willinger, W. Wavelet analysis of conservative cascades. *Bernoulli*, 9:97—135, 2003.

[RY91] Revuz, D. and Yor, M. *Continuous martingales and brownian motion*. Springer, 1991.

[SC94] Georgakakos, K., Cârsteanu, A., Sturdevant, P. and Cramer, J. Observation and Analysis of Midwestern Rain Rates. *Journal of Applied Meteorology*, 33, 1994.

[Sch93] Schweizer, M. Approximating random variables by stochastic integrals, and applications in Financial Mathematics. Habilitationsschrift and der Universität Göttingen, January 1993.

[Sch94] Schweizer, M. Aproximating random variables by stochastic integrals. *The Annals of Probability*, 22(3), 1994.

[SG01] Purdy, J.-C., Harris, D., Austin, G.-L., Seed, A.-W. and Gray, W. A case study of orographic rainfall processes incorporating multiscaling characterization techniques. *Journal of Geophysical Research*, 106(D8):7837—7845, 2001.

[Sig99] Sigma. Natural catastrophes and man-made disasters 1998: Storms, hail and ice cause billion-dollar losses. Sigma publication 1, Swiss Re, Zürich, 1999.

[Sig02] Sigma. El seguro en América Latina: ante la oportunidad de crecimiento y el reto de mejorar la rentabilidad. Sigma publication 2, Swiss Re, Zürich, 2002.

[Sig04] Sigma. World insurance in 2003: insurance industry on the road to recovery. Sigma publication 3, Swiss Re, Zürich, 2004.

[SL87] Schertzer, D. and Lovejoy, S. Physical modeling and analysis of rain and clouds by anisotropic scaling multiplicative processes. *Journal of Geophysical Research*, 92D(8), 1987.

[SL89] Schertzer, D. and Lovejoy, S. Nonlinear variability in geophysics: multifractal analysis and simulation. *In: [Pie89]*, pages 49—79, 1989.

[SL91a] Schertzer, D. and Lovejoy, S., editors. *Geophysics, Scaling and Fractals*. Kluger, The Nederlands, 1991.

[SL91b] Schertzer, D. and Lovejoy, S. Scaling non-linear variability in geodynamics: multiple singularities, observables, universality classes, nonlinear variability. *In: [SL91a]*, 1991.

[SL92] Schertzer, D. and Lovejoy, S. Hard and soft multifractals. *Physica - Section A*, 185:187—194, 1992.

[SL97] Schertzer, D. and Lovejoy, S. Universal multifractals do exist!: Comments on “a statistical analysis of mesoscale rainfall as a random cascade”. *Journal of Applied Meteorology*, 36:1296—1303, 1997.

[SS95] Georgakakos, K., Sharifi, M.-B. and Sturdevant, P.-L. Analysis of high-resolution rainfall data. *In: [Kun95]*, 1995.

[SS03] Dahlströhm, K., Skea, J. and Stahel, W. Innovation, Insurability and Sustainable development: Sharing Risk Management between Insurers and the State. *The Geneva Papers on Risk and Insurance*, 28, 2003.

[ST94] Samorodnitstky, G. and Taqqu, M.-S. *Stable non-gaussian random processes*. Stochastic Modeling. Chapman & Hall, 1994.

[Sub99] Ministry of Finance and Public Credit (SHCP), Subministry of Expenditure (SSE). Exposición de Motivos e Iniciativa de Derecho para el Presupuesto de Egresos de la Fe-deración, 1999. Estados Unidos Mexicanos.

[TV99] Troutman, B. and Vecchia, A. Estimation of Rényi exponents in random cascades. *Bernoulli*, 5:191—207, 1999.

[VD93] Hubert, P., Tessier, Y., Lovejoy, S., Schertzer, D., Schmitt, F., Ladoy, P. Carbonnel, J.-P., Violette, S. and Desurosne, I. Multifractals and extreme rainfall events. *Geophysical Research Letters*, 20(10), 1993.

[Ven02] Veneziano, D. Large deviations of multifractal measures. *Fractals*, 10:117—129, 2002.

[VF02a] Veneziano, D. and Furcolo, P. Multifractality of rainfall scaling of intensity-duration-frequency curves. *Water Resources Research*, 38(12), 2002. doi: 10.1029/2001WR000372.

[VF02b] Veneziano, D. and Furcolo, P. Scaling of multifractal measures under affine transformations. *Fractals*, 10(2):147—156, 2002.

[VI02] Veneziano, D. and Iacobellis, V. Multiscaling pulse representation of temporal rainfall. *Water Resources Research*, 38(8), 2002. doi: 10.1029/2001WR000522.

[WB04] Wenzel, F., Bonjer, K., Fiedrich, F., Lungu, D., Marmureanu, G., Wirth, W. and Böse, M. Real-time earthquake information systems. *In [MP04]*, pages 199–206, 2004.

[Wor04] World Bank. World development indicators database. Electronic publication, http://www.worldbank.org/data/dataquery.html, August 2004.

[WP02] Freeman, P.-K., Martin, L.-A., Linnerooth-Bayer, J., Mechler, R., Saldaña, S., Warner, Koko and Pflug, G. National systems for comprehensive disaster management: Financing reconstruction. Technical report, International Institute of Applied Systems Analysis, 2002.